Molecular Characterization of Two *myo*-Inositol Oxygenases in *Arabidopsis thaliana*

Shannon Recca Alford

Dissertation submitted to the faculty of the Virginia Polytechnic Institute and State University in partial fulfillment of the requirements for the degree of

Doctor of Philosophy
In
Biochemistry

Dr. Glenda E. Gillaspy, Chair
Dr. Elizabeth A. Grabau
Dr. John M. McDowell
Dr. Zhijian Tu
Dr. Robert H. White

February 12, 2009
Blacksburg, VA

Keywords: inositol, *myo*-inositol oxygenase, D-glucuronic acid, ascorbic acid, inositol-(1,4,5)-trisphosphate, phosphatidylinositol, *Arabidopsis thaliana,* gas chromatography

Molecular Characterization of Two *myo*-Inositol Oxygenases in *Arabidopsis thaliana*

Shannon Recca Alford

ABSTRACT

Understanding how plants respond to stress is of importance, considering the increasing need to feed a growing population and supply its energy. Plants have complex systems for detecting, and responding to stresses. One stress-responsive system involves *myo*-inositol (Ins). Ins is a precursor for cell wall components, inositol trisphosphate ($Ins(1,4,5)P_3$) and phosphatidylinositol phosphate signaling molecules, and an alternate ascorbic acid (AsA) synthesis pathway. The enzyme, *myo*-inositol oxygenase (MIOX) is encoded by four genes in Arabidopsis and catalyzes the first step of Ins catabolism producing D-glucuronic acid (DGlcA).

This research focuses on MIOX metabolism of Ins during plant growth and stress responses. I have examined *miox* mutants for alterations in metabolism and signaling. MIOX2 and MIOX4 expression patterns correlate with *miox* mutant root growth in varying nutrient conditions, and changes in flowering time. In *miox2* mutants, I found an increase in Ins in most tissues, which was accompanied by cold- and abscisic (ABA)-sensitivity; however, *miox4* mutants are ABA- insensitive, and have a small increase of Ins in flowers. MIOX2:GFP fusion protein accumulates in the cytoplasm and MIOX4:GFP accumulates in the cytoplasm and nucleus.

Overexpresser $MIOX4^+$ plants provide a model system to examine how directing carbon from Ins into DGlcA impacts Ins levels and Ins signaling. I have examined $MIOX4^+$ plants for alterations in MIOX4 RNA and protein, and measured Ins by gas chromatography (GC). My results indicate that $MIOX4^+$ tissues are impacted differently by the MIOX4 transgene, with decreases in Ins after seed imbibition, and increased Ins levels later in development. Ins depletion in seedlings was correlated with a decrease in $Ins(1,4,5)P_3$. To determine the impact of reducing Ins and $Ins(1,4,5)P_3$ in $MIOX4^+$ seedlings, I examined processes known to involve $Ins(1,4,5)P_3$ signaling. $MIOX4^+$ seed have increased seed dormancy, NaCl-sensitivity, and ABA-insensitivity. These results

suggest MIOX affects Ins signaling in response to ABA. Together, these data indicate that transcriptional control of MIOX2 and MIOX4 results in distinct roles in plant growth, and that MIOX2 and MIOX4 function in metabolic and signaling processes critical for growth, nutrient sensing, and stress responses.

ACKNOWLEDGEMENTS

I have learned and matured as a scientist under the advising and mentoring of several people while here at Virginia Tech, including and especially Glenda Gillaspy, whose scientific creativity still marvels me; my committee members: Dr. Elizabeth Grabau, Dr. John McDowell, Dr. Zhijian (Jake) Tu, and Dr. Robert White; and a patient mentor Dr. Javad Torabinejad. I would like to thank to Dr. Craig Nessler and Dr. Argelia Lorence for supplying MIOX4^{+} transgenic seeds, anti-MIOX4 antibody, and critical comments on all things MIOX. I would also like to thank Blair Lyons, Nicole Fontaine, Pyae Hein, and Bhadra Gunesekera for assistance in physiological experiments; David Ruggio, Tatiana Boluarte, and Kim Harich for assistance in protocol development and with GC measurements; Dr. David Schmale III for his assistance in using the GC/MS; Dr. Chieh-Ting Wang for his guidance in performing qPCR; Dr. Keith Ray and Dr. Rich Helm for lipid measurements and protein sequencing; Janet Donahue for running a marathon with the anti-MIOX antibody and helpful experimental advice; Raimund Tenhaken for MIOXp:GUS seed; Kansas State Lipidomics for protocols; my fellow comrades in arms-pipettes, who have always been a source of encouragement, humor, and perspective when things get tough in the trenches-lab, specifically Elitsa Ananieva, Natasha Safaee, and William Slade; and finally my friends in Graduate Christian Fellowship at Virginia Tech and Blacksburg Christian Fellowship who have offered escape, sound advice, accountability, encouragement, and sympathy during my graduate career.

I cannot express acknowledgements without recognizing my always patient, ever-encouraging, and completely understanding best friend and husband, Jarrod Alford. To be the spouse of a graduate student is to strive alongside that student toward the end goal. I am not sure which of us will be happier when I am finished. I also thank my parents for never questioning my desire to do this thing called graduate school and offering nothing but support for my decisions. Finally, and what I consider most importantly, I will acknowledge my Lord and Savior Jesus Christ, whose life, death, and resurrection give me purpose, strength, hope, and joy to live.

TABLE OF CONTENTS

LIST OF FIGURES

CHAPTER I

CHAPTER II

CHAPTER III

LIST OF ABBREVIATIONS

ABA	abscisic acid
AsA	L-ascorbic acid
CaMV	cauliflower mosaic virus
DAG	diacylglycerol
DGK	diacylglycerol kinase
DGlcA	D-glucuronic acid
GC	gas chromatography
GFP	green fluorescent protein
GUS	β-glucuronidase
IMP	*myo*-inositol monophosphatase
Ins	*myo*-inositol
Ins(1,4,5)P_3	*myo*-inositol-(1,4,5)-trisphosphate
$InsP_6$	inositol hexakisphosphate
InsPs	inositol phosphates
MIOX	*myo*-inositol oxygenase
MIOX4$^+$	transgenic plants overexpressing the MIOX4 gene
MIPS	*myo*-inositol-1-phosphate synthase
MS	Murashige & Skoog (plant culture salts)
NaCl	sodium chloride
PA	phosphatidic acid
PC	phosphatidylcholine
PLC	phospholipase C

PLD	phospholipase D
PtdIns	phosphatidylinositol
PtdInsPs	phosphatidylinositol phosphates
qPCR	quantitative PCR
WT	wild type

.

CHAPTER I

INTRODUCTION AND OBJECTIVES

MYO-INOSITOL

Cellular Uses

myo-inositol (Ins) is a cyclohexane derived polyol first isolated in animals, that is synthesized by both eukaryotes and prokaryotes (Michell, 2007, 2008). In multicellular eukaryotes, Ins is a component involved in many crucial cellular compounds, including those involved in signal transduction (phosphatidylinositol (PtdIns), PtdIns phosphates (PtdInsPs), and Ins phosphates (InsPs)), hormone regulation (indole acetic acid conjugates), stress tolerance (ononitol and pinitol), and phosphorus storage (inositol hexakisphosphate) (Loewus and Loewus, 1983; Loewus and Murthy, 2000; Raboy, 2003; Gillaspy *et al*., 2004). The primary breakdown product of Ins, D-glucuronic acid (DGlcA), is utilized for synthesis of cell wall pectic non-cellulosic compounds, and in some organisms, L-ascorbic acid (AsA, Vitamin C) (Loewus and Murthy, 2000). Therefore, Ins synthesis and catabolism impacts compounds involved in many critical biochemical pathways (Figure 1).

Synthesis

Although organisms incorporate Ins into various compounds, there is only one biosynthetic route to produce Ins. Several biochemists (Eisenberg *et al.*, 1964; Chen and Charalampous, 1966; Sherman *et al.*, 1969; Loewus, 1977; Loewus and Loewus, 1980; Loewus *et al.*, 1980) defined the pathway of synthesis of Ins beginning with the conversion of glucose-6-phosphate to *myo*-inositol-1-phosphate (InsP) catalyzed by the *myo*-inositol-1-phosphate synthase enzyme (MIPS; EC 5.5.1.4) (Majumder *et al.*, 1997), followed by the dephosphorylation of InsP catalyzed by *myo*-inositol monophosphatase (IMP; EC 3.1.3.25) (Parthasarathy *et al.*, 1994), finally yielding free Ins.

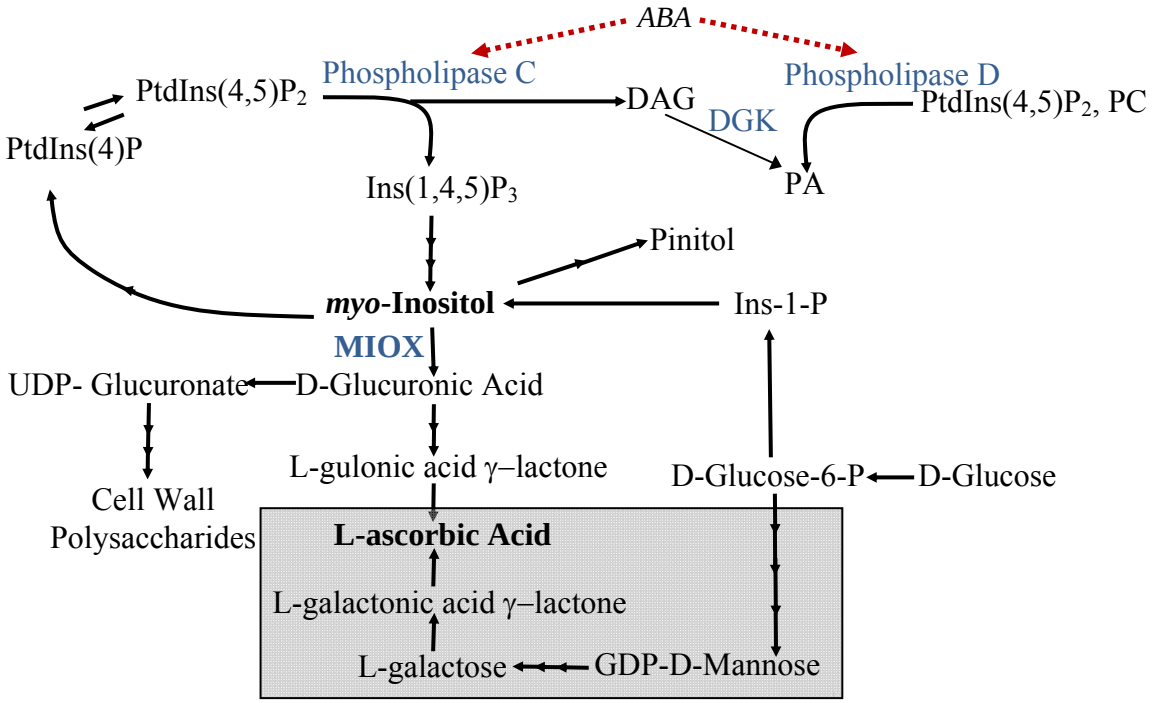

Figure 1. Inositol Signaling and Metabolism Pathways. Ins is incorporated in the signaling molecule Ins(1,4,5)P_3 and can be methylated to form the osmolyte pinitol. Ins is also a precursor for cell wall polysaccharides and AsA via oxidation by *myo*-inositol oxygenase (MIOX). The Smirnoff-Wheeler AsA synthesis pathway is highlighted in gray. PtdIns(4,5)P_2 = phosphatidylinositol-(4,5)-bisphosphate; PtdIns(4)P = phosphatidylinositol-(4)-monophosphate; Ins(1,4,5)P_3 = inositol-(1,4,5)-trisphosphate; DAG=diacylglycerol; DGK=diacylglycerol kinase; PA=phosphatidic acid; PC=phosphatidylcholine. *ABA* represents an abscisic acid signal (in red) stimulating PLD and PLC. Enzymes are in blue.

Catabolism

The first step of Ins catabolism is catalyzed by the enzyme *myo*-inositol oxygenase (MIOX; E.C. 1.13.99.1), which Reddy's group purified (Koller and Hoffmann-Ostenhof, 1979; Reddy *et al.*, 1981; Arner *et al.*, 2001). Recently the crystal structure of mouse MIOX was solved (Brown *et al.*, 2006), revealing a monomeric, single-domain protein. MIOX catalyzes the breakdown of Ins by oxidation to DGlcA with the incorporation of a single oxygen atom from molecular oxygen (Moskala *et al*., 1981).

Signaling

In the Ins signaling pathway, activation of phospholipase C (PLC) catalyzes the hydrolysis of PtdIns(4,5)P_2 to diacylglycerol and Ins(1,4,5) trisphosphate (Ins(1,4,5)P_3) (Figure 1) (Stevenson *et al*., 2000; Berridge, 2005; Munnik and Testerink, 2008). In plants, Ins(1,4,5)P_3 is thought to bind to intracellular receptors, which results in the release of Ca^{2+} (Berridge, 1993), however, no Ins(1,4,5)P_3 receptor has been identified (Krinke *et al*., 2007). From physiological, biochemical, and genetic studies, we know that Ins signaling is critical in the response to gravity (Perera *et al.*, 1999; Perera *et al.*, 2001; Perera *et al.*, 2006), blue light (Chen *et al.*, 2008), abscisic acid (ABA) (Sanchez and Chua, 2001; Xiong *et al.*, 2001; Burnette *et al.*, 2003), salt (DeWald *et al*., 2001; Takahashi *et al*., 2001), cold (Xiong *et al*., 2001), and pathogens (Ortega and Perez, 2001; Andersson *et al.*, 2006). Another important signaling molecule, phosphatidic acid (PA) can be produced by hydrolysis of lipid molecules by a phospholipase D (PLD) or via sequential action of PLC and a diacylglycerol (DAG) kinase (DGK) (see Figure 1) (Wang, 2005). PA has also been implicated in several similar signaling pathways as Ins(1,4,5)P_3 including ABA, salt, cold, and pathogen response (Munnik and Testerink, 2008).

Metabolism in Plants

Loewus was the first to address the question of what happens to Ins once synthesized (Roberts *et al.*, 1967). Labeling maize root tips with inositol-2-(^{14}C) showed that between 50-71% of the incorporated label was oxidized to DGlcA and acted on by the Ins oxidation pathway to produce pectic cell wall polysaccharides (Figure 1) (Loewus and Murthy, 2000). Similarly, studies on cultured plant cells indicate that ~23% of labeled Ins stays unmetabolized as free Ins, ~6% ends up in galactinol, and ~16% becomes incorporated into the phospholipids (Jung *et al.*,

1972). Other studies show that this phospholipid pool is ~93% PtdIns, ~1.7% PtdInsP, and ~0.8% $PtdInsP_2$ (Cho *et al.*, 1993). Thus DGlcA, free Ins, and PtdIns represent the major destinations of Ins, whereas, auxin conjugates, pinitol, raffinose (from galactinol), alternate Ins isomers, and Ins hexakisphosphate ($InsP_6$) are minor. There are exceptions to this generalization, for example, $InsP_6$ is highly abundant in seeds, and pinitol accumulation occurs in many species in response to stress (Bohnert *et al.*, 1995; Nelson *et al.*, 1998; Vera-Estrella *et al.*, 1999; Raboy, 2001).

The Ins oxidation pathway impacts two important aspects of plant physiology. The production of pectic cell wall polysaccharides is of vital importance as they are required for structural support (Loewus, 1965). Cell wall polysaccharides can also be produced from the sugar nucleotide oxidation pathway via glucose, but under certain conditions (when Ins levels are high or glucose levels are low), the Ins oxidation pathway can play a major role in cell wall polysaccharide formation. This role is supported by evidence from labeling studies in pollen (Loewus and Loewus, 1980), and studies on Arabidopsis implicating Ins oxidation at the early seedling stage (Seitz *et al.*, 2000). The second important aspect of Ins oxidation concerns a debated alternate pathway for production of AsA. In animals (except humans and a few others), oxidation of Ins produces DGlcA which can be converted to L-gulonic acid and then to L-gulonic acid γ-lactone (Banhegyi *et al.*, 1997). The conversion of L-gulonic acid γ-lactone to AsA is catalyzed by the L-gulonolactone oxidase enzyme, which is missing in humans (Nishikimi *et al.*, 1994). Humans, therefore, require plant-derived AsA to provide this important water-soluble antioxidant. Lorence *et al.* (2004) overexpressed the MIOX4 gene in transgenic Arabidopsis and found a 2-3 fold increase in AsA, suggesting a direct link between Ins oxidation and AsA synthesis. Endres and Tenhaken (2008) have recently challenged that data by demonstrating there is not an increase of AsA in $MIOX4^+$ plants.

MYO-INOSITOL OXYGENASE

MIOX in Animals

The animal MIOX enzyme was identified and shown to utilize both *myo*- and D-*chiro* inositol substrates (Arner *et al.*, 2001). In animals, the single MIOX gene is almost exclusively expressed in the kidneys (Arner *et al.*, 2006). In a model for type-2 diabetes, increased MIOX activity correlates with increased hyperglycemia (Nayak *et al.*, 2005). Both *myo*- and D-*chiro* Ins are known components of endogenous Ins phosphoglycans, which have been reported to act as insulin mediators (Frick *et al*., 1998; Nascimento *et al*., 2006); therefore, MIOX manipulation is an important target for scientists studying diabetes. Furthermore, evidence supports that administration of D-*chiro*- or *myo*-inositols, lowers blood glucose in diabetes and enhances insulin action (Brautigan *et al*., 2005; Nascimento *et al*., 2006).

MIOX in Plants

Although animals have a single MIOX gene, plants contain gene families encoding MIOX enzymes. For example, *Oryza sativa* (rice) contains two predicted MIOX genes, *Populus trichocarpa* (poplar) contains three predicted MIOX genes (http://www.floralgenome.org/tribe.php), and *Arabidopsis thaliana* contains four MIOX genes, named after their chromosomal locations (MIOX1:At1g14520; MIOX2: At2g19800; MIOX4:At4g26260; MIOX5: At5g56640) (Kanter *et al.*, 2005; Torabinejad and Gillaspy, 2005). The four MIOX isoforms are 66–84% identical at the amino acid level. Lorence *et al.* (2004) showed that the MIOX4 gene encodes a functional and active MIOX enzyme, and that the same catalytic domain in all four Arabidopsis MIOX has Ins oxygenase activity (personal communication). Tenhaken's group found that MIOX1 and MIOX2 are expressed in almost all plant tissues, whereas the expression of MIOX4 and MIOX5 is largely restricted to flowers and maturing pollen (Kanter *et al*., 2005). Disruption of MIOX1 or MIOX2 can diminish the amount of Ins incorporated into the cell wall fraction, thus these genes have been shown to actively impact the production of cell wall compounds (Kanter *et al*., 2005).

Arabidopsis MIOX and Nutrients

Recent publications have implicated Arabidopsis MIOX2 and MIOX4 in nutrient sensing or response pathways. Baena-Gonzalez *et al.* (2007) compiled published microarray data of Arabidopsis plants exposed to different nutrient conditions to analyze gene expression. They found that MIOX2 expression increases upon growth in low nutrient conditions, including sucrose starvation, starvation-induced senescence, extended night, and dark-induced senescence. They also reported that MIOX2 expression decreases upon treatment with high nutrients, including glucose, CO_2, and sucrose (Baena-Gonzalez *et al*., 2007). Gibon *et al*. (2006) saw similar results when 3-week-old Arabidopsis plants were subjected to an extended period of darkness resulting in induction of MIOX2 and MIOX4 expression.

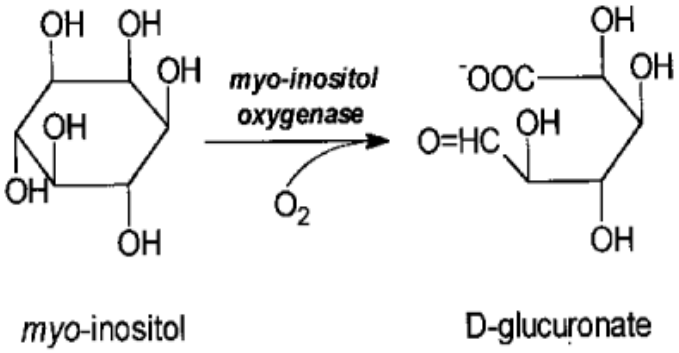

Figure 2. *myo*-Inositol Oxygenase Mechanism. MIOX catalyzes the breakdown of Ins by oxidation to DGlcA with the incorporation of a single oxygen atom from molecular oxygen (Moskala *et al*., 1981).

OBJECTIVES

The goal of this research is to understand the molecular processes by which the plant cell coordinates Ins catabolism with its varying needs. As MIOX can potentially control the cellular pool of Ins available for Ins signaling and Ins metabolism, I hypothesize the MIOX enzymes have specialized roles in providing inositol for downstream pathways. Further, the data available at the beginning of my work indicated that control of MIOX activity could be provided transcriptionally and at the level of subcellular localization. The research presented here addresses this hypothesis with the following two objectives:

Objective 1. Molecular Characterization of MIOX2 and MIOX4

Examination of MIOX Expression Patterns

Phenotypic and Metabolic Characterization of miox2 and miox4 Mutants

Complementation of miox2 and miox4 Mutants

Analysis of Protein Levels of MIOX:GFP Seedlings

Subcellular Localization of MIOX2:GFP and MIOX4:GFP Fusion Proteins

Objective 2. Characterization of MIOX4 Overexpressers: "A *myo*-Inositol Oxygenase Gain-of-Function in Arabidopsis Alters Inositol Metabolism and Signaling"

Examination of MIOX4 Transgene Expression in MIOX4^{+} Plants

Phenotypic and Metabolic Characterization of MIOX4 Overexpressers

Analysis of Protein Levels of MIOX4^{+} and MIOX2^{+} Tissues

Metabolic Characterization of MIOX2 Overexpressers

CHAPTER II

OBJECTIVE 1. Molecular Characterization of MIOX2 and MIOX4

ABSTRACT

myo-inositol (Ins) is a precursor for cell wall components, is used as a backbone of inositol trisphosphate (Ins(1,4,5)P_3) and phosphatidylinositol phosphate signaling molecules, and it is debated about whether it is also a precursor in an alternate ascorbic acid (AsA) synthesis pathway. Oxidation of Ins by the enzyme *myo*-inositol oxygenase (MIOX) produces D-glucuronic acid (DGlcA), which is further altered to produce cell wall polysaccharides and possibly AsA. The Arabidopsis genome contains four genes predicted to encode MIOX enzymes. It was shown that plants ectopically expressing the MIOX4 gene from Arabidopsis ($MIOX4^+$) produced higher levels of AsA in some tissues, and that mutants of two of the MIOX genes have reduced Ins incorporation in cell wall material.

I have examined the loss-of-function MIOX mutants for impacts on metabolism and signaling alterations. First, I measured alterations in Ins levels and other metabolites of the *miox* mutant plants by GC analysis. In the *miox2* mutant plants, I found a significant increase in Ins in most tissues, indicating a lack of Ins oxidation. Increases of Ins in *miox2* mutants were accompanied by sensitivity to cold and ABA, a plant drought hormone that uses Ins(1,4,5)P_3 as a second messenger. In *miox4* mutants I found a small increase of Ins in flowers accompanied by an insensitivity to ABA. I have observed changes in flowering time and root growth related to nutrient levels in the *miox2* and *miox4* mutants. Together, these results suggest that MIOX expression affects a plant's ability to respond to ABA, and indicates that MIOX expression impacts Ins signaling as well as metabolism. To determine the subcellular location of MIOX2 and MIOX4, I examined MIOX:GFP fusion protein expression in transgenic plants. I found MIOX2 is restricted to the cytoplasm and MIOX4 accumulates in both the cytoplasm and nucleus of certain cells. My results help us understand how MIOX function impacts Ins metabolism and signaling and thus a plant's response to external stresses.

INTRODUCTION

myo-Inositol (Ins) is a cyclic polyol that is synthesized by both eukaryotes and prokaryotes (Michell, 2007, 2008), and is used in signaling transduction pathways, hormone regulation, stress tolerance, phosphorus storage, and for metabolic purposes (Loewus and Loewus, 1983; Loewus and Murthy, 2000; Gillaspy *et al.*, 2004). D-glucuronic acid (DGlcA), the breakdown product of Ins, is utilized for synthesis of cell wall pectic non-cellulosic compounds and Vitamin C, L-ascorbic acid (AsA), in some organisms (Loewus and Murthy, 2000). Therefore, Ins metabolism impacts compounds involved in many different and critical biochemical pathways (Figure 1).

The first step of Ins catabolism is catalyzed by the enzyme *myo*-inositol oxygenase (MIOX; EC 1.13.99.1) (Koller and Hoffmann-Ostenhof, 1979; Reddy *et al.*, 1981; Arner *et al.*, 2001). The breakdown of Ins involves oxidation to DGlcA by the incorporation of a single oxygen atom from molecular oxygen (Figure 2) (Moskala *et al.*, 1981). MIOX is encoded by a four member gene family in Arabidopsis (At1g14520, At2g19800, At4g26260, and At5g56640) (Lorence *et al.*, 2004; Kanter *et al.*, 2005). The four genes are very well conserved and are differentially regulated during development with MIOX2 (At2g19800) being the predominantly expressed gene, while MIOX4 (At4g26260) and MIOX5 (At5g56640) are expressed mostly during reproductive stages (Kanter *et al.*, 2005). Disruption of MIOX1 (At1g14520) or MIOX2 can diminish the amount of Ins incorporated into the cell wall fraction, thus these genes have been shown to actively impact the production of cell wall compounds (Kanter *et al.*, 2005).

Recent data links MIOX expression with nutrient sensing in plants. Gibon *et al.* (2006) examined MIOX2 and MIOX4 expression under extended dark conditions and conditions with high and low in vivo sugars. Expression of both genes was reduced under the starvation conditions, including extended darkness and low sugars, while expression levels of both genes were elevated under non-starvation conditions with excess sugar (Gibon *et al.*, 2006). Baena-Gonzalez *et al.* (2007) examined microarray data to determine that MIOX2 is expressed more in several starvation conditions, and expressed less when plants are provided excess carbon sources. The latter group indicated that overexpression of Sucrose nonfermenting-1-related kinase, SnRK1.1, a regulator of nutrient sensing, also causes an increase in MIOX2 transcript levels. They examined physiological effects of SnRK1.1 overexpression in root growth assays and observed altered growth depending on nutrient conditions. These data indicate that plants

elevate MIOX2 and MIOX4 expression in low nutrient conditions and decrease expression when ample carbon is present, thus the oxidation of Ins may be an important adaptation to altered nutrient status in regulating plant growth.

To understand the roles MIOX2 and MIOX4 play in Ins signaling, nutrient sensing, and Ins metabolism, I have examined *miox2* and *miox4* mutants, MIOX promoter GUS plants, and MIOX:GFP fusion proteins. Here I report that both *miox* mutants have elevated Ins in some tissues; however they have opposite responses to ABA and nutrients, and in time to flowering. Differences in these responses may be explained by differential expression patterns and differences in the subcellular location of the proteins. These data further define the distinct roles MIOX2 and MIOX4 have in the plant cell.

MATERIALS AND METHODS

Plant Growth and Germination Experiments

Arabidopsis thaliana ecotype Columbia plants were used for all experiments. For seed germination experiments, age-matched WT and mutant seeds were harvested on the same day from plants grown in parallel on the same shelf of a growth rack and were stored at 23°C in the dark for at least 30 days before germination. For ABA studies, WT and mutant seeds were surface-sterilized and plated on 0.5x MS salts (pH 5.8) and 0.8% agar containing 0, 0.5, 1, or 2 μM ABA. Each agar plate was divided into sections, and >50 seeds of WT or mutant type were plated per section. Plates with seeds were stored in the dark at 4°C for at least 3 days then transferred to 23°C under continuous light. Germination assays were performed in triplicate. A seed was scored as germinated when the radicle protruded through the seed coat. For root growth experiments, seeds were surface-sterilized and plated on 0.8% agar medium, 0.5x MS + 0.8% agar medium and 0.5x MS + 0.8% agar medium + 3% glucose. Each agar plate was divided into sections, and >10 seeds of WT or mutant type were plated per section. Plates were wrapped in foil and placed at 4°C for three days before moving to room temperature. Plates were oriented vertically to allow measurements of root length. Root length experiments were performed in triplicate or more. For GC analyses of seedlings, WT and mutant seeds were surface-sterilized, placed in petri dishes on pre-wetted sterile filter paper, stratified at 4°C, germinated and grown for 5 days under continuous 100-200 μE light at room temperature, and frozen in N_2(l) for sample preparation. For flowering time and GC analyses of older tissues, WT and mutant seeds were placed on pre-wetted Pro Mix potting soil and grown under l6 hours of light/day in a growth room set at 22°C and 24°C night and day temperature and watered every other day with measured amounts. Regular-light conditions of 100-200 μE for 16 h days and low-light conditions of 40 μE for 16 h days were provided by a mixture of fluorescent and incandescent lamps or fluorescent lamps only.

Promoter GUS Analysis

For expression analysis of p:GUS (β-Glucuronidase) lines, WT, MIOX2p:GUS, and MIOX4p:GUS seeds were surface-sterilized grown on soil or on the “no” (agar), “low” (agar + ½ MS salts), and “optimal” (agar+ ½ MS salts+ 3% glucose) nutrient conditions. Whole

seedlings were removed at 5-7 days from the plates and tissues were harvested at appropriate times. The seedlings were placed in GUS staining buffer (0.1% Trion X-100, 50 mM phosphate buffer, 0.5 mM $K_4Fe(CN)_6$ x $3H_2O$, 0.5 mM $K_3Fe(CN)_6$, 2 mM 5-bromo-4-chloro-3-indolyl β-D-glucuronide cyclohexamine salt) vacuum-infiltrated for 20 minutes, incubated in the stain for several hours at 37°C, and then cleared of chlorophyll with subsequent 70% and 95% ethanol extractions at 4°C, according to the published protocol (Jefferson, 1987). Stained seedlings and tissues were photographed using an Olympus SZX16 stereoscope with an attached Olympus DP71 camera with DP Controller software (Olympus Corp., Japan).

Mutant Isolation

Potential MIOX2(At2g19800) and MIOX4 (At4g26260) mutants were identified from the Salk T-DNA lines (Alonso *et al*., 2003) through the analysis of the SiGnAL database (http://www.signal.salk.edu/cgi-bin/tbnaexpress). Seeds for *miox2-1* (Salk_002569), *miox2-2* (Salk_040608), *miox4-1* (Salk_018395), and *miox4-2* (Salk_027238) mutants were obtained from the Ohio State University Arabidopsis Biological Resource Center. To map the T-DNA insertion sites, genomic DNA was isolated from leaves of the mutant lines using a DNeasy kit (QIAGEN Inc., Valencia, CA) according to the manufacturer's instructions. DNA from segregating plants was screened with PCR using the SALK LB primers and the MIOX gene-specific primers. To analyze the *miox2-1* line, annealing at 59°C was performed with the LB primer and the following forward and reverse primers: *2-1for*, 5'-AACCATGATATCAACAACCC-3' and *2-1rev*, 5'- TGCTGGCCAAAAAGTATGGC-3'. To analyze the *miox2-2* line, annealing at 60°C was performed with the LB primer and the following forward and reverse primers: *2-2for*, 5'-ATTATGAGAATGGTGAAAGC-3' and *2-2rev*, 5'-GGCTCCTGCCTTGTGCAATG-3'. To analyze the *miox4-1* line, annealing at 55°C was performed with the LB primer and the following forward and reverse primers: *4-1for*, 5'-ATGACGATCTCTGTTGAGAAGC-3' and *4-1rev*, 5'-TCACCACCTCAAGTTTTCCGGG-3'. To analyze the *miox4-2* line, annealing at 60°C was performed with the LB primer and the following forward and reverse primers: *4-2for*, 5'-CTTGTTGCATGTGTGTTAGACAC-3' and *4-2rev*, 5'-ACCAACAACAGCCCATTGAG-3'.The resulting PCR fragments were sequenced and compared to the genomic sequence for each gene to map the T-DNA insertion. In the case of *miox2-1*, the 3'UTR insertion was found to be located 272 bp past the stop codon of MIOX2.

For *miox4-2*, the 5'UTR insertion was found to be located 13 bp before the start codon of MIOX4. Additionally, in the case of *miox4-2*, a second LB forward primer PCR product was also apparent indicating that a second T-DNA was present in tandem in the *miox4-2* gene.

RT-PCR

Total RNA was extracted from 100 mg flash-frozen 6-week-old leaves, and open flowers from WT and mutant plants using an RNeasy kit (QIAGEN Inc., Valencia, CA). Extracted RNA concentrations were measured using a NanoDrop ND-1000 Spectrophotometer (Thermo Scientific NanoDrop Technologies, LLC, Wilmington, DE). cDNA was synthesized from 1 μg of RNA using an iScript cDNA Synthesis Kit (Bio-Rad Laboratories, Hercules, CA). For MIOX2 gene-specific amplification, the *2-2for* primer and *2cDNArev* primer were used in 30 cycles of PCR amplification (1 min 95°C, 1 min 54°C, 1.5 min 72°C) resulting in a 780 bp product. For MIOX4 gene-specific amplification, the *4-1for* primer and *4-1rev* primer were used in 30 cycles of PCR amplification (1 min 95°C, 1 min 56°C, 2 min 72°C) resulting in a 954 bp product. Actin amplification has been described and generated a 425 bp product (Berdy *et al*., 2001).

Flowering Time Assays

WT and mutant plants were grown as described previously under long-day (16 hrs) or short-day (8 hrs) conditions. Careful attention was given to growing plants side-by-side or in the same pot for comparison. Plants were examined at the point of inflorescence emergence. Plants were removed from soil, inverted, and rosette leaves were removed in developmental order to facilitate counting. Fifteen or more plants per variant were examined.

Gas Chromatography/ Mass Spectrometry Analyses

For sample preparation, frozen 5-day-old seedlings, 6-wk-old leaves, open flowers, and green, elongated siliques were ground into a powder, and 1mL of 60% methanol was mixed with the powder. D-*chiro*-inositol (2 mg) was added to the mixture as an internal standard. The mixture was incubated at 70°C for approximately 1.5 hours. The insoluble portion was removed by centrifugation at 13200 rpm for 10 minutes. The supernatant was dried in a speed-vacuum chamber (Savant) and reconstituted in 200 μL of water, filtered through a 0.2 μM Tuffryn®

syringe filter (Pall Gelman Laboratory, Ann Arbor, MI), and dried again. The dried sample was reduced by mixing with 100 μL of 10 mM dithiothreitol for 10 minutes and dried again. Derivatization reagent (1:1 mixture of pyridine and bis(trimethyl-silyl)trifluoro-acetamide + 1% trimethylchlorosilane; Alltech, State College, PA) was freshly prepared. For sample derivatization, 250 μL of the reagent was added to the dried sample. The sample was sonicated and heated at 80°C for at least 45 minutes until the entire sample was in solution. The sample was transferred to an autosample vial, and 250 μL of hexanes were added to the sample.

For compound identification, retention times of peaks were compared to those of known metabolite standards. Additionally, peaks were identified by comparison of mass spectral data using GC/MS. Plant samples and standards were separated by a 6890-N GC on an HP-5MS capillary column 30 m X 0.25 mm i.d. (Agilent Technologies, Inc. Santa Clara, CA) with helium as the carrier gas with pressure-controlled flow set at 9.1 psi. The injection port was set at 250°C, the oven was set on a gradient from 75°C to 274°C at 6.5C°/min, and compounds were subjected to electrospray ionization and detected by a 5975 MS (Aglient Technologies, Inc. Santa Clara, CA). The mass spectrum for each peak of interest was compared with a library, from Agilent Data Analysis software, of known spectral data for compound identification (Aglient Technologies, Inc. Santa Clara, CA). Identification of pinitol and L-gulonic acid γ-lactone were specifically confirmed by creating selective ion chromatograms to isolate their specific peaks.

For compound quantification, the sample was injected with a split of 10 mL/min and separated by Clarus 500 GC (Perkin Elmer Instruments, Shelton, CT) on a Rtx®-5 fused capillary column 30 m X 0.32 mm i.d. (Restek, Bellefonte, PA) with helium as the carrier gas with pressure-controlled flow set at 6.5 psi with a linear velocity of 1 mL/min. The injection port was set at 225°C, the oven was set on a gradient from 75°C to 274°C at 6.5C°/min, and the flame ionization detector was set at 280°C. Standard curves displaying peak area versus μg/mL were generated for Ins, AsA, L-gulonic acid γ-lactone, D/L-galactose, D-glucose, L-galactonic acid γ-lactone, and pinitol. Peak area was quantified by Totalchrom software (Perkin Elmer, Shelton, CT), adjusted based on recovery of the known internal standard, and converted to μg/ml based on the standard curves. The values were then converted to μg/g fresh weight based on the original sample weight. At least 3-5 independent replicates were averaged together to determine data points.

Western Blotting

Conditions have been previously reported (Burnette *et al*., 2003). Briefly, tissues were ground in liquid nitrogen, homogenized and resuspended with a pestle in SDS-bromophenol blue loading dye, boiled, and the supernatant was loaded onto a polyacrylamide gel for separation. SDS-PAGE was followed by Western blotting with a 1:20000 dilution of rabbit anti-MIOX antibody (provided by the Nessler lab from Cocalico Biologicals Inc., Reamstown, PA) or blotting with a 1:1000 dilution of rabbit anti-GFP antibody (Invitrogen Molecular Probes, Eugene, OR). A secondary goat, anti-rabbit horse radish peroxidase antibody (Bio-Rad Laboratories, Hercules, CA) was used at a 1:2000 dilution. Immunoreactive bands were detected using an ECL Plus Western Blotting Detection System (Amersham, Buckinghamshire, UK) and imaged with a Bio-Rad Gel-Doc system with Quantity One Software (Bio-Rad). Ponceau S staining of blots prior to antibody incubation was performed to ensure that equal amounts of extracts were analyzed.

GFP Fusion Construction and GFP Imaging

The 2255 bp genomic region of MIOX2, minus the stop codon, was amplified by high-fidelity PCR using Phusion polymerase (New England BioLabs, Ipswich,MA), confirmed by sequencing, cloned into the pENTR/D-TOPO vector (Invitrogen), and recombined via the Gateway system (Invitrogen) using the manufacturer's instructions into pK7FWG2. The resulting 35S cauliflower mosaic virus promoter:MIOX2:green fluorescent protein (GFP) construct was transformed into *Agrobacterium tumefaciens* by cold shock and was used in the transformation of *miox2-2* and WT plants as described (Bechtold *et al*., 1993). MIOX2:GFP and MIOX2:GFP/*miox2-2* seedlings were identified on 50 μg/mL kanamycin plates and by screening for GFP production using an Olympus SZX16 stereoscope equipped with fluorescence optics with an attached Olympus DP71 camera with DP Controller software (Olympus Corp., Japan). Two independent, complemented lines (MIOX2:GFP/*miox2-2* C14 and MIOX2:GFP/*miox2-2* F2) and two independent WT background lines (MIOX2:GFP M4 and MIOX2:GFP C9) with detectable GFP expression were used for subcellular localization.

The 948 bp coding region of MIOX4, minus the last two codons, was amplified by high-fidelity PCR using Phusion polymerase (New England BioLabs), confirmed by sequencing, cloned into the pENTR/D-TOPO vector (Invitrogen), and recombined via the Gateway system

(Invitrogen) using the manufacturer's instructions into pK7FWG2. The resulting 35S cauliflower mosaic virus promoter:MIOX4:GFP construct was transformed into *Agrobacterium tumefaciens* by cold shock and was used in the transformation of *miox4-2* and wild-type plants as described (Bechtold *et al*., 1993). MIOX4:GFP and MIOX4:GFP/*miox4-2* seedlings were identified on 50 μg/mL kanamycin plates and by screening for GFP production using the Olympus SZX16 stereoscope equipped with fluorescence optics. One complemented line (MIOX4:GFP/*miox4-2*) and one WT background line (MIOX4:GFP) with detectable GFP expression were used for subcellular localization.

Three to five-day-old seedlings were imaged utilizing an Axioimager with Axiovision software (Zeiss). Z-stack series of 15 to 20 1-μm sections were collected, and deconvolution with an iterative algorithm was applied. The resulting deconvolved images were reconstituted into a single image using the maximal intensity projection function of Axiovision. To visualize nuclei, seedlings were stained with 1 μg mL^{-1} DAPI (Molecular Probes) solution for 5 min, excess liquid was removed, and the seedlings were mounted in water. Photographs were taken with a Zeiss MC100 camera. GFP was imaged with a filter set consisting of an excitation filter of 540 to 580 nm, a dichroic mirror of 595 nm, and a barrier filter of 600 to 660 nm. DAPI staining was visualized with a standard UV fluorescence filter set. For plasmolysis experiments, seedlings were floated in 800 or 1000 mM NaCl for 15 minutes, followed by imaging.

RESULTS

MIOX Expression Patterns

To examine the spatial and temporal expression of MIOX2 and MIOX4 within tissues, I obtained MIOX2p:GUS and MIOX4p:GUS seed from the Tenhaken lab (Kanter *et al*., 2005). Because there are reported changes in expression of MIOX2 and MIOX4 dependent on nutrient conditions (Gibon *et al*., 2006; Baena-Gonzalez *et al*., 2007), I carefully examined seedlings grown on various nutrient conditions. The seeds were surface-sterilized and grown on soil or on "no" (agar), "low" (agar + 0.5 x MS salts), and "optimal" (agar+ 0.5 x MS salts + 3% glucose) nutrient conditions. Whole seedlings were removed at 5-7 days from the plates and tissues were harvested at appropriate times, incubated with GUS stain, and then cleared of chlorophyll with subsequent ethanol extractions.

MIOX2p:GUS seedlings showed intense staining, indicative of high expression, in the cotyledons and root, especially in the vascular cylinder and the root tip, in the no nutrient conditions (Figure 3). When given low nutrients, the intensity of MIOX2p:GUS staining decreases, with moderate expression present in the cotyledons and root (Figure 3). When grown with optimal nutrients, MIOX2p:GUS seedlings have greatly decreased expression, with staining restricted mostly to the primary root and lateral roots (Figure 4). Thus, the presence of nutrients represses MIOX2 gene expression in seedlings. In later stages of development, the MIOX2p:GUS construct directs expression in the anthers, developing seeds within the pistil, on the stigmatic surface, and in stipules found in the rosette, and no staining was observed in mature leaves (Figure 5-6).

MIOX4p:GUS plants were also examined under these conditions. There was no obvious staining in the MIOX4p:GUS seedlings grown in the no nutrient conditions (Figure 3). However, when given low nutrients, the MIOX4p:GUS construct directs low level expression in the cotyledons and in the root vascular cylinder (Figure 3). With optimal nutrient conditions, MIOX4p:GUS seedlings show staining only in the end of the primary root, with no staining in the quiescent zone, and staining in the root cap (Figure 4). In later stages of development, there is high expression of GUS in the sepals, young petals, anthers, and top of the pistil, and in stipules found in the rosette (Figure 5-6). As was the case with MIOX2, there was no expression of MIOX4 in mature leaves (Figure 6).

Overall, I conclude that the regulation of MIOX2 and MIOX4 expression in various nutrient conditions is different. MIOX2 is highly expressed in no nutrient condition, while MIOX4 expression is off (Figure 3). In low nutrient conditions, the expression patterns look similar; however, MIOX4 expression is less intense (Figure 3). Given optimal nutrients, both MIOX2 and MIOX4 promoters are turned off in the cotyledons; however, MIOX2 is still expressed along the primary root (Figure 4), while MIOX4 expression is only detectable in the root tip (Figure 4). There are some differing expression patterns in older tissues as well. Both genes are expressed in male and female organs; however, MIOX4 staining indicates expression in all the floral whorls, including sepals, petals, stamen, and carpal, while MIOX2 is only detectable in the inner two whorls. Both MIOX2 and MIOX4 expression is seen in an emerging meristematic tissue, the stipules, yet neither is detectable in mature leaves.

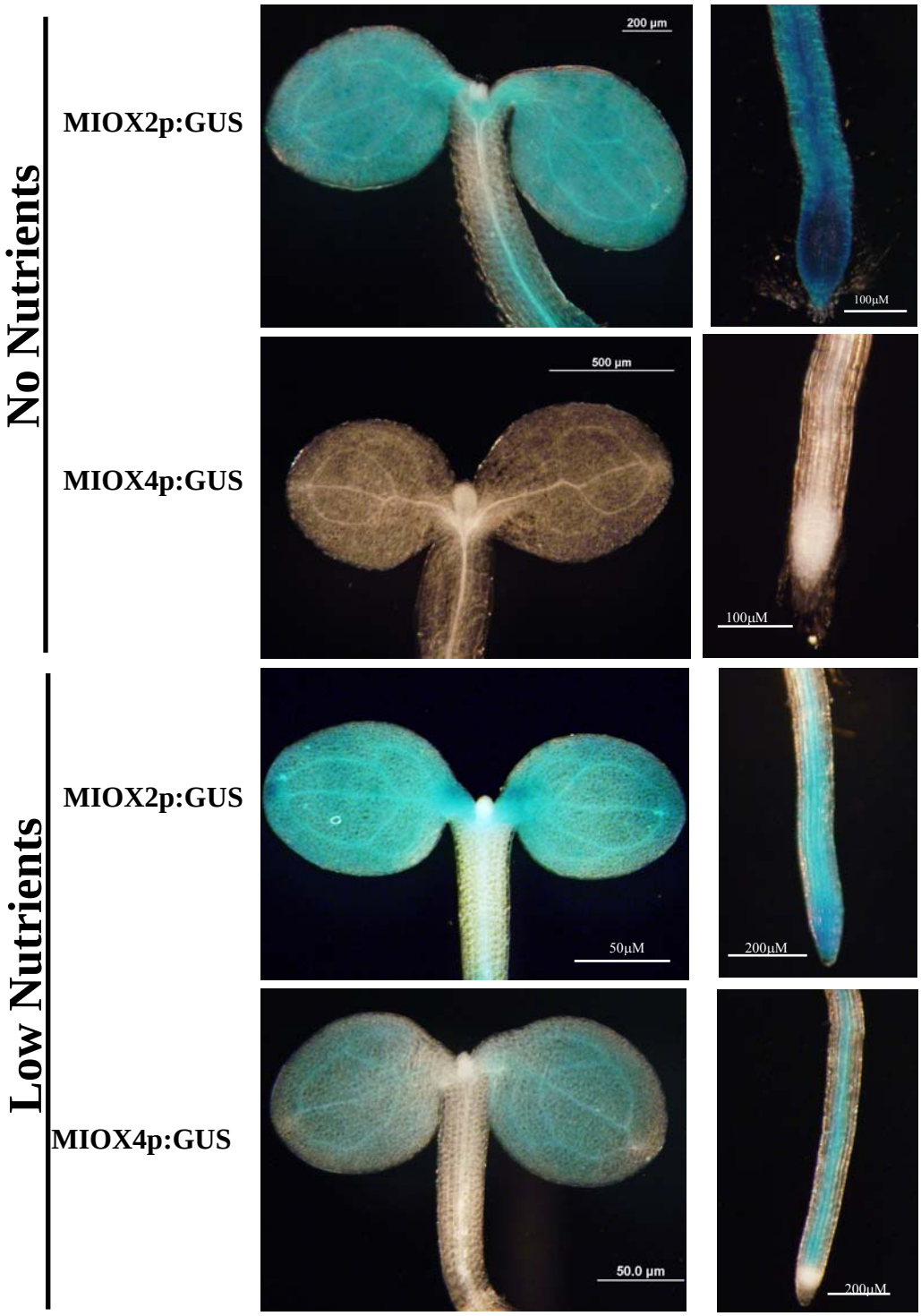

Figure 3. Promoter Analysis with MIOXp:GUS Seedlings on No and Low Nutrients. WT, MIOX2p:GUS, and MIOX4p:GUS 5-7 day-old seedlings were grown on no nutrient (upper) or low nutrient (lower) conditions, stained for GUS expression, and examined. Pictures are representative of staining patterns observed in 5-10 seedlings for each condition. WT samples showed no staining.

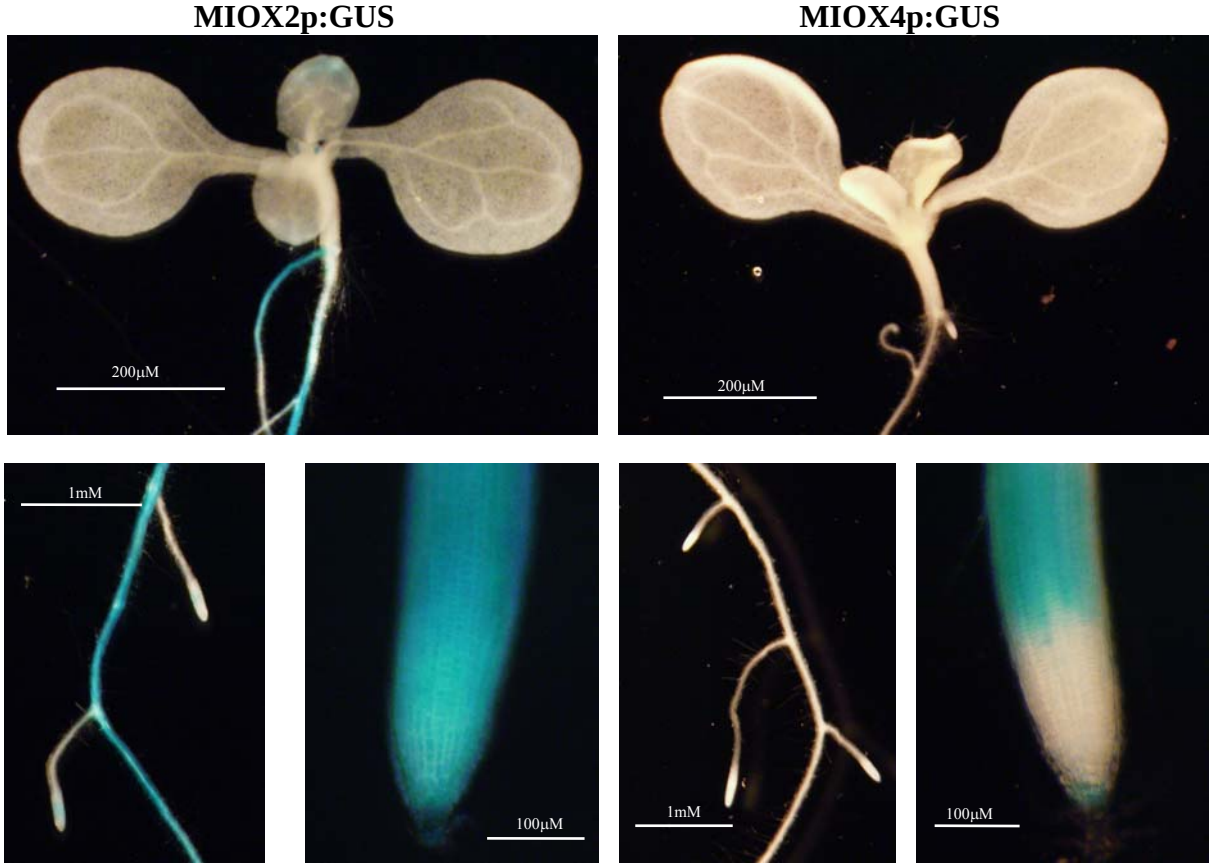

Figure 4. Promoter Analysis with MIOXp:GUS Seedlings on Optimal Nutrients. WT, MIOX2p:GUS (left) , and MIOX4p:GUS (right) 5-7 day-old seedlings were grown on optimal nutrient conditions, stained for GUS expression, and examined. Pictures are representative of staining patterns observed in 5-10 seedlings for each condition. WT samples showed no staining.

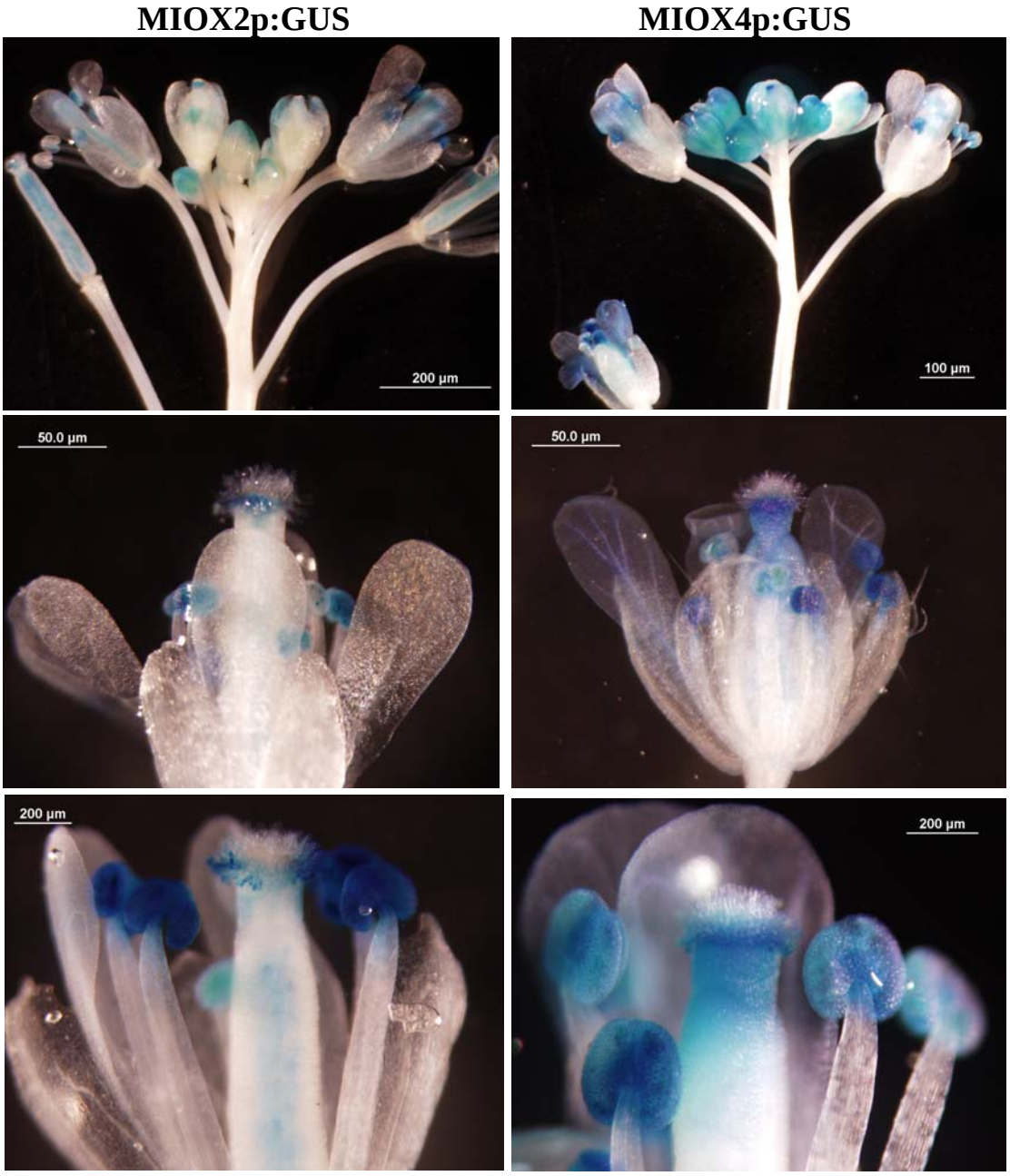

Figure 5. Promoter Analysis with MIOXp:GUS Flowers. WT, MIOX2p:GUS (left) , and MIOX4p:GUS (right) floral structures were stained for GUS expression, and examined. Pictures are representative of staining patterns observed in approximately 5 floral clusters. WT samples showed no staining.

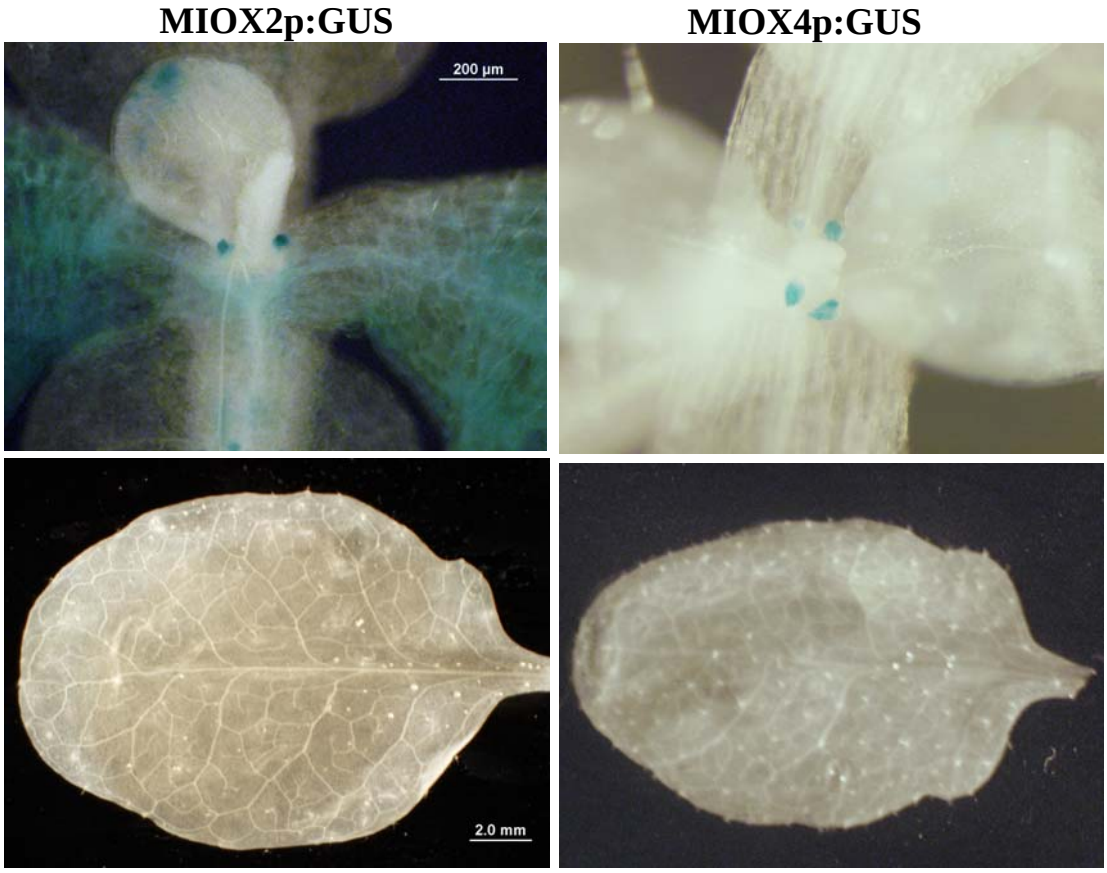

Figure 6. Promoter Analysis with MIOXp:GUS Tissues. WT, MIOX2p:GUS (left) , and MIOX4p:GUS (right) tissues were stained for GUS expression, and examined. Pictures are representative of staining patterns observed in 5-10 samples. WT samples showed no staining.

Identification of miox2 and miox4 Mutant Lines

To determine the physiological function of the MIOX2 and MIOX4 genes, I isolated T-DNA insertion mutants for these genes from the Salk collection (Alonso *et al*., 2003). Two putative T-DNA mutant lines for each gene were obtained from the Arabidopsis Biological Resource Center, and named *miox2-1* (SALK_002569), *miox2-2* (SALK_040608), *miox4-1* (SALK_018395), and *miox4-2* (SALK_027238). The T-DNA insertions in the MIOX2 gene were confirmed by PCR using a T-DNA left border primer and MIOX2 gene-specific primers (*2-1for* and *2-1rev*), resulting in the amplification of a 1050 bp fragment in *miox2-1* mutants (Figure 7A, upper). Using a T-DNA left border primer and MIOX2 gene-specific primers (*2-2for* and *2-2rev*), amplification resulted in an 873 bp fragment in *miox2-2* mutants (Figure 7A, upper). Sequencing of the amplified fragments showed that the T-DNA insertions were in the 3'UTR for *miox2-1* and in the sixth exon for *miox2-2* (Figure 7A, upper). The T-DNA insertions in the MIOX4 gene were confirmed by PCR using a T-DNA left border primer and MIOX4 gene-specific primers (*4-1for* and *4-1rev*), resulting in the amplification of a 635 bp fragment in *miox4-1* mutants (Figure 7A, lower). Using a T-DNA left border primer and MIOX4 gene-specific primers (*4-2for* and *4-2rev*), amplification resulted in two fragments, 697 bp and 1101 bp, in *miox4-2* mutants (Figure 7A, lower). Sequencing of the amplified fragments showed that the T-DNA insertions were in the third intron for *miox4-1* and a tandem insertion in the 5'UTR for *miox4-2* (Figure 7A, lower).

To verify the decrease or lack of expression in *miox2* and *miox4* homozygous mutant lines, I examined RNA levels in the mutant lines compared to WT levels. I used RNA isolated from leaves and flowers, for MIOX2 and MIOX4 analysis, respectively, and semi-quantitative RT-PCR to determine whether *miox2* and *miox4* mutants retained expression. Primers specific for an Actin gene (ACT8) were used as a positive control. Using primers specific for MIOX2 (*2-2for* and *2cDNArev*), I detected a 780 bp PCR product corresponding to MIOX2 in WT leaves and small amounts of this product in the *miox2-1* and *miox2-2* mutants (Figure 7B, left). Using primers specific for MIOX4 (*4-1for* and *4-1rev*), I detected a 954 bp PCR product corresponding to MIOX4 in WT flowers and very small amounts of this product in the *miox4-1*; however, this PCR product was not detectable in *miox4-2* mutants (Figure 7B, right). I conclude that the *miox2* mutants have reduced MIOX2 expression, the *miox4-1* mutant has greatly reduced MIOX4 expression, and the *miox4-2* mutant is totally lacking in MIOX4 expression. From these

analyses, I conclude that these mutants are suitable for examining the consequences of eliminating or reducing MIOX2 or MIOX4 expression. Under standard laboratory conditions, *miox2* and *miox4* mutants exhibited normal growth and development except for alterations in flowering (described on page 62).

It should be noted that I also obtained eight other lines of seeds from the Salk collection for two T-DNA insertional mutations within MIOX1 and MIOX2 genes and four T-DNA insertional mutations in MIOX5. These additional eight lines were screened by PCR with gene specific and T-DNA specific primers, as described previously. In total I screened twelve T-DNA lines, and I identified two independent homozygous mutant lines for each of the four MIOX genes in Arabidopsis. Expression levels were measured for each of the eight mutant lines by RT-PCR, four of which were described above. Expression levels of MIOX1 and MIOX5 in homozygous T-DNA lines are not reduced in leaves and flowers, respectively (data not shown). Because of the complexity of this gene family and the availability of transcriptional mutants, I have focused on *miox2* and *miox4* mutants.

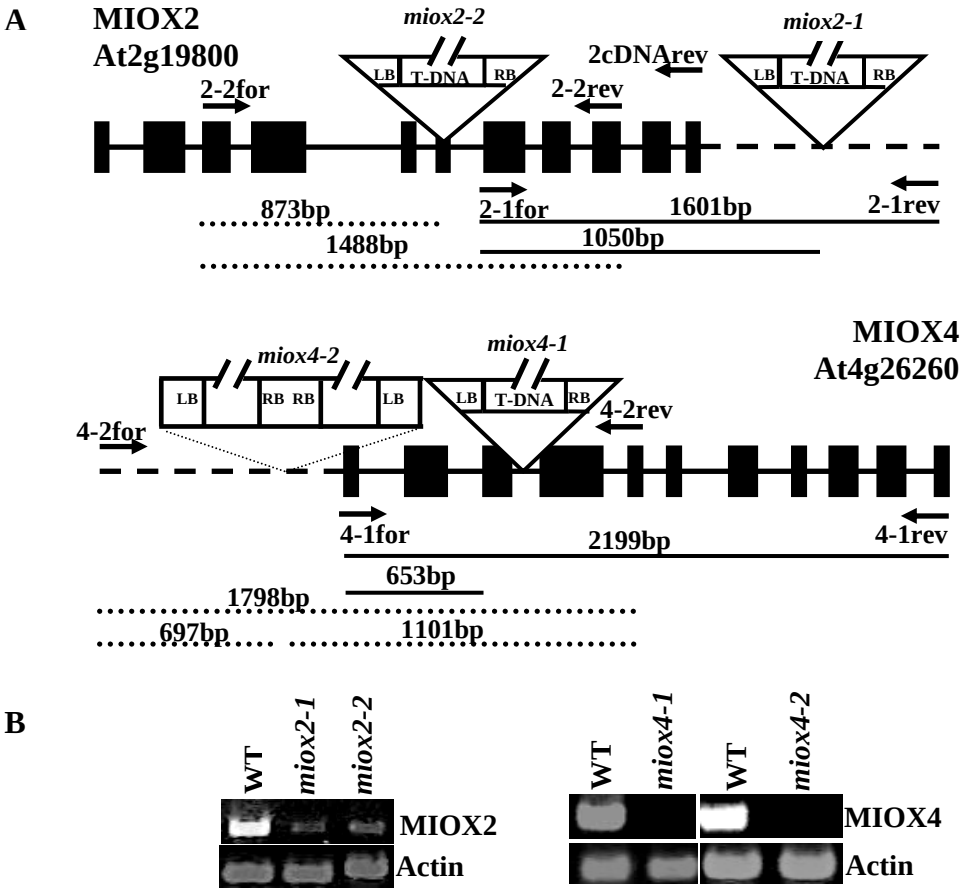

Figure 7. Characterization of MIOX2 and MIOX4 T-DNA Insertional Mutants. A) MIOX2 (upper) and MIOX4 (lower) gene maps showing locations of T-DNA insertions. Black boxes represent exons, black lines represent introns, dashed lines represent UTR. LB: T-DNA left border, RB: T-DNA right border. Arrows indicate primers. The regions of MIOX2/4 genes amplified by PCR for *miox2-1*/*miox4-1* insertions are indicated by solid lines, and the regions of MIOX2/4 genes amplified by PCR for *miox2-2*/*miox4-2* insertions are indicated by dotted lines. **B**) RT-PCR analysis of MIOX2 and MIOX4 transcript in WT, *miox2* (left panel), and *miox4* (right panel) mutant tissues. Actin transcript analysis was a control. Primer sequences can be found in "Materials and Methods."

Nutrient Sensitivity of miox Mutant Roots

To determine whether MIOX2 or MIOX4 impact growth under various nutrient conditions, I performed root length assays in the presence of no nutrients and added nutrients, which are the conditions used for promoter GUS analysis. WT, *miox2-1*, *miox2-2, miox4-1,* and *miox4-2* seed were grown on agar medium containing no, low and optimal nutrients and examined for root elongation for up to 9 days.

When *miox2* mutants are grown on no nutrients, root growth is increased as compared to WT (Figure 20A, left). The *miox2* roots grew longer (*miox2-1*) or approximately the same (*miox2-2*) as WT roots on low nutrients (Figure 20B, left). In contrast, the *miox2* roots grew shorter on optimal nutrients as compared to WT roots (Figure 20C), suggesting that reduced expression of MIOX2 results in nutrient level sensitivity during root elongation. These responses are similar to the response of the SnRK1.1 overexpresser recently described by Sheen's group (Baena-Gonzalez *et al*., 2007). This group speculates that the SnRK1.1 nutrient and stress sensor turns on genes required to adapt to low nutrients which provides a growth advantage under low nutrients and a disadvantage under high nutrients.

Upon measuring *miox4* mutant roots, I observed a decrease in growth on no nutrients as compared to WT roots (Figure 20A, right). In contrast, when grown on low nutrients, *miox4* roots grew longer as compared to WT roots (Figure 20B, right). The *miox4* roots grew shorter on optimal nutrients as compared to WT roots (Figure 20C); however, the differences were diminished over time. I conclude that *miox4* mutants have altered growth under various nutrient conditions. The *miox2* and *miox4* mutants show opposite phenotypes when grown on no nutrient conditions; however, they show the same root growth responses to low and optimal conditions. Taken together with expression data (Figures 3-4 & 7), I conclude that in conditions when expression is induced for MIOX2 and MIOX4, native MIOX2 and MIOX4 function to suppress root elongation, which manifests in longer roots in the corresponding mutant.

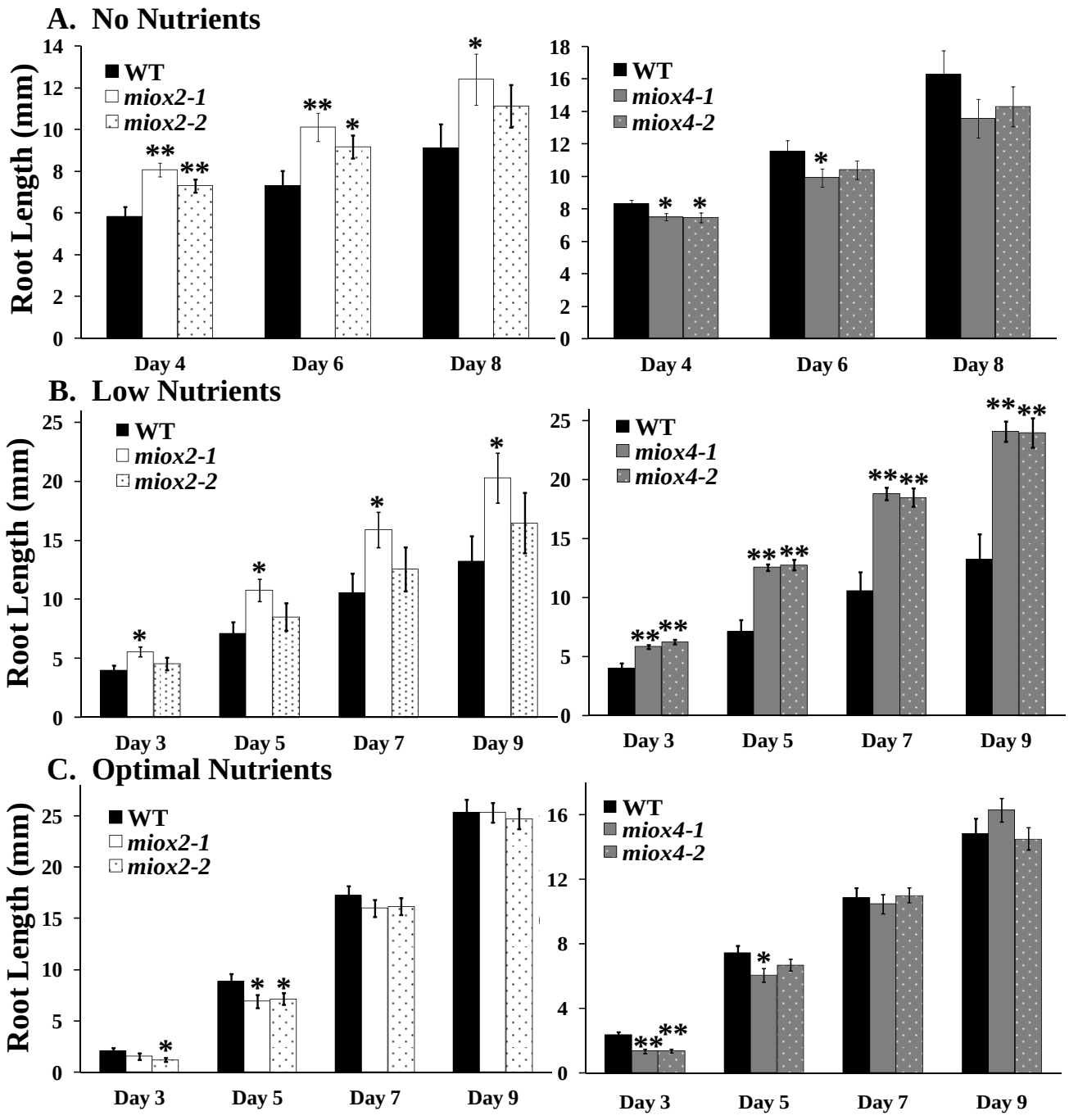

Figure 8. Root Growth in Different Nutrient Conditions. WT and mutant seeds were surface-sterilized, placed on agar with different nutrients **A)** no nutrients containing water + agar, **B)** low nutrients containing 0.5x MS salts + agar, and **C)** optimal nutrients containing 0.5x MS salts + 3% glucose + agar, stratified for 3d at 4°C, then placed at room temperature under long-day conditions. Root length was measured every other day. Bars represent the mean ±SE where n=3-5, with each replicate containing 10-15 seedlings. ** indicates p-value ≤0.005, and * indicates p-value ≤0.05.

Flowering Time of miox Mutant Plants

Flowering time alterations were also observed during growth of *miox* mutant plants under normal laboratory conditions. To investigate the observed change in flowering time in *miox* mutant plants, I performed flowering time assays. WT, *miox2-1*, *miox2-2*, *miox4-1*, and *miox4-2* seeds were sowed on pre-wetted soil in pots, and, after stratification for 3 days at 4^{o} C in the dark, pots were moved to long-day conditions and allowed to grow to flowering. Rosette leaves were counted upon appearance of the inflorescence tissue. The *miox2-1* and *miox2-2* plants were found to have more rosette leaves upon inflorescence initiation than WT when grown under long-day conditions (Figure 9A left and B upper), but no difference was observed when plants were grown under short-day conditions (data not shown). The *miox4-1* and *miox4-2* plants were found to have fewer rosette leaves upon inflorescence initiation than WT when grown under long-day conditions (Figure 9A right and B lower). The *miox4-1* plants were also observed to have fewer rosette leaves than WT when grown under short-day conditions (Figure 9C). The *miox2* mutant plants were also examined under short-day conditions, but the data were inconclusive. I conclude that reduced expression of MIOX2 results in delayed flowering time under long-day conditions, and reduced expression of MIOX4 results in earlier flowering time. These opposing flowering time phenotypes are likely the result of different metabolic states of the *miox2* and *miox4* mutants and different expression patterns of MIOX2 versus MIOX4.

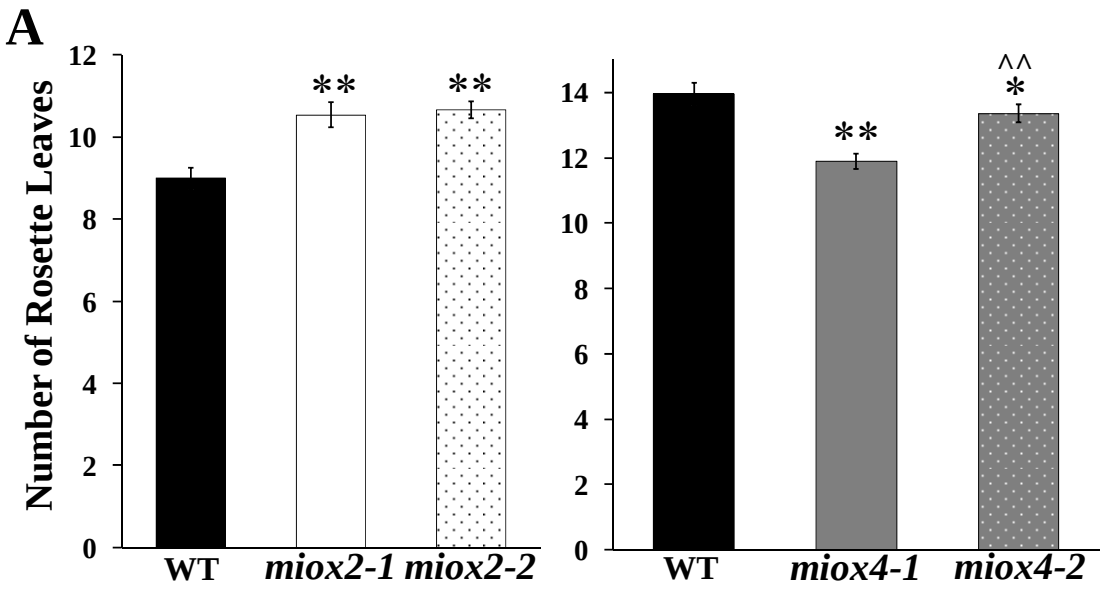
A
Number of Rosette Leaves
12
10
8
6
4
2
0
**
**
WT
miox2-1
miox2-2
14
12
10
8
6
4
2
0
**
^^
*
WT
miox4-1
miox4-2

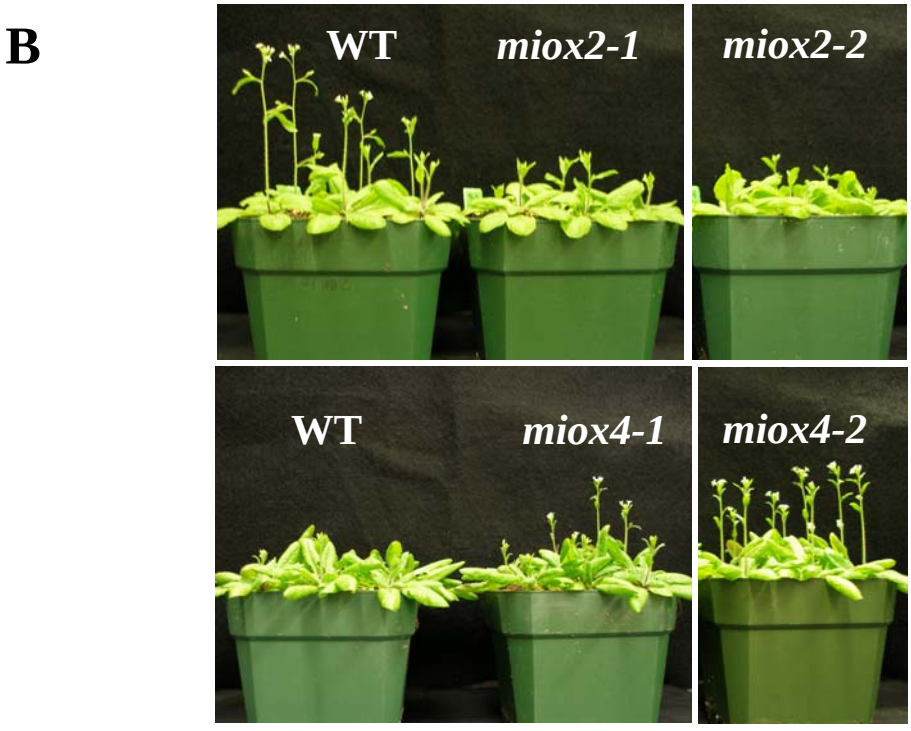
B
WT
miox2-1
miox2-2
WT
miox4-1
miox4-2

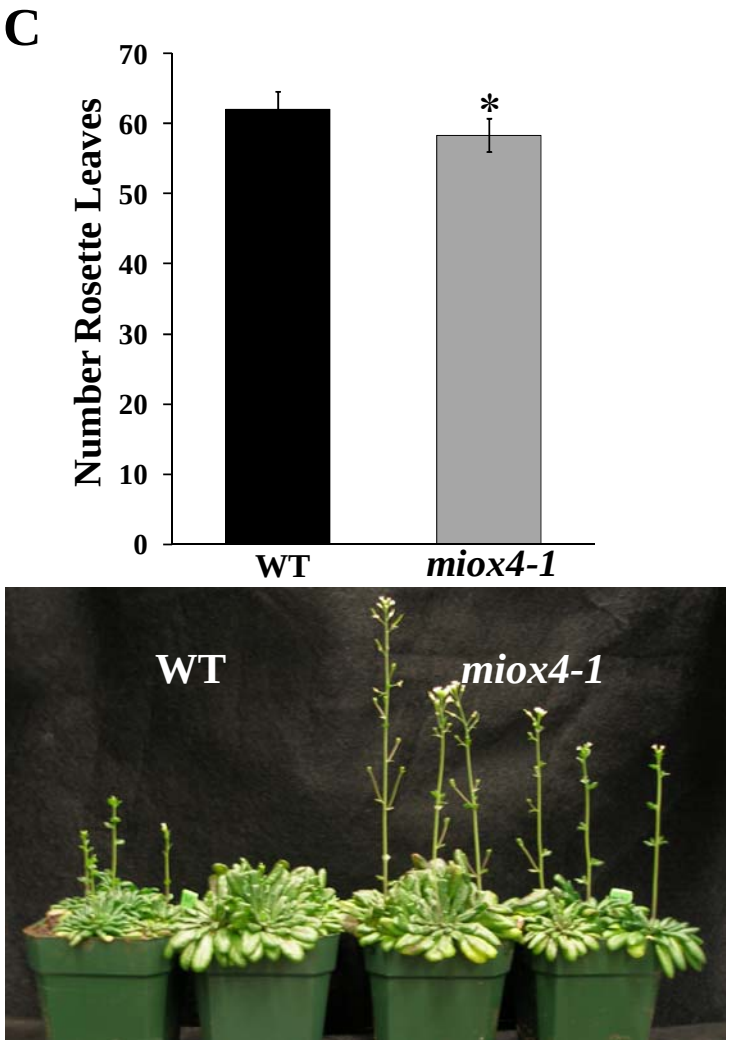

Figure 9. Comparison of *miox* Mutants in Flowering Time. WT, *miox2*, and *miox4* mutant seeds were sown on pre-wetted soil, stratified at 4°C for 3 days, and then placed in a growth chamber under **A-B)**long day (16hrs light) or **C)**short day (8 hrs light) conditions. Rosette leaves were counted. Values represent the mean ±SE where n=15-38 plants. ** indicates a p value < 0.0005, * indicates p-value ≤0.1, ^^ indicates p-value <0.0005 of *miox4-2* vs *miox4-1*.

Inositol Metabolite Profile of miox Mutant Plants

To determine how metabolism is perturbed in the *miox* mutants and to correlate the observed phenotypes with metabolic alterations, I quantified specific metabolites in the mutant plants. Metabolites of interest included the MIOX substrate, Ins, and product DGlcA and other known or hypothesized compounds in the AsA synthesis pathways (Wheeler *et al.*, 1998; Smirnoff *et al.*, 2001) (Michell, 2007, 2008), including, AsA, L-galactonic acid γ-lactone, D/L-galactose, and D-glucose (see Figure 1). Standard curves for each metabolite were generated using commercially available standards. Peaks within chromatograms were identified by comparison to the retention times of standards and by parallel GC/MS analysis. Peak areas were quantified from chromatograms and normalized to the amount of sample material and internal standards.

Regarding *miox2* mutants, I expected to see decreased Ins oxidation and further metabolic alterations, when compared to WT plants. I found an increase of Ins in seedlings, leaves, and flowers, but not in siliques of *miox2* mutants (Figure 10). Despite the increase in Ins in those tissues, there is no measurable change in DGlcA levels. There is a minor AsA decrease in *miox2-2* seedlings, and a minor increase in AsA in *miox2-1* leaves, but no other changes are evident in AsA levels. Levels of the AsA precursor, L-galactonic acid γ-lactone, are not especially altered in any tissue, with a minor increase in *miox2-2* leaves and minor decreases in siliques. There are some alterations in the two sugars examined, galactose and glucose. Galactose levels are increased in the *miox2-1* mutant seedlings and flowers and *miox2-2* flowers, while there is a small decrease in *miox2-2* seedlings and siliques. Glucose levels are decreased in *miox2* mutant seedlings and siliques and increased in *miox2* mutant leaves. From this metabolic analysis, I conclude that reduced expression of MIOX2 leads to a build-up of Ins and some other alterations in related metabolites, which suggests a reduction in oxidation of Ins.

Regarding *miox4* mutants, I expected to see increased Ins when metabolite levels were compared to WT levels. I found that the only substantial increase in Ins is within the *miox4* flowers (Figure 11). There are minor decreases in Ins in *miox4-1* seedlings and *miox4-2* leaves. There is a decrease in DGlcA in the *miox4-1* seedlings and minor increases in *miox4-1* leaves and siliques. AsA levels are essentially unchanged in the *miox4* mutants, except for an increase in *miox4-1* leaves. Levels of the AsA precursor, L-galactonic acid γ-lactone, are increased in *miox4-2* seedlings and *miox4-1* leaves, and levels are decreased in *miox4* flowers. Galactose

levels are virtually unchanged in all tissues except for a decrease in *miox4-2* leaves. In the case of glucose levels, there is a decrease in *miox4-1* seedlings, and there are statistically significant increases in *miox4-2* seedlings and siliques. Taking these *miox4* mutant data together, I conclude that reduced expression of MIOX4 leads to small perturbances in Ins oxidation, seen mostly in flowers and other alterations in related metabolites.

In addition to analyzing the *miox2* and *miox4* mutants by GC, I have analyzed metabolite profiles of MIOX2:GFP and MIOX4:GFP plants, described in the "Subcellular Localization" section. These GFP fusions are expressed under control of the 35S CaMV promoter, and should function as overexpressers of MIOX2 and MIOX4.

In MIOX2:GFP plants, there are decreased Ins levels in all tissues examined, increased DGlcA in all tissues except seedlings, and increased downstream product, AsA, in all tissues except seedlings (Figure 10). There is an increase in the AsA precursor, L-galactonic acid γ-lactone, in leaves. There is an increase in galactose in seedlings and siliques, but a sharp decrease in galactose in flowers. Glucose levels are decreased in all tissues, except leaves where there is an increase. These data indicate that the MIOX2:GFP fusion protein results in Ins decreases, DGlcA increases, and changes in other downstream metabolite levels, and strongly suggest that the MIOX2:GFP fusion protein is catalytically active.

I expected the MIOX4:GFP transgenic line to behave similarly to the MIOX4^{+} plants described in Chapter III, because they are both overexpressing the MIOX4 gene. The pattern of Ins levels in MIOX4:GFP plants is, in fact, very similar to MIOX4^{+} plants, in that there is an Ins decrease in seedlings and there are Ins increases in mature tissues (Figures 11& 22). There is a decrease in DGlcA in seedlings and an increase in siliques. There is a decrease in AsA levels in seedlings, and substantial increases in AsA in leaves, flowers, and siliques. L-galactonic acid γ-lactone levels follow a similar trend of AsA levels, in that there are increased levels in leaves, flowers, and siliques. There is a decrease of galactose in seedlings, but a sharp increase in flowers, which is opposite what I observed in MIOX2:GFP flowers. Finally, glucose levels are decreased in seedlings and increased in siliques, a finding similar to the MIOX4^{+} glucose levels. These data indicate that the MIOX4:GFP fusion protein is likely to be catalytically active as its presence results in Ins decreases and product increases.

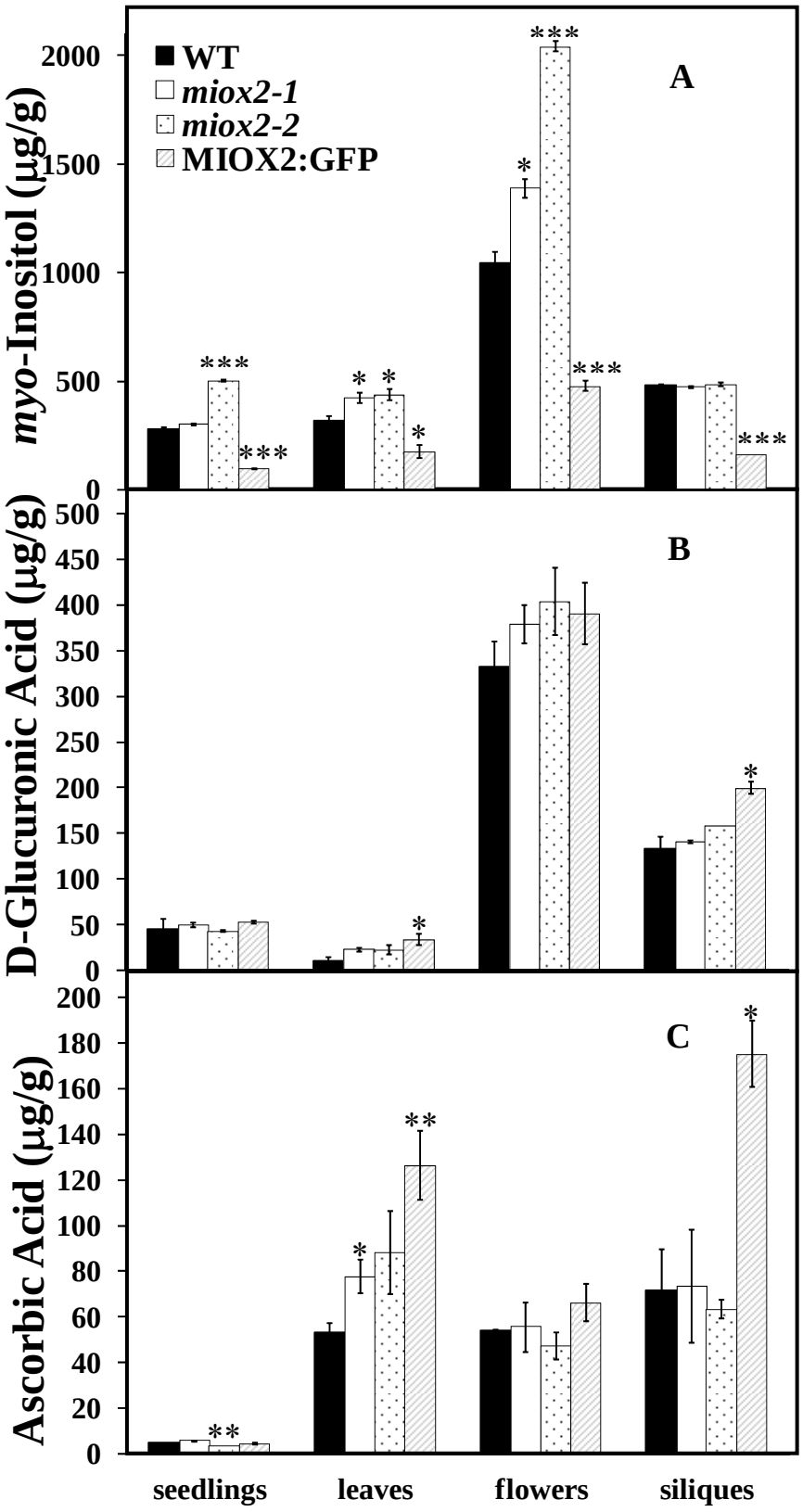
WT
miox2-1
miox2-2
MIOX2:GFP
A
B
C
myo-Inositol (µg/g)
D-Glucuronic Acid (µg/g)
Ascorbic Acid (µg/g)
2000
1500
1000
500
0
450
400
350
300
250
200
150
100
50
180
160
140
120
80
60
40
20
seedlings
leaves
flowers
siliques

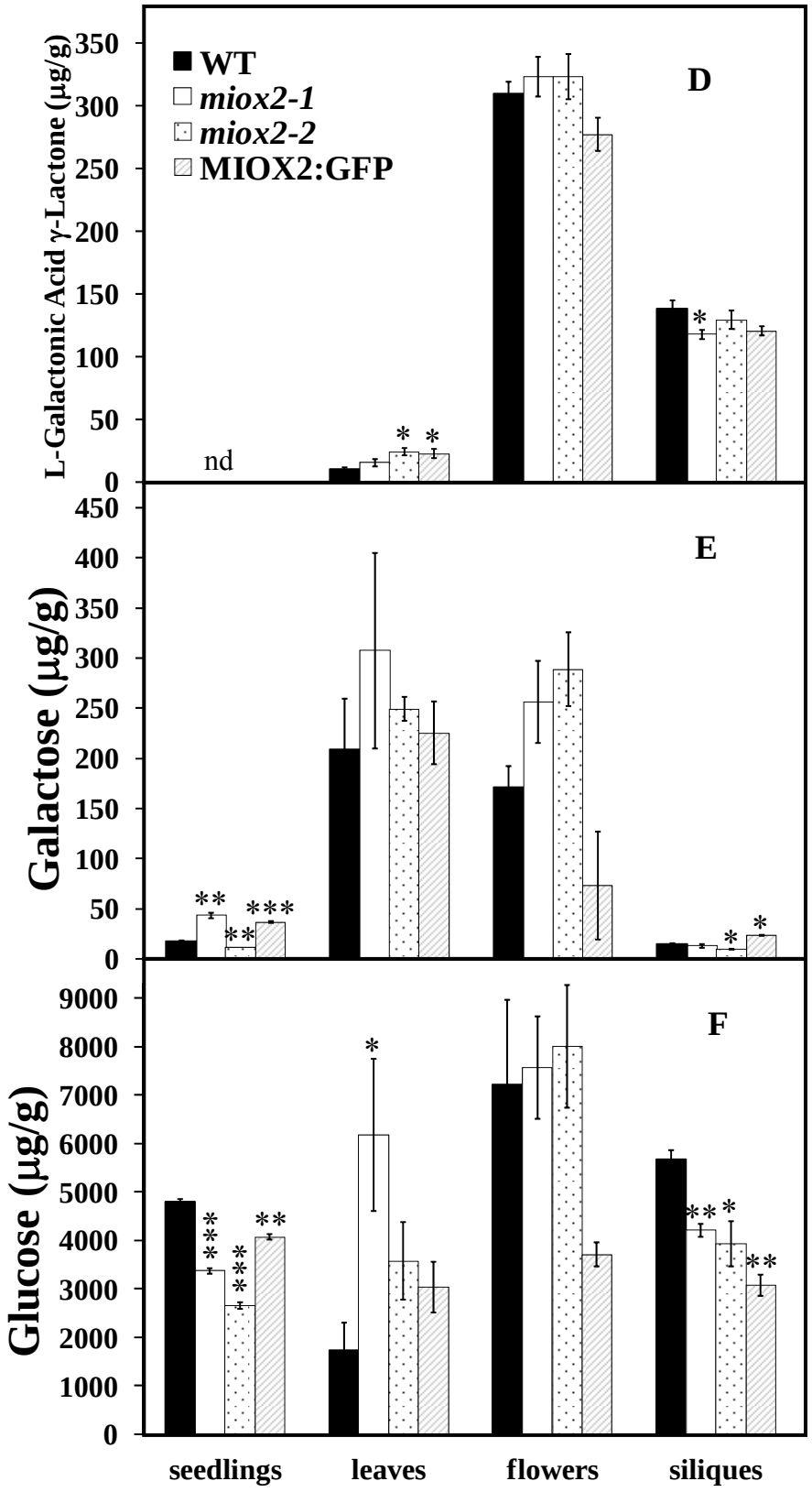
WT
miox2-1
miox2-2
MIOX2:GFP
D
E
F
L-Galactonic Acid γ-Lactone (μg/g)
Galactose (μg/g)
Glucose (μg/g)
nd
seedlings
leaves
flowers
siliques

Figure 10. Metabolite Levels of WT, *miox2* Mutant, and MIOX2:GFP Tissues. Tissues were harvested, ground in liquid nitrogen, extracted, reduced, derivatized, and analyzed by GC. Amounts are given in μg/g fresh tissue. **A)** Ins, **B)** DGlcA, **C)** AsA, **D)** L-galactonic acid γ-lactone, **E)** galactose, and **F)** glucose were measured by GC for WT, *miox2* mutants, and MIOX2:GFP lines. Bars represent the mean ±SE where n=3-5 independent, biological replicates, with each seedling replicate containing hundreds of 5-day-old seedlings, each leaf replicate contained 3-5 6-wk-old leaves, each flower replicate contained 50-100 open flowers, and each silique replicate contained 30-50 green, elongated siliques. *** indicates p-value ≤0.0005,** indicates p-value ≤0.005, and * indicates p-value ≤0.05 as compared to WT. "nd" represents values below detectable limits.

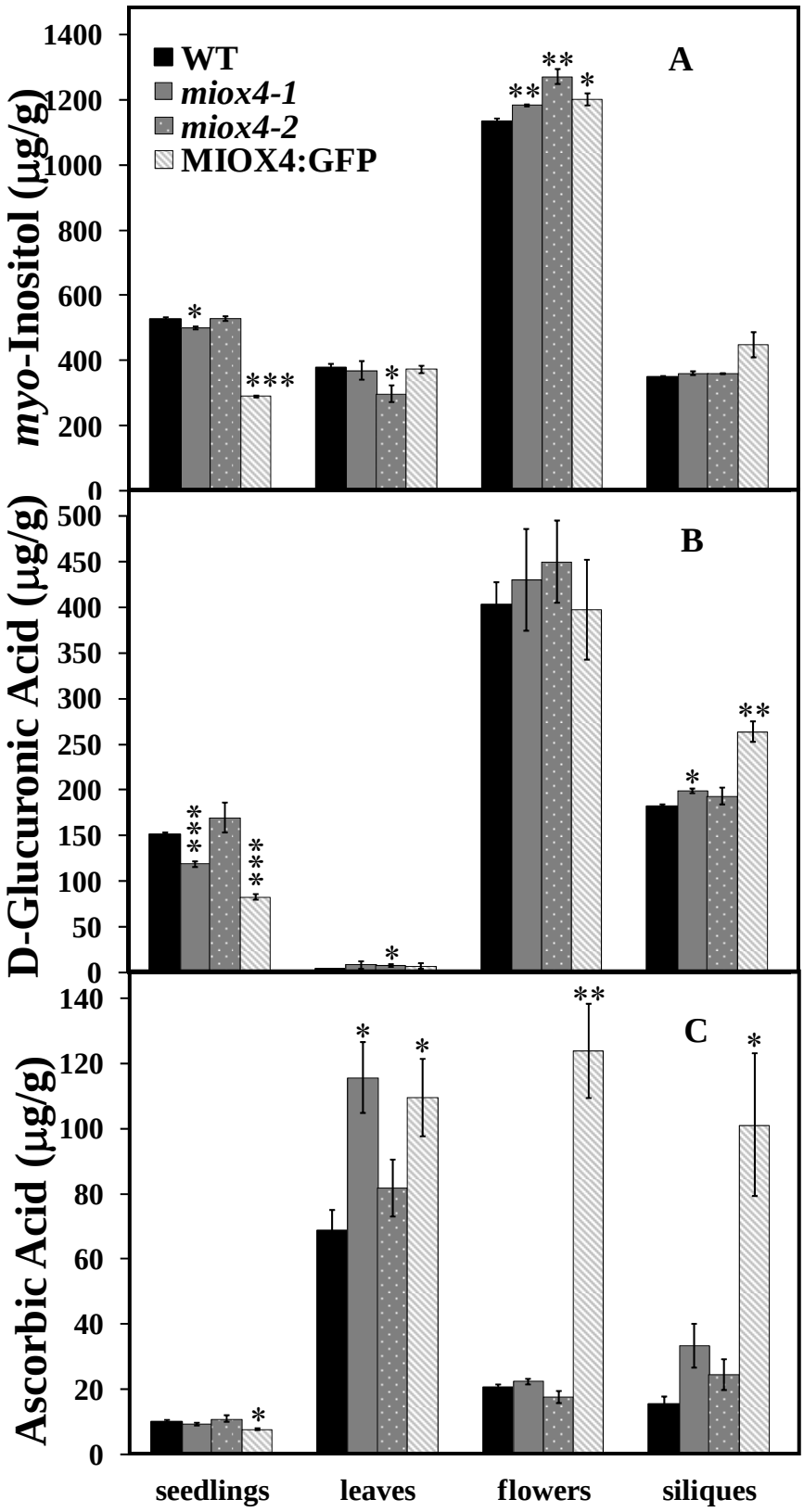
WT
miox4-1
miox4-2
MIOX4:GFP
A
B
C
myo-Inositol (µg/g)
D-Glucuronic Acid (µg/g)
Ascorbic Acid (µg/g)
seedlings
leaves
flowers
siliques

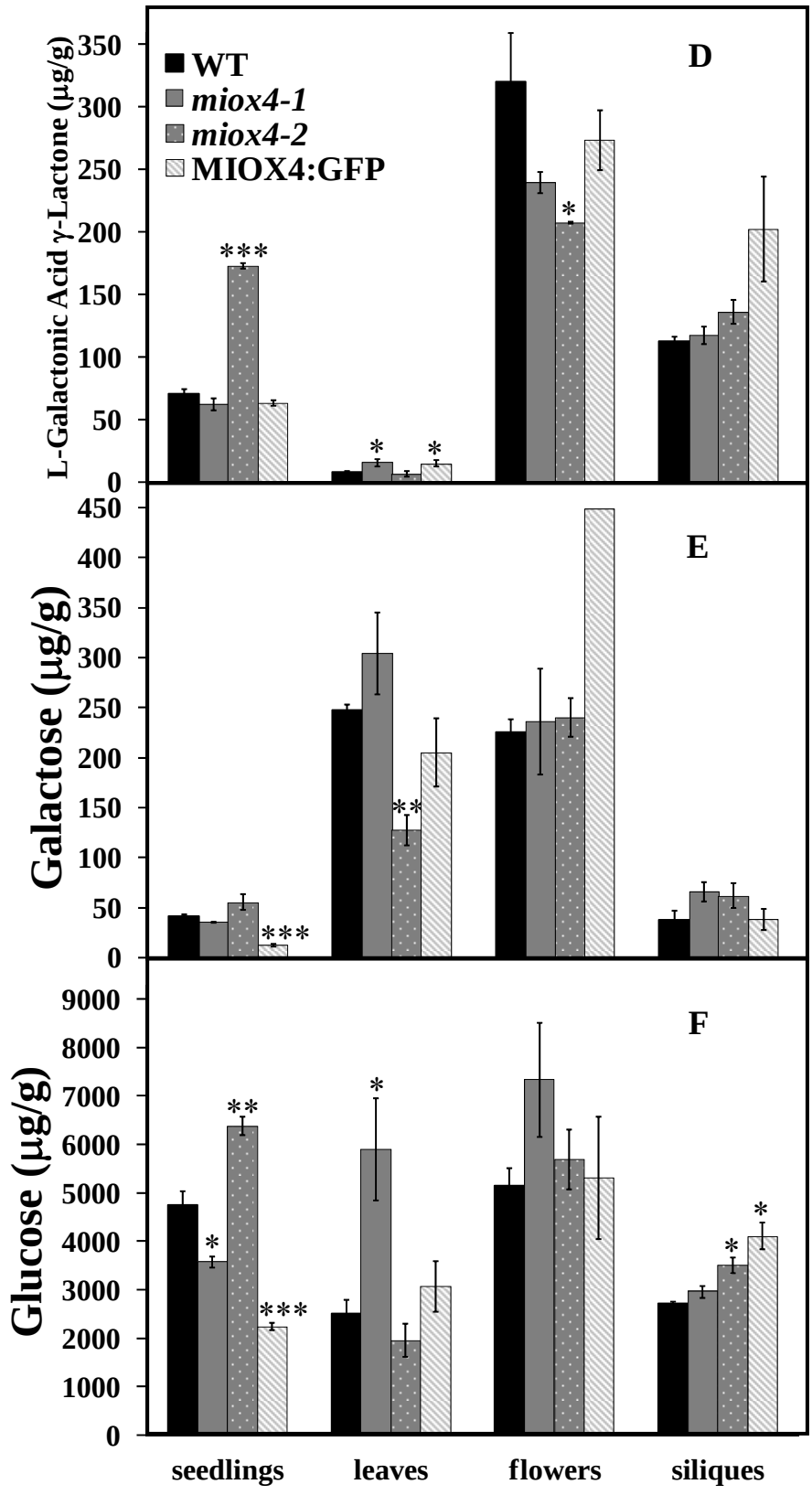
WT
miox4-1
miox4-2
MIOX4:GFP
D
E
F
L-Galactonic Acid γ-Lactone (μg/g)
Galactose (μg/g)
Glucose (μg/g)
seedlings
leaves
flowers
siliques

Figure 11. Metabolite Levels of WT, *miox4* Mutant, and MIOX4:GFP Tissues. Tissues were harvested, ground in liquid nitrogen, extracted, reduced, derivatized, and analyzed by GC. Amounts are given in μg/g fresh tissue. **A)** Ins, **B)** DGlcA, **C)** AsA, **D)** L-galactonic acid γ-lactone, **E)** galactose, and **F)** glucose were measured by GC for WT, *miox4* mutants, and MIOX4:GFP lines. Bars represent the mean ±SE where n=3-5 independent, biological replicates, with each seedling replicate containing hundreds of 5-day-old seedlings, each leaf replicate contained 3-5 6-wk-old leaves, each flower replicate contained 50-100 open flowers, and each silique replicate contained 30-50 green, elongated siliques. *** indicates p-value ≤0.0005,** indicates p-value ≤0.005, and * indicates p-value ≤0.05 as compared to WT.

Response of miox Mutants to Abscisic Acid

MIOX2 expression is down-regulated in response to several conditions of stress, including ABA, salt, and cold, suggesting certain stresses may alter Ins metabolism resulting in a decrease in Ins oxidation (Zimmermann *et al*., 2004). This decrease in oxidation could result in more available Ins that could be used for Ins(1,4,5)P_3 signaling. Many studies have linked Ins(1,4,5)P_3 accumulation in plants with ABA sensitivity. ABA application to seedlings induces a transient increase in Ins(1,4,5)P_3, indicated in Figure 1 by ABA stimulation of phospholipase C, and changes in Ins(1,4,5)P_3 have been correlated with altered ABA sensitivity in seed germination and stomatal closure assays (Gilroy *et al*., 1990; Burnette *et al*., 2003). For example, *5ptase* mutants containing elevated Ins(1,4,5)P_3 are ABA hypersensitive (Gunesekera *et al*., 2007), while seed overexpressing the At5PTase2 gene contain reduced Ins(1,4,5)P_3 and are ABA-insensitive in seed germination assays (Sanchez and Chua, 2001). My data with MIOX4$^+$ seedlings, reported in Chapter III, shows the same trend in decreased Ins(1,4,5)P_3 levels and resulting ABA-insensitivity (Figures 23 & 27). To determine whether the increased Ins levels present in *miox* mutants alters ABA sensitivity, we performed seed germination assays in the presence of ABA.

I produced age-matched seed populations that were harvested from WT, *miox2-1*, *miox2-2, miox4-1, and miox4-2* plants grown at the same time under identical conditions and plated these seed on 0.5xMS medium containing 0 and 2 μM ABA. After stratification for 3 days at 4^o C in the dark, plates were moved to continuous light and examined for radicle protrusion from the seed coat (germination) after 3 days. The *miox2* mutant seeds were more sensitive to 2μM ABA, germinating slower, as compared to WT seeds (Figure 12A). I also compared the time course for germination of *miox2* seed in the presence of 2μM ABA and found that this ABA sensitivity continued over the course of 7 days (Figure 12B). I conclude that reduced expression of MIOX2 results in ABA-sensitivity during seed germination.

The *miox4-1* and *miox4-2* seeds were insensitive to ABA, germinating faster, as compared to WT seeds (Figure 12A). I also compared the time course for germination of *miox4* seed in the presence of 2μM ABA and found that this ABA insensitivity continued over the course of 7 days (Figure 12C). I conclude that reduced expression of MIOX4 results in ABA-insensitivity during seed germination.

Taking these data together, I observe opposite phenotypes of *miox2* and *miox4* seeds in ABA germination assays where *miox2* mutants are sensitive to ABA and *miox4* mutants are insensitive to ABA. This difference in germination suggests that MIOX2 and MIOX4 could differentially impact Ins(1,4,5)P_3 signaling, specifically in the ABA response.

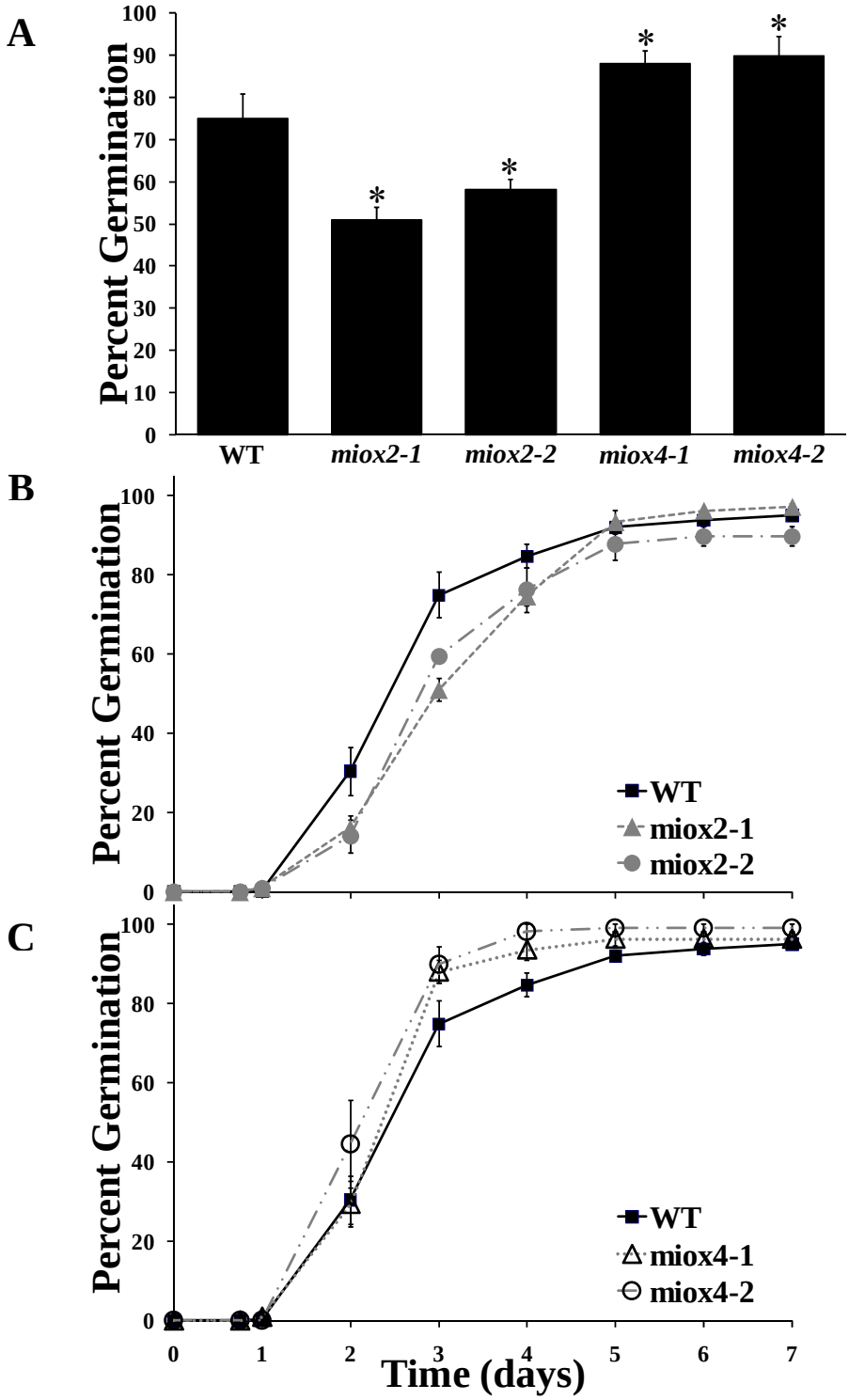

Figure 12. Examination of ABA Sensitivity of *miox* Mutant Seeds. WT and *miox* mutant seeds were surface sterilized and plated on 0.5x MS agar medium with ABA. Seeds were stratified at 4°C for 3 days then placed at 23°C under continuous light. Germination was scored daily for 7 days. **A)** Germination was measured at day 3 on 2μM ABA. **B)** Germination of WT

and *miox2* mutant seeds and **C)** WT and *miox4* mutant seeds on 2μM ABA over 7 days is shown. Values represent the mean ± SE of three replicates where seed # is ~50 per variant. * indicates p-value ≤0.05.

Response of miox2 Mutants to NaCl and Cold

To determine whether the increase of Ins in *miox2* mutant plants has an affect on Ins(1,4,5)P_3 signaling via stimuli other than ABA, I performed root length assays in the presence of NaCl and germination assays in the cold. WT, *miox2-1*, and *miox2-2* seed were plated on 0.5xMS medium. Solutions of 0, 50, and 100mM NaCl were added to the medium for root length assays. After stratification for 3 days at 4^{o} C in the dark, plates were moved to long-day conditions and examined for root length for 14 days, or plates were moved to 4°C long-day conditions and examined for germination. The *miox2* roots grew longer on 100mM NaCl as compared to WT roots (Figure 13A-B). The *miox2-2* mutant seed germinated slower, thus were more sensitive to cold (Figure 13C). I conclude that reduced expression of MIOX2 results in salt insensitivity seen in root growth, and increased seed sensitivity to cold.

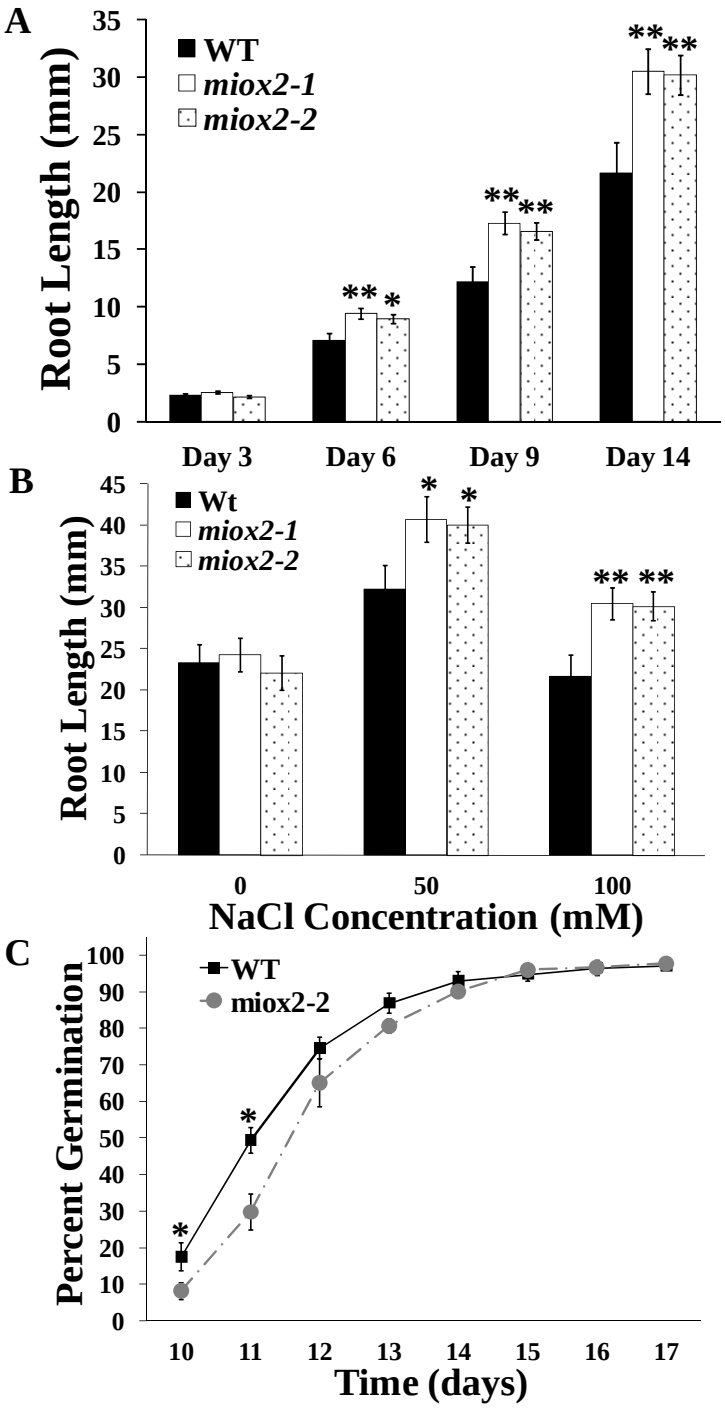

Figure 13. Examination of Salt and Cold Sensitivities of *miox2* Mutants. WT, *miox2-1*, and *miox2-2* seeds were surface-sterilized and plated on 0.5x MS agar medium. NaCl solutions were added for the root length assay. **A-B)** Seeds were stratified at 4°C for 3 days then placed at 23°C under long-day conditions and measured for 14 days. **A)** Root length on 100 mM NaCl is shown. **B)** Root length measured at Day 14 on 0, 50, and 100 mM NaCl is shown. Values represent the mean ± SE (n= 3 biological replicates, where each replicate contained 10 seedlings). **C)** Seeds were stratified at 4°C for 3 days then placed at 8°C under long-day

conditions. Values represent the mean ± SE (n= 3 biological replicates, where each replicate contained 50-60 seeds). * indicates a p-value <0.05 and ** indicates a p-value <0.005.

Complementation of miox2 and miox4 Mutants

To further address whether root length alterations and germination sensitivities of the mutants of *miox* mutants are due to loss of MIOX2 and MIOX4 expression, I expressed MIOX2:Green fluorescent protein (GFP) fusion protein under control of the 35S CaMV promoter in *miox2-2* mutants (MIOX2:GFP/*miox2-2* plants). I identified several lines of MIOX2:GFP/*miox2-2* plants and characterized one of these alongside WT and *miox2* mutants. A similar strategy was implemented to complement the *miox4* mutants. I expressed MIOX4:GFP fusion protein under control of the 35S CaMV promoter in *miox4-2* mutants (MIOX4:GFP/*miox4-2* plants). I identified several lines of MIOX4:GFP/*miox4-2* plants and characterized one of these alongside WT and *miox4* mutants.

To address germination phenotypes, age-matched seed populations, that were harvested from all MIOX2:GFP and MIOX4:GFP plants, were plated on 0.5xMS medium containing 0, and 2μM ABA. After stratification for 3 days at 4^{o} C in the dark, plates were moved to long-day conditions and examined for radicle protrusion from the seed coat (germination) for 7 days. MIOX2:GFP/ *miox2-2* seeds were as sensitive to 2 μM ABA as the *miox2* mutants (Figure 14A). MIOX4:GFP/ *miox4-2* seeds were as insensitive to 2 μM ABA as the *miox4* mutants (Figure 14A). I conclude that alterations in ABA-sensitivity cannot be complemented by the MIOX2:GFP or MIOX4:GFP constructs.

To address root growth phenotypes, age-matched seed populations that were harvested from all MIOX2 seed variants were plated on agar medium containing 0.5xMS agar medium + 3% glucose (optimal nutrients). After stratification for 3 days at 4^{o} C in the dark, plates were moved to long-day conditions and examined for root length for 9 days. The MIOX2:GFP/ *miox2-2* roots grew shorter on optimal nutrients as compared to WT and *miox2-2* roots (Figure 14B). I conclude that, under these conditions, root growth alterations of *miox2-2* seeds cannot be complemented by the MIOX2:GFP construct. However, the MIOX2:GFP/ *miox2-2* seedlings have reduced root growth under both conditions tested and might, therefore, impart a novel impact on seedling growth.

To further understand whether the complemented lines, MIOX2:GFP/ *miox2-2* and MIOX4:GFP/ *miox4-2*, were complemented with respect to their Ins metabolic alterations, these plants were analyzed for Ins and other metabolite levels.

For the *miox2* mutant complementation, the changes observed in Ins and DGlcA levels were compared with levels in the MIOX2:GFP/ *miox2-2* plants. Ins levels are decreased in all tissues for the complemented line compared to WT and *miox2-2* levels, similarly to the MIOX2:GFP overexpression line (Figure 14C, left). Also, DGlcA levels are increased in some tissues (Figure 14D, left). I conclude that the metabolite alterations observed in miox2 mutants were not complemented upon insertion of the MIOX2:GFP construct in plants. Although the alterations in Ins and DGlcA in MIOX2:GFP plants suggests that the MIOX2:GFP construct is catalytically active, the construct does not complement the phenotypes of the *miox2-2* mutant. Indeed the alterations in substrates and products in the MIOX2:GFP/*miox2-2* line indicate the likelihood that this plant behaves metabolically like an overexpresser of MIOX2.

Regarding *miox4* complementation, Ins levels are greatly increased in seedlings and flowers compared to WT and *miox4-2* levels, and Ins levels are decreased in seedling compared to WT (Figure 14C, right). DGlcA levels are increased in seedlings and siliques compared to WT and *miox4-2* levels (Figure 14D, right). I conclude that the metabolite alterations observed in *miox4* mutants were not complemented upon insertion of the MIOX4:GFP construct in plants. The greatly increased Ins levels in seedlings and flowers suggests that the complemented line is functioning to reduce MIOX activity in some feedback mechanism or stimulates Ins synthesis, as noted for the $MIOX4^{+}$ overexpressers examined in Chapter III.

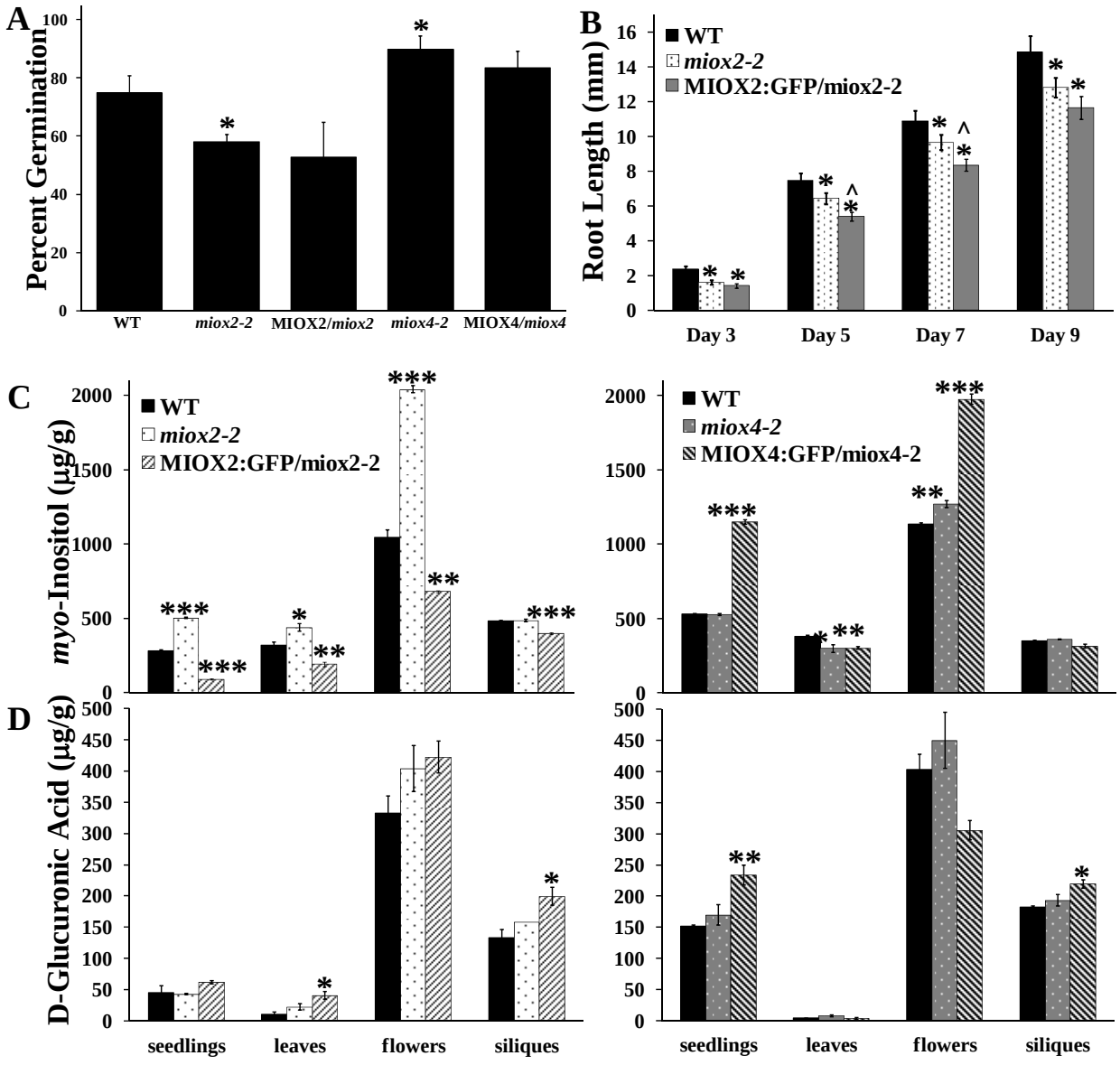

Figure 14. MIOX Complementation. WT, *miox2-2*, MIOX2:GFP/*miox2-2, miox4-2,* and MIOX4:GFP/*mox4-2* seeds were analyzed for complementation of phenotypes. Seeds were surface-sterilized, and placed on growth medium, stratified for 3d at 4°C, then placed at room temperature under long-day conditions. **A)** Germination is shown on 2 µM ABA. Germination was scored daily. Bars represent the mean ±SE where n= 50 seeds for assay performed in triplicate. **B)** Root growth is shown on optimal nutrients containing 0.5x MS salts + 3% glucose + agar, and root length was measured every other day. Bars represent the mean ±SE where n= 3-5, with each replicate containing 10-15 seedlings. **C-D)** Ins and DGlcA were measured by GC for each mutant and complement line. Bars represent the mean ±SE where n= 3-5, with each seedling replicate containing hundreds of seedlings, each leaf replicate contained 3-5 leaves,

each flower replicate contained 50-100 flowers, and each silique replicate contained 30-50 siliques.*** indicates p-value ≤ 0.0005,** indicates p-value ≤ 0.005, and * indicates p-value ≤ 0.05 as compared to WT. ^ indicates p-value ≤ 0.06 as compared to *miox2-2*.

Protein Levels of MIOX:GFP Seedlings

To determine whether the MIOX:GFP fusion proteins accumulate, described in the "Complementation" and "Subcellular Localization" sections, seedlings were analyzed by western blotting with the anti-MIOX4 antibody described in Chapter III and the anti-GFP antibody. The upper panel of Figure 15, showing a membrane blotted with anti-MIOX4, indicates that there is accumulation of the MIOX2:GFP and MIOX4:GFP fusion proteins in the WT and mutant backgrounds. The MIOX4:GFP bands appear more intense than the bands showing MIOX2:GFP fusion protein. This is likely because the anti-MIOX4 antibody was produced against MIOX4 recombinant protein, and could cross-react better with MIOX4 versus MIOX2. There is an abundant non-specific 50 kD band in the seedling extracts denoted with an asterisk. The native MIOX proteins, described in Chapter III as a 45 kD band, are detectable in *miox4-2* and WT seedling extracts (upper panel). The lower panel of Figure 15, showing a membrane blotted with anti-GFP, indicates that there is a large accumulation of the MIOX2:GFP fusion protein in the WT and mutant backgrounds. However, the MIOX4:GFP fusion protein is barely detectable in the WT and mutant backgrounds, although it is clearly detectable with the anti-MIOX4 antibody. MIOX2:GFP exhibits the highest level of protein accumulation in the WT background. Taking these data together, I conclude that MIOX2:GFP and MIOX4:GFP fusion proteins accumulate in the WT and mutant backgrounds.

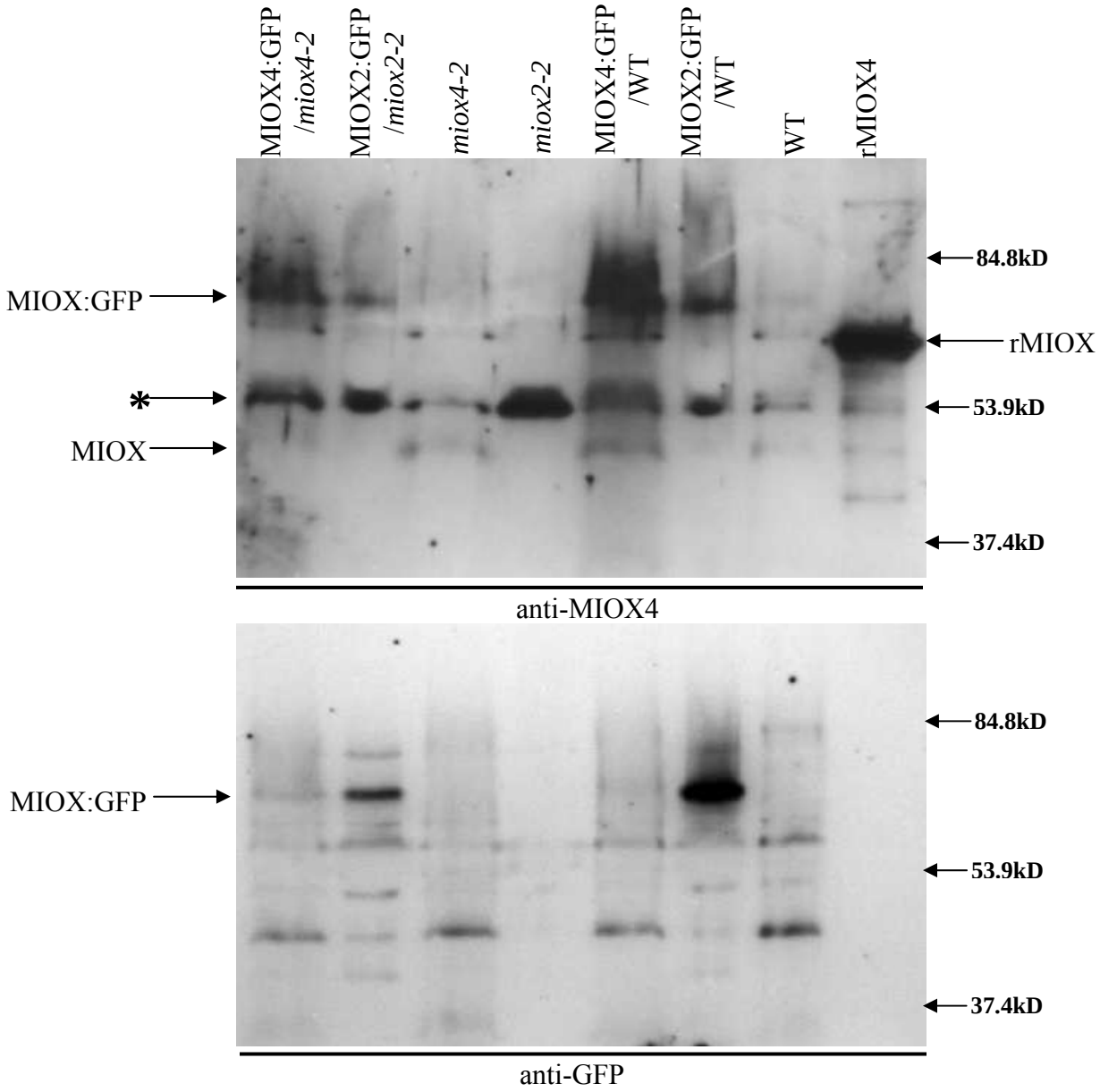

Figure 15. Western Blot of MIOX:GFP and MIOX Mutant Seedlings. Denatured extracts were separated by SDS-PAGE, transferred to the membrane, and blotted. **upper)** extracts were blotted with the anti-MIOX4 antibody. **lower)** extracts were blotted with the anti-GFP antibody. * denotes the 50kD non-specific band.

Subcellular Localization of MIOX2:GFP and MIOX4:GFP Fusion Proteins

In addition to the spatial regulation confirmed by examination of MIOXp:GUS plants, I wanted to determine if the two MIOX gene products are located in different cellular compartments. Using the protein subcellular localization prediction program, WoLF PSORT, I found differences in predicted subcellular locations for the MIOX gene products (Horton *et al*., 2006). WoLF PSORT predicts that MIOX1 and MIOX2 are most likely located in the cytosol while MIOX4 and MIOX5 are likely located in the nucleus.

To empirically determine the subcellular locations of MIOX2 and MIOX4 proteins, I created MIOX:GFP gene fusion constructs to direct expression of the fusion proteins in transgenic plants. To create a MIOX2:GFP construct, I generated genomic DNA to clone the MIOX2 gene following the scheme described in the Materials and Methods. Genomic DNA was used because a full length MIOX2 cDNA clone could not be amplified by PCR, nor were suitable MIOX2 clones available. To create a MIOX4:GFP construct, a full length MIOX4 cDNA clone in a pUNI vector, from the Arabidopsis Biological Resource Center, was incorporated according to the scheme described in the Materials and Methods. The MIOX2:GFP and MIOX4:GFP constructs were used in transformation of WT and *miox* mutant plants.

To examine the localization of the MIOX2:GFP fusion protein, I performed imaging experiments with MIOX2:GFP plants and *miox2-2* mutants complemented with the MIOX2:GFP construct (MIOX2:GFP/ miox*2-2* plants). Because MIOX2:GFP plants have decreased Ins levels (see Figure 10), suggesting that the fusion protein is catalytically active, it is likely that this fusion protein undergoes the same post-translational modifications and subcellular localization as the native MIOX2 protein. I was able to identify GFP expressing plants easily with an Olympus SZX16 stereoscope with dual-fluorescent optics, and examination of flowers (Figure 16B) and seedlings (Figure 16C, right) in comparison to WT flowers (Figure 16A) and seedlings (Figure 16C, left) . I analyzed T2 progeny from two independent MIOX2:GFP and MIOX2:GFP/ miox*2-2* lines with fluorescence deconvolution microscopy, and found a similar pattern of location in all four lines. GFP fluorescence was associated with the cytoplasm in all cells within the cotyledon epidermis (Figure 17A), hypocotyls (Figure 17B), seedling roots (Figure 17C) and root tips (Figure 17D). To confirm the cytoplasmic localization, I treated the seedlings with 0.8 M NaCl to plasmolyze the cells, causing the cytoplasm to retract from the cell

wall. Based on the plasmolysis results (Figure 17E-F), GFP fluorescence is only in the cytoplasm. I conclude that the MIOX2 protein is localized in the cytoplasm of seedlings.

To investigate the subcellular location of MIOX4:GFP fusion protein, I performed imaging experiments with MIOX4:GFP plants and *miox4-2* mutants complemented with the MIOX4:GFP construct (MIOX4:GFP/ miox*4-2* plants). Since the MIOX4:GFP construct results in decreased Ins levels in MIOX4:GFP seedlings (see Figure 11), it is likely that this fusion protein undergoes the same post-translational modifications and subcellular localization as the native MIOX4 protein. I analyzed T1 progeny from two independent MIOX4:GFP lines and one MIOX4:GFP/ miox*4-2* line with fluorescence deconvolution microscopy, and found a similar pattern in all three lines. GFP fluorescence was associated with the cytoplasm in cells in the cotyledon epidermis (Figure 18A), hypocotyls (Figure 18B), seedling roots (Figure 18C) and root tips (Figure 18D). To confirm the cytoplasmic localization, I performed a plasmolysis experiment using 1 M NaCl. Examination of the plasmolyzed roots and hypocotyls revealed GFP fluorescence in the cytoplasm (Figure 18E-F). In addition to its cytoplasmic location, MIOX4:GFP was also found in nuclei from some, but not all, root tip cells (Figure 18D). To confirm the nuclear localization of the MIOX4:GFP fusion protein in the root tip, I stained MIOX4:GFP/ miox*4-2* seedlings with the nuclear dye 4',6-diamidino-2-phenylindole (DAPI) and imaged for GFP and DAPI fluorescence simultaneously. In the region examined, approximately 65% of root nuclei exhibiting DAPI fluorescence also had GFP fluorescence (insets of Figure 19A&B, denoted with yellow arrows), and the overlay indicates fluorescence of both fluorophores from the same nuclei (Figure 19C, denoted with yellow arrows). I conclude that the MIOX4 protein is localized in the cytoplasm and also within some root nuclei in seedlings.

I have also transformed *miox2-2* mutants with the MIOX4:GFP construct to test whether there is complementation provided by MIOX4:GFP for the loss of MIOX2. All MIOX4:GFP/*miox2-2* transformants have kanamycin resistance, from the mutant background, but very little GFP fluorescence was detectable in the T_0 transformants. Five putative transformants were identified and screened further. However, in these putative lines, GFP fluorescence is not detectable at levels comparable to the other MIOX4:GFP transgenics, therefore, I have not moved forward with these lines.

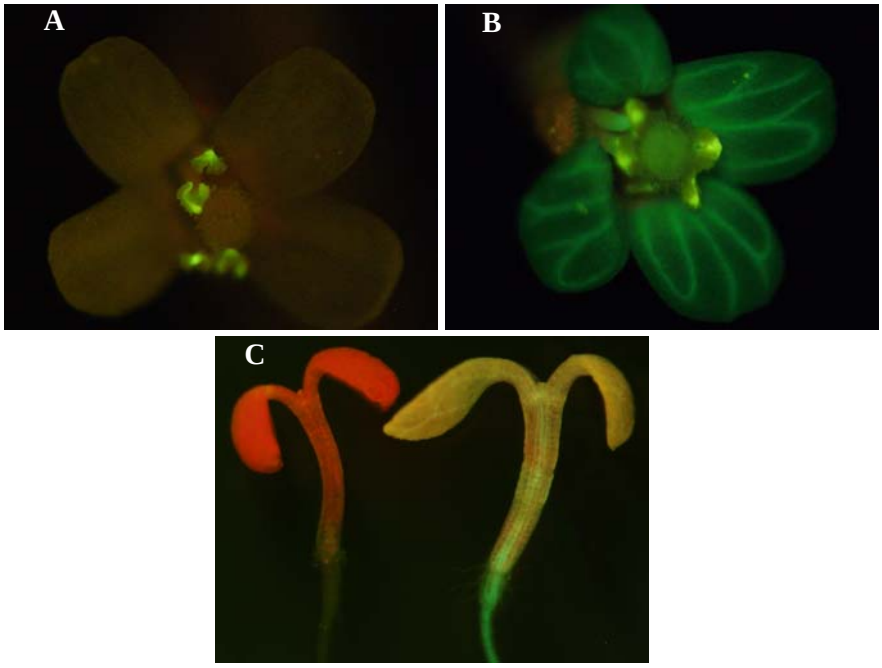

Figure 16. GFP-tagged MIOX2 in Arabidopsis Plants. GFP-tagged MIOX2 was expressed in the WT and *miox2-2* mutant backgrounds **A)** WT flower and **B)** MIOX2:GFP/ *miox2-2* flower under dual chlorophyll and GFP fluorescence filter; **C)** WT (left) and MIOX2:GFP/ *miox2-2* (right) seedlings under dual chlorophyll and GFP fluorescence filter. Note that chlorophyll fluoresces red in A-C.

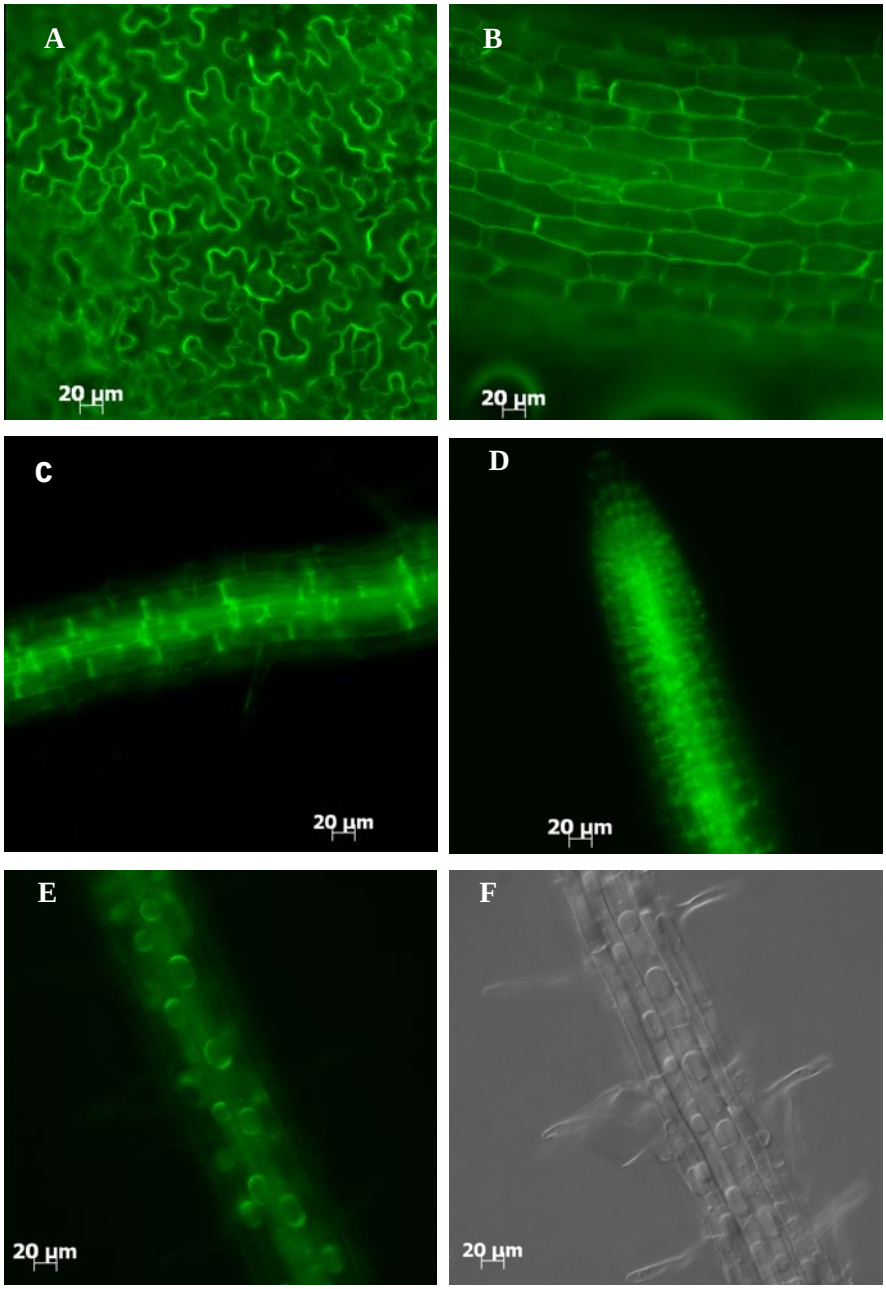

Figure 17. Subcellular Localization of GFP-tagged MIOX2 in Arabidopsis Seedlings. GFP-tagged MIOX2 was expressed in the WT and *miox2-2* mutant backgrounds, and the subcellular location in **A)** cotyledons, **B)** hypocotyls, **C-F)** and roots from twelve-day old seedlings was examined with fluorescence deconvolution microscopy. **A-E)** GFP fluorescence; **E-F)** root plasmolyzed with 0.8 M NaCl, **F)** differential interference contrast of plasmolyzed root in E; In panels A-F, the bar = 20 µm.

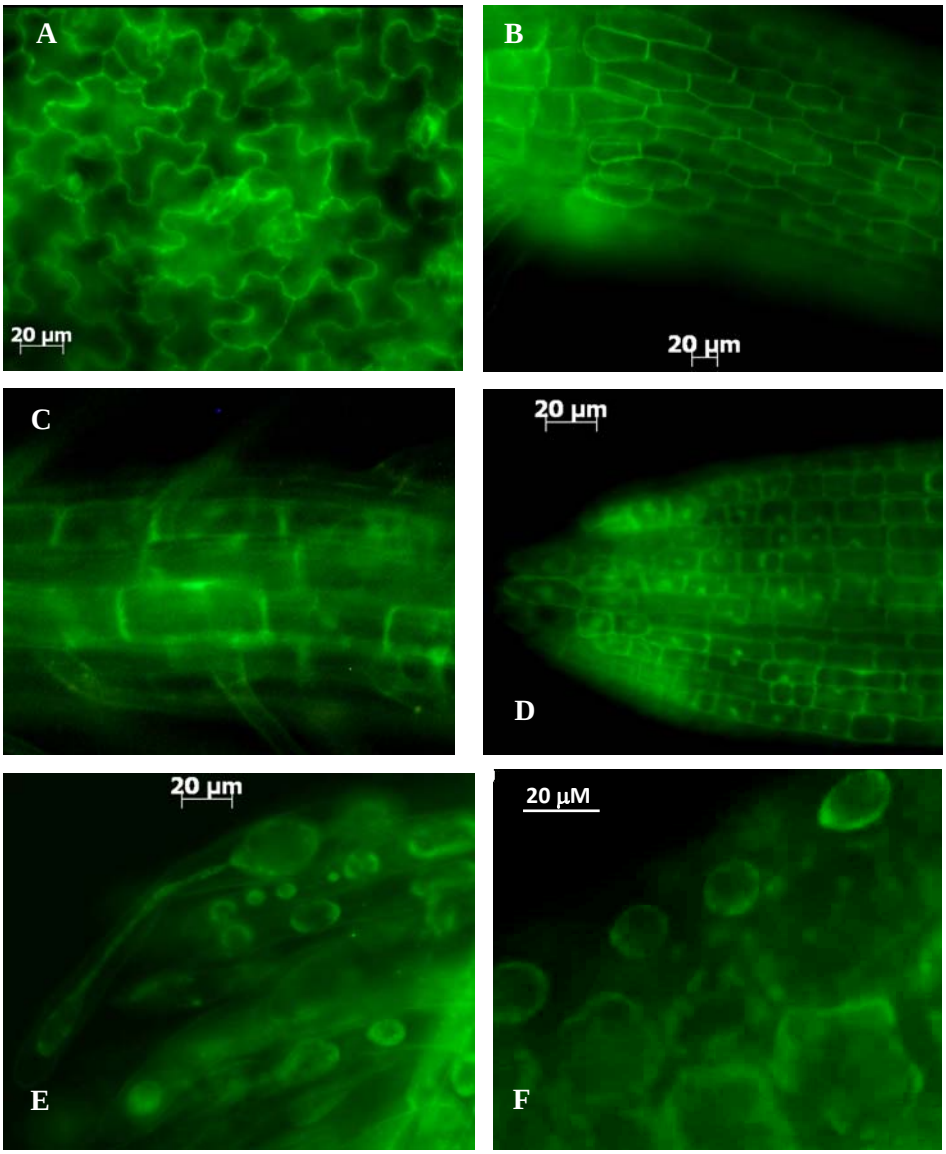

Figure 18. Subcellular Localization of GFP-Tagged MIOX4 in Arabidopsis Seedlings. GFP-tagged MIOX4 was expressed in the WT and *miox4-2* mutant backgrounds, and the subcellular location in **A)** epidermal cells, **B)** hypocotyls, **C-E)** and roots from three-four-day old seedlings was examined with fluorescence deconvolution microscopy. **A-F)** GFP fluorescence; **D)** root tip cells; **E)** root hair cells plasmolyzed with 1 M NaCl; and **F)** hypocotyl cells plasmolyzed with 1 M NaCl. In panels A-F, the bar = 20 µm.

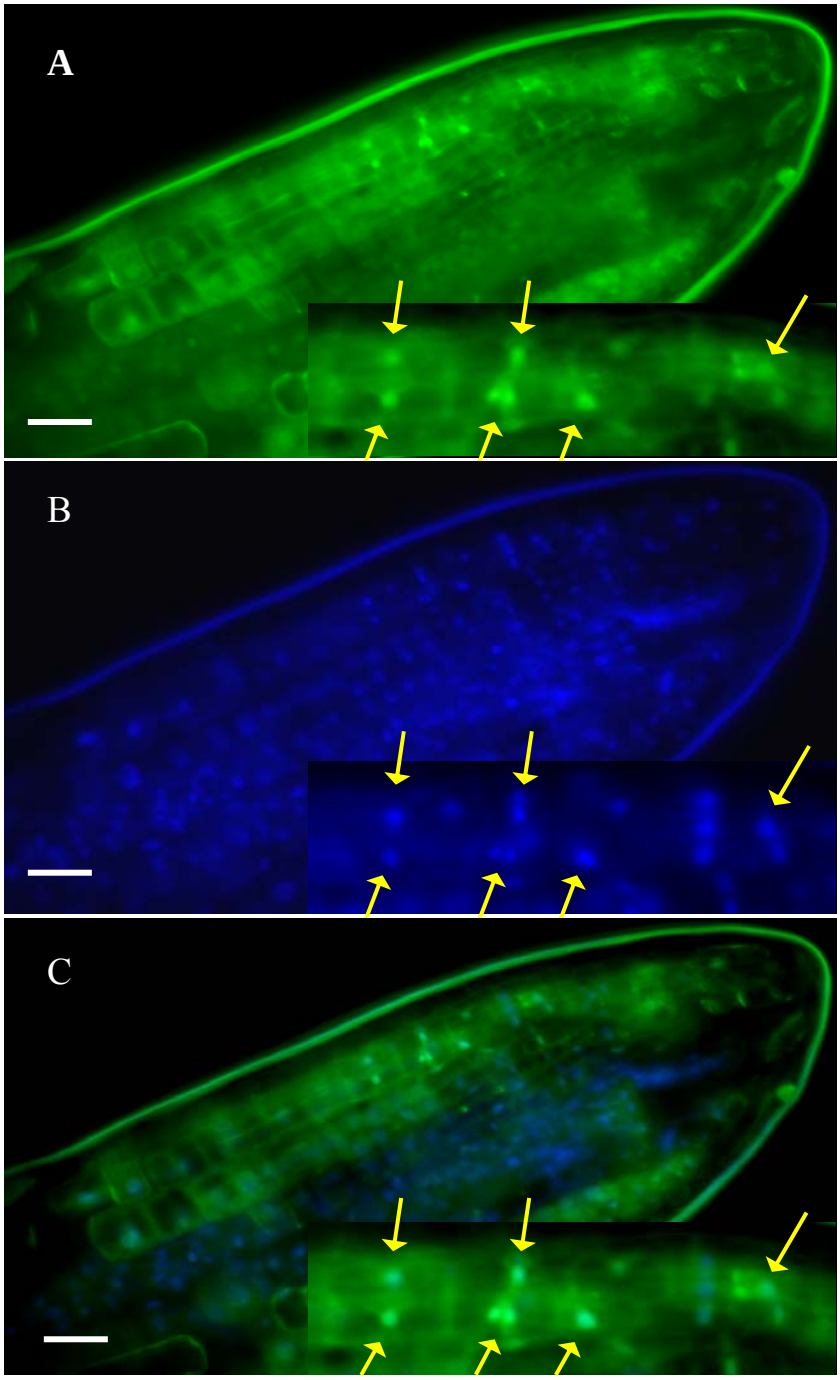

Figure 19. DAPI Staining of MIOX4:GFP Roots. GFP-tagged MIOX4 was expressed in the WT and *miox4-2* mutant backgrounds, and the subcellular location in roots from three to four day-old seedlings was examined with fluorescence deconvolution microscopy. **A)** GFP fluorescence; **B)** DAPI fluorescence; **C)** Overlay of DAPI and GFP fluorescence. In panels A-C, the bar = 20 μm. Yellow arrows in each inset indicate GFP & DAPI fluorescing nuclei.

DISCUSSION

Plant growth and responses to environmental stimuli are affected by the molecule Ins. Ins is the precursor to InsP signaling molecules, cell wall components, and it has been shown to play a role in AsA synthesis (Lorence *et al*., 2004), a debated topic (Endres and Tenhaken, 2008). Plant cells maintain a pool of free Ins to distribute for various needs, and oxidation of Ins, by MIOX, results in a progression of Ins to cell wall and/or AsA synthesis as opposed to use in signal transduction pathways (Loewus and Murthy, 2000). Arabidopsis contains a gene family encoding MIOX isoforms, and presumably these MIOX isoforms provide a way to regulate MIOX at the transcriptional level or provide different catalytic functions within the plant. I report here that MIOX2 and MIOX4 differ with respect to their transcriptional regulation and subcellular location. These differences likely impact Ins oxidation in different ways as is evidenced by the opposite nature of *miox2* and *miox4* phenotypes under several circumstances.

MIOX2 and MIOX4 Expression Patterns are Dependent on Nutrient Conditions

Microarray data suggest that MIOX2 is the most constitutively expressed MIOX in the Arabidopsis gene family, and that MIOX4 and MIOX5 likely provide most or all of the Ins oxidation that leads to cell wall and/or AsA synthesis in flowers and fruits (see Figure 20). Previously reported findings indicated that MIOX4 is not expressed in seedlings (Kanter *et al*., 2005); however, my examination of MIOX2 and MIOX4 promoter:GUS plants revealed expression of both genes in seedlings which varied depending on nutrient conditions. One possible reason for the discrepancy between my results and those of Kanter *et al.* is the inclusion of sucrose in their media. Whereas, my results in Figure 4 show that sucrose suppresses most of MIOX2 and MIOX4 expression. My results with MIOX2p:GUS and MIOX4p:GUS plants also confirms the microarray data showing that MIOX2 expression is upregulated in response to limited carbon conditions, and MIOX2 is downregulated in response to added carbon sources (Gibon *et al*., 2006; Baena-Gonzalez *et al*., 2007). In general, expression of MIOX2 and MIOX4 is induced under no or low nutrients, indicating that Ins oxidation could play a role in adaptation to low nutrients. Furthermore, MIOX expression might allow for use of Ins as an alternative carbon source.

My analysis of later developmental stages, including leaves and reproductive tissues, agrees with the previously published data on these MIOX2p:GUS and MIOX4p:GUS plants

(Figure 5-6) (Kanter *et al*., 2005). Of notable importance is the finding of expression in the meristematic stipules of both MIOX2 and MIOX4 (Figure 6). This finding indicates that both genes might play a role in early development of undifferentiated tissue, likely in supplying UDP-DGlcA necessary for cell wall building.

Physiological and Metabolic Changes in miox2 and miox4 Plants Correlate with Expression Patterns

I have shown that loss-of-function mutants defective in MIOX2 and MIOX4 isoforms have unique phenotypes and metabolic profiles. Specifically, loss of MIOX2 results in increased Ins (Figure 10), and MIOX2 seems to be required to suppress root elongation under no or low nutrient conditions (Figure 8). Nelson *et al.* (1998) have suggested that Ins is present in the phloem and serves to signal the photosynthetic capacity of the shoot to the roots, which will in turn sustain membrane biosynthesis depending on the photosynthetic capacity. Thus, the increase in Ins in *miox2* mutants could provide a signal to the roots that the photosynthetic capacity has been met for increased root cell membrane biosynthesis and subsequent elongation. Under optimal conditions, however, MIOX2 is repressed in WT seedling shoots, so that under these conditions *miox2* mutants now receive a different signal, likely because Ins is not oxidized in root either, resulting in suppressed root elongation as compared to WT seedlings (Figure 4 & 8).

In addition to the seedling root growth alterations, I observed delayed flowering in the *miox2* mutants (Figure 9). Ohto *et al.* (2001) described delayed flowering time in plants supplemented with sucrose or glucose. They conclude that the excess sugar delays progression of the late rosette phase from maturing into the reproductive phase. The increase of Ins and glucose in *miox2* mutant leaves (Figure 10), could likewise signal a new nutritional status to the meristem resulting in an increase in days to flowering.

By analyzing *miox2* seed and seedlings, I was able to correlate the increased Ins with ABA- and cold- sensitivity, and NaCl-insensitivity (Figures 10 & 12-13). The increased Ins could result in increased Ins(1,4,5)P_3. For example, genetic mutants such as *sac9* and *fry1* (a phosphoinositide phosphatase and an Ins polyphosphate phosphatase) contain elevated Ins(1,4,5)P_3 and are salt-, cold- and ABA-hypersensitive, demonstrating a role for Ins(1,4,5)P_3 in mediating the effects of those stimuli (Xiong *et al*., 2001; Williams *et al*., 2005). Additionally,

Hong *et al.* (2008) have observed phenotypes similar to the *miox2* mutants, in that phospholipase D mutants that were ABA-sensitive and had delayed flowering. Although ABA- and cold-sensitivity likely result from increased Ins(1,4,5)P_3, the NaCl-insensitivity, seen in the root growth of *miox2* mutants, seems to be opposite the ABA-and cold- sensitivities (Figure 13). Therefore, the NaCl-insensitivity might occur specifically because of the increase in Ins in seedlings. The excess Ins could be functioning as an osmolyte during salt stress (Ishitani *et al*., 1996; Nelson *et al*., 1998), irrespective of Ins(1,4,5)P_3 signaling.

Regarding the *miox4* mutants, loss of MIOX4 results in no large changes of Ins levels in seedlings (Figure 11). However, MIOX4 seems to be required to promote root elongation under no nutrient conditions (Figure 8). Because MIOX4 is not natively expressed under the no nutrient conditions, it would seem that a *miox4* mutant would not display any phenotypes under those conditions (Figure 3). However, I observed a decrease in root length under no nutrient conditions (Figure 8), the mechanism resulting in this phenotype is unclear. Perhaps a more careful dissection of shoot and root metabolite analysis in varying nutrient conditions would clearly define the role of Ins in *miox4* root growth phenotypes. Under low nutrients MIOX4 is expressed in the shoot, and therefore potentially elevated Ins levels in the *miox4* shoot could provide a signal to the roots that the photosynthetic capacity has been met for increased root cell membrane biosynthesis resulting in elongation. In optimal nutrients, MIOX4 is not expressed in the shoot (Figure 4), thus under these conditions, WT seedlings would not receive information about photosynthetic capacity based on MIOX4 function. However, the shorter *miox4* roots in optimal conditions (Figure 8) could be the result of a discreet Ins pool in the root that is not oxidized in the mutant, resulting in fewer cell wall components and shorter roots. Together these data of *miox2* and *miox4* mutants suggest that MIOX2 and 4 functions are both involved in controlling Ins metabolism to regulate root growth; however, the differences in their expression patterns dictate slightly different areas within the seedling for their function.

In addition to the seedling root growth alterations, I observed early flowering in the *miox4* mutants (Figure 9). Unlike, the *miox2* mutants, there are not major alterations of Ins levels in the *miox4* leaves which would result in altered flowering time. In addition to sugar regulation over flowering time (Ohto *et al*., 2001), research suggests that flowering time is regulated by a chromatin-mediated repression system (Takada and Goto, 2003). Localization data indicates that MIOX4 is present in nuclei of some cells (Figures 18-19), therefore, MIOX4

could potentially play a role in transcriptional regulation of genes controlling flowering time, functioning to repress flowering.

I observed ABA- insensitivity in germinating *miox4* seed (Figure 12). It is unclear why this insensitivity occurs; however, it is possible that reduced Ins oxidation in the *miox4* seed results in a compensatory reduction of Ins synthesis. A discreet decrease in Ins levels in seed could give rise less Ins(1,4,5)P_3 and ABA-insensitivity. This alteration could be resolved by measuring Ins in seed.

From metabolic analysis, I have observed that MIOX2 impacts Ins levels more than MIOX4. This greater impact is evident by the increase of Ins in most tissues in *miox2* mutants, and by the decrease of Ins levels in all MIOX2:GFP tissues (Figure 10). However, Ins levels are not altered as much in the *miox4* mutants or MIOX4:GFP overexpressers (Figure 11), nor in the $MIOX4^+$ overexpressers (described in Chapter III, Figure 22). This difference in metabolic impact might be explained by native gene expression patterns showing that MIOX2 is more constitutively expressed than the other three MIOX (Figure 20), thus western blot data confirms that the plant might tolerate greater overexpression of MIOX2 versus MIOX4 (Figure 15). Despite the greater perturbances of Ins catabolism in MIOX2:GFP plants, I have found increased AsA levels in both MIOX2:GFP and MIOX4:GFP tissues (Figures 10 & 11). Without a metabolic flux analysis, I cannot determine whether the alterations in AsA are due to the alterations in Ins catabolism; however, the data are consistent with the possibility that Ins oxidation feeds into AsA synthesis, at least under some conditions.

One important consideration of working with loss-of-function mutants is complementation of mutant phenotypes and metabolic alterations with a copy of the WT gene. Since T-DNA mutants can carry multiple gene disruptions, complementation, in addition to examining multiple mutant lines, is an important control to ensure that differences in mutants are due to a single gene disruption. I used the 35S CaMV promoter to drive expression of MIOX2:GFP and MIOX4:GFP gene fusions in the appropriate mutant background, and did not observe complementation in either case. As well, potentially complemented lines had altered Ins levels similar to gain-of-function MIOX plants. Thus, it is likely that the lack of complementation seen in my work is due to use of the 35S promoter. Future efforts should utilize the native MIOX2 and MIOX4 promoters. It is also possible that use of a GFP fusion inhibits correct protein-protein interactions required for regulation of MIOX activity. Although

other GFP fusion proteins have provided complementation for mutants in our lab (Ananieva *et al*., 2008; Ercetin *et al*., 2008), fusion proteins have not served double duty in the case of *miox* complementation.

In conclusion, the data reported in this Chapter support the original hypothesis that MIOX enzymes are encoded by multiple genes that have specialized roles in Ins metabolism. Specifically, it appears that MIOX2 has a more prominent role in providing Ins oxidation for the needs of the plant in many different tissues. MIOX4 likely plays a supplementary role in some tissues; furthermore, the nuclear localization of MIOX4 indicates that it might also have a specialized role in Ins catabolism that remains to be characterized.

CHAPTER III

OBJECTIVE 2. Characterization of MIOX4 Overexpressers "A *myo*-Inositol Oxygenase Gain-of-Function in Arabidopsis Alters Inositol Metabolism and Signaling"

Adapted from: **Alford, S.R. and Gillaspy, G.E. in preparation for *Plant Physiology***

ABSTRACT

myo-Inositol (Ins) is used in plant cells as a backbone of inositol phosphate and phosphatidylinositol phosphate signaling molecules as well as a precursor for several other inositol-containing molecules. For example, the oxidation of Ins by the enzyme *myo*-inositol oxygenase (MIOX) produces D-glucuronic acid (DGlcA), which can be further metabolized to UDP-glucuronate and AsA. It has been speculated that MIOX oxidization of cellular Ins could act to regulate the balance of metabolic and signaling needs for Ins. Transgenic plants overexpressing the MIOX4 gene ($MIOX4^+$) provide a model system to examine how re-directing carbon from Ins into DGlcA impacts Ins levels and Ins signaling. We have examined developmental alterations in MIOX RNA and protein levels, along with Ins and other metabolites in $MIOX4^+$ and wild type plants. Our results indicate that $MIOX4^+$ tissues are impacted differently than WT by the MIOX4 transgene, with resulting decreases in cellular Ins in early stages after seed imbibition, and increased Ins levels in later developmental stages such as leaves, flowers, siliques and, dry seed. The Ins depletion in seedlings was correlated with a decrease in second messenger Ins-(1,4,5)-trisphosphate ($Ins(1,4,5)P_3$), but no change in phosphatidylinositol was found. To determine the impact of reducing Ins and $Ins(1,4,5)P_3$ in $MIOX4^+$ seedlings, we examined physiological processes known to involve $Ins(1,4,5)P_3$ signaling. We found that $MIOX4^+$ seeds have a small increase in seed dormancy, are sensitive to sodium chloride (NaCl), and are abscisic acid (ABA)-insensitive. Lastly, we report that in contrast to MIOX4 overexpression, MIOX2 overexpression reduces Ins more consistently throughout development, thus MIOX2 is a better candidate for future manipulation of the Ins metabolism pathway.

INTRODUCTION

myo-Inositol (Ins) is a 6 member carbon ring polyol that is synthesized by both eukaryotes and prokaryotes (Michell, 2007, 2008). In multicellular eukaryotes, Ins is involved in many crucial cellular compounds, including those involved in signal transduction (phosphatidylinositol (PtdIns), PtdIns phosphates (PtdInsPs), and Ins phosphates (InsPs)), hormone regulation (indole acetic acid conjugates), stress tolerance (ononitol and pinitol), and phosphorus storage (inositol hexakisphosphate) (Loewus and Loewus, 1983; Loewus and Murthy, 2000; Raboy, 2003; Gillaspy *et al*., 2004). D-glucuronic acid (DGlcA), the breakdown product of Ins, is utilized for synthesis of cell wall pectic non-cellulosic compounds and Vitamin C, L-ascorbic acid (AsA), in some organisms (Loewus and Murthy, 2000). Therefore, Ins metabolism impacts compounds involved in many different and critical biochemical pathways (Figure 1).

The first step of Ins catabolism is catalyzed by the enzyme *myo*-inositol oxygenase (MIOX; EC 1.13.99.1) (Koller and Hoffmann-Ostenhof, 1979; Reddy *et al.*, 1981; Arner *et al.*, 2001). The breakdown of Ins involves oxidation to DGlcA by the incorporation of a single oxygen atom from molecular oxygen (Figure 2) (Moskala *et al*., 1981) . MIOX is encoded by a four member gene family in Arabidopsis (At1g14520, At2g19800, At4g26260, and At5g56640) (Lorence *et al.*, 2004; Kanter *et al.*, 2005). The four genes are very well conserved and are differentially regulated during development with MIOX2 (At2g19800) being the predominantly expressed gene, while MIOX4 (At4g26260) and MIOX5 (At5g56640) are expressed mostly during reproductive stages (Kanter *et al*., 2005). Disruption of MIOX1 (At1g14520) or MIOX2 can diminish the amount of Ins incorporated into the cell wall fraction, thus these genes have been shown to actively impact the production of cell wall compounds (Kanter *et al*., 2005).

There is a debate regarding whether MIOX oxidation of Ins can redirect carbon towards AsA production, an important issue for engineering plants with increased nutritional value (Zhang *et al.*, 2007). An earlier report with plants overexpressing the MIOX4 gene from Arabidopsis ($MIOX4^{+}$) showed that these plants synthesize higher levels of AsA (Lorence *et al*., 2004), presumably from increased oxidation of Ins into DGlcA. Recently another group found that $MIOX4^{+}$ plants do not contain greatly altered AsA levels, even though small amounts of Ins oxidation were noted. It was concluded that MIOX does not redirect carbon into AsA production (Endres and Tenhaken, 2008).

We are primarily interested in a related issue: whether the signaling pool of Ins is impacted by MIOX function, and whether alterations in Ins levels can alter the signaling capacity of these plants. In the Ins signaling pathway, activation of phospholipase C (PLC) catalyzes the hydrolysis of PtdIns(4,5)P_2 to diacylglycerol and Ins(1,4,5) trisphosphate (Ins(1,4,5)P_3) (Figure 1) (Stevenson *et al.*, 2000; Berridge, 2005). In plants, Ins(1,4,5)P_3 is thought to bind to intracellular receptors, which results in the release of Ca^{2+} (Berridge, 1993), however, no Ins(1,4,5)P_3 receptor has been identified (Krinke *et al*., 2007). From physiological, biochemical, and genetic studies, we know that Ins signaling is critical in the response to gravity (Perera *et al.*, 1999; Perera *et al.*, 2001; Perera *et al.*, 2006), blue light (Chen *et al.*, 2008), abscisic acid (ABA) (Sanchez and Chua, 2001; Xiong *et al.*, 2001; Burnette *et al.*, 2003), salt (DeWald *et al*., 2001; Takahashi *et al*., 2001), cold (Xiong *et al*., 2001), and pathogens (Ortega and Perez, 2001; Andersson *et al.*, 2006). Another important signaling molecule, phosphatidic acid (PA) can be produced by hydrolysis of lipid molecules by a phospholipase D (PLD) or via a PLC-DGK (diacylglycerol kinase) coupled activity (see Figure 1) (Wang, 2005). PA has also been implicated in several similar signaling pathways as Ins(1,4,5)P_3 including ABA, salt, cold, and pathogen response (Testerink and Munnik, 2005). Thus it is of interest to determine how increased Ins oxidation by MIOX4 may impact physiological events.

To address whether oxidation of Ins in MIOX4$^+$ plants impacts Ins signaling, we have measured Ins metabolites and Ins(1,4,5)P_3 in different MIOX4$^+$ and wild type (WT) tissues. Our results indicate that mass levels of Ins are reduced in MIOX4$^+$ seedlings, but not in other tissues. Further, we show that this "Ins depletion" is accompanied by a reduction in Ins(1,4,5)P_3, an increase in PA, alterations in seed dormancy, and ABA- and NaCl-sensitivity. These data indicate that increased MIOX activity can impact the ability of seedlings to regulate Ins metabolism and signaling.

MATERIALS AND METHODS

Plant Growth and Germination Experiments

Arabidopsis thaliana ecotype Columbia plants were used for all experiments. MIOX4$^+$ transgenic line L2 was used for all experiments (Lorence *et al*., 2004) because this line contained the highest expression of MIOX4 RNA and the largest increase in AsA (3-fold increase). For seed germination experiments, age-matched WT and transgenic seeds were harvested on the same day from plants grown in parallel on the same shelf of a growth rack and were stored at 4°C in the dark for at least 30 days before germination. For ABA and NaCl studies, WT and MIOX4$^+$ seeds were surface-sterilized and plated on 0.5x MS salts (pH 5.8) and 0.8% agar containing 0, 0.5, 1, or 2 μM ABA, or 0, 75, 100, or 125 mM NaCl. Each agar plate was divided into sections, and 25 or 56 seeds of WT or MIOX4$^+$ type were plated per section. Plates with seeds were stored in the dark at 4°C for at least 3 days then transferred to 23°C under continuous light. For dormancy experiments, WT and MIOX4$^+$ seeds were harvested and germinated immediately on 0.5x MS and 0.8% agar or allowed to ripen for 12 days before germinating. Germination assays were performed in triplicate. A seed was scored as germinated when the radicle protruded through the seed coat. For hypocotyl and root growth experiments, seeds were surface-sterilized and plated on 0.5x MS and 0.8% agar medium. Plates were wrapped in foil and placed at 4°C for three days before moving to room temperature. Plates were oriented vertically to allow measurements of hypocotyl and root length. For RNA, GC, and Ins(1,4,5)P_3 measurements of seedlings, WT and MIOX4$^+$ seeds were surface-sterilized, placed in petri dishes on pre-wetted sterile filter paper, stratified at 4°C, germinated and grown for 5 days under continuous light at room temperature, and frozen in N_2(l) for sample preparation. For the RNA measurement, water loss experiments, and GC analyses of older tissues, WT and MIOX4$^+$ seeds were placed on pre-wetted Pro Mix potting soil and grown under l6 hours of light/day in a growth room set at 22°C and 24°C night and day temperature. Visible radiation (100-320 μmol m^{-2} s^{-1} for 16 h) was provided by a mixture of fluorescent/metal halide/high pressure sodium lamps or fluorescent lamps only.

Gene Expression Measurements

RNA was extracted from frozen 5-day-old seedlings, 6-week-old leaves, open flowers, and green elongated siliques from WT and MIOX4^{+} plants using an RNeasy kit (QIAGEN Inc., Valencia, CA). Extracted RNA concentrations were measured using a NanoDrop ND-1000 Spectrophotometer (Thermo Scientific NanoDrop Technologies, LLC, Wilmington, DE). cDNA was synthesized from the RNA using an iScript cDNA Synthesis Kit (Bio-Rad Laboratories, Hercules, CA). Quantitative PCR was performed using SYBR GREEN reagents (Applied Biosystems, Foster City, CA) on a 7300 Real-Time PCR System (Applied Biosystems, Foster City, CA). Expression was calculated using the 7300 System SDS software (Applied Biosystems, Foster City, CA) where WT seedling tissue expression was normalized to 1, and the Arabidopsis gene Actin8 was used as the endogenous control.

Gas Chromatography/ Mass Spectrometry Analyses

For sample preparation, frozen seedlings and tissues were ground into a powder, and 1 mL of 100% ethanol (for 6-wk-old leaves, open flowers, and green, elongated siliques) or 1 mL 60% methanol (for dry seed, 24hr imbibed seed, and 5-day-old seedlings) was mixed with the powder. The 60% methanol extraction was performed to increase extraction of compounds that are present in lower levels. D-*chiro*-inositol (2 mg) was added to the mixture as an internal standard. The mixture was incubated at 70°C for approximately 1.5 hours. The insoluble portion was removed by centrifugation at 13200 rpm for 10 minutes. The supernatant was dried in a speed-vacuum chamber (Savant) and reconstituted in 200 μL of water, filtered through a 0.2 μM Tuffryn® syringe filter (Pall Gelman Laboratory, Ann Arbor, MI), and dried again. The dried sample was reduced by mixing with 100μL of 10mM dithiothreitol for 10 minutes and dried again. Derivatization reagent (1:1 mixture of pyridine and bis(trimethyl-silyl)trifluoro-acetamide + 1% trimethylchlorosilane; Alltech, State College, PA) was freshly prepared. For sample derivatization, 250 μL of the derivatization reagent was added to the dried sample. The sample was sonicated and heated at 80°C for at least 45 minutes until the entire sample was in solution. The sample was transferred to an autosample vial, and 250 μL of hexanes were added to the sample.

For compound identification, retention times of peaks were compared to those of known metabolite standards. One analyte peak was found for D-*chiro*-inositol, L-gulonic acid γ-lactone,

AsA, L-galactonic acid γ-lactone, and pinitol, while under these conditions D-glucose is represented by two peaks (two isomers). D- and L-galactose are not separated under these conditions, thus we have quantified values from a single, combined peak. Ins is represented by three peaks; however, two of these peaks have a negligible area, so we have used the single dominant peak for Ins quantification. Additionally, peaks were identified by comparison of mass spectral data using GC/MS. Plant samples and standards were separated by a 6890-N GC on an HP-5MS capillary column 30 m X 0.25 mm i.d. (Agilent Technologies, Inc. Santa Clara, CA) with helium as the carrier gas with pressure-controlled flow set at 9.1 psi. The injection port was set at 250°C, the oven was set on a gradient from 75°C to 274°C at 6.5C°/min, and compounds were submitted to electrospray ionization and detected by a 5975 MS (Aglient Technologies, Inc. Santa Clara, CA). The mass spectrum for each peak of interest was compared with a library, from Agilent Data Analysis software, of known spectral data for compound identification (Aglient Technologies, Inc. Santa Clara, CA). Identification of pinitol and L-gulonic acid γ-lactone were specifically confirmed by creating selective ion chromatograms to isolate their specific peaks.

For compound quantification, the sample was injected with a split of 10mL/min and separated by Clarus 500 GC (Perkin Elmer Instruments, Shelton, CT) on a Rtx®-5 fused capillary column 30 m X 0.32 mm i.d. (Restek, Bellefonte, PA) with helium as the carrier gas with pressure-controlled flow set at 6.5 psi with a linear velocity of 1 mL/min. The injection port was set at 225°C, the oven was set on a gradient from 75°C to 274°C at 6.5C°/min, and the flame ionization detector was set at 280°C. Standard curves displaying peak area versus μg/mL were generated for Ins, AsA, L-gulonic acid γ-lactone, D/L-galactose, L-galactonic acid γ-lactone, and pinitol (Figure 21). Peak area was quantified by Totalchrom software (Perkin Elmer, Shelton, CT), adjusted based on recovery of the known internal standard, and converted to μg/ml based on the standard curves. The values were then converted to μg/g fresh weight based on the original sample weight. The D-glucose levels were calculated based on peak area of the MIOX4^{+} sample peak compared to the WT sample peak area. The D-glucose values for MIOX4^{+} samples were then represented as a percent of the WT values At least 2-5 different, independent extracts were analyzed and averaged together to determine WT and MIOX4^{+} data points for each tissue.

Ins(1,4,5)P_3 Measurements

Frozen 5-day-old seedlings were scraped from filter paper and ground to a fine powder in N_2(l). The powder was transferred to a tube, weighed, mixed with 500µL of cold 20% perchloric acid, and incubated on ice for 20 minutes. The precipitated protein was removed by centrifugation at 4°C for 20 minutes at 2000x g. The supernatant was neutralized to pH 7 with KOH. The assay was performed on the neutralized supernatant using an Ins(1,4,5)P_3 mass measurement kit (Amersham-Pharmacia Biotech, United Kingdom) according to the manufacturer's protocol. Controls for non-specific binding were included. The Ins(1,4,5)P_3 content was calculated based on a standard curve.

Lipid Extraction and Mass Spectrometry Analysis

For extraction of phospholipids from plant material, 5-day-old WT and MIOX4$^+$ seedlings, grown on sterile filter paper (50-60 mg fresh weight) at the same time and conditions, were harvested. Extraction of phospholipids was performed as in (Devaiah *et al*., 2006). Extracted plant material was dried and weighed to determine dry weight. For quantification of extracted phospholipids was performed essentially as described previously (Devaiah *et al*., 2006). The dried phospholipid extract was dissolved in 1 ml chloroform and 25 µL was mixed with 1 ml chloroform/methanol/300 mM ammonium acetate in water (300/665/35) containing 0.66 nmol 14:0-16:0 PC (Avanti Polar Lipids, Inc.), 0.66 nmol di24:0 PC (Avanti), 0.24 nmol di14:0 PS (Avanti), 0.24 nmol di16:0 PS (Avanti), 0.16 nmol di8:0 PI (Cayman Chemical) and 0.16 nmol di16:0 PI (Cayman). Samples were introduced into an Applied Biosystems 4000 Q-Trap mass spectrometer at 30 microliters per minute via a Harvard syringe pump and a Turbo V electrospray ion source. Mass spectrometer settings were the same as previously described (Devaiah *et al*., 2006) except the m/z scan ranges for PC and PI were adjusted to acquire data corresponding to the internal standards listed above. Multiple continuum scans were averaged in multiple channel acquisition (MCA) mode; 8, 160, 18 and 78 scans were averaged per sample for scans specific to PC, PI, PA/PG and PS, respectively.

For data analysis, Analyst software (ver.1.4.2) was used for data processing. Averaged spectra were smoothed (when necessary) and centroided. Peaks were binned based on isotope distribution and compared utilizing Excel software from Microsoft. Peaks were normalized both to (1) the sum of the intensities of both internal standards to provide % intensity, and (2) dry

weight of sample, resulting in "% intensity mg^{-1} dry wt". Statistical analysis of p-values for peaks was generated by one-tailed t-test comparison with WT peaks.

Water Loss Measurements

Rosette leaves from age-matched WT and $MIOX4^{+}$ 5-week-old plants were detached, weighed immediately, placed under continuous light, and weighed at time points from 0 to 450 minutes. Water loss was calculated as a percentage of the initial fresh weight.

Western Blotting

Conditions have been previously reported (Burnette *et al*., 2003). Briefly, tissues were ground in liquid nitrogen, homogenized and resuspended with a pestle in SDS-bromophenol blue loading dye, boiled, and the supernatant was loaded onto a polyacrylamide gel for separation. SDS-PAGE was followed by Western blotting with a 1:20000 dilution of rabbit anti-MIOX antibody (provided by the Nessler lab from Cocalico Biologicals Inc., Reamstown, PA) or blotting with a 1:1000 dilution of rabbit anti-GFP antibody (Invitrogen Molecular Probes, Eugene, OR). A secondary goat, anti-rabbit horse radish peroxidase antibody (Bio-Rad Laboratories, Hercules, CA) was used at a 1:2000 dilution. Immunoreactive bands were detected using an ECL Plus Western Blotting Detection System (Amersham, Buckinghamshire, UK) and imaged with a Bio-Rad Gel-Doc system with Quantity One Software (Bio-Rad). Ponceau S staining of blots prior to antibody incubation was performed to ensure that equal amounts of extracts were analyzed.

Construction of MIOX2 Overexpressers

The 2255 bp genomic region of MIOX2 open reading frame minus the stop codon was amplified by high-fidelity PCR, confirmed by sequencing, cloned into the pENTR/D-TOPO vector (Invitrogen), and recombined via the Gateway system (Invitrogen) using the manufacturer's protocol into pK7FWG2. The resulting 35S CaMVp:MIOX2:GFP construct was transformed into *Agrobacterium tumefaciens* by cold shock and was used to transform WT plants (Bechtold *et al*., 1993). MIOX2:GFP seedlings were identified on 50 μg/mL kanamycin plates and by screening for GFP production using an Olympus SZX16 stereoscope with fluorescence optics with an Olympus DP71 camera with DP Controller software (Olympus Corp., Japan).

RESULTS

MIOX4 Transgene Expression in MIOX4$^+$ Plants

To characterize expression of MIOX4, we compared published literature on MIOX4$^+$ plants, complied microarray data, and quantified MIOX4 RNA. Previous studies on the MIOX4 gene were focused on whether a gain of function in MIOX4 can impact AsA synthesis in plants (Lorence *et al*., 2004). MIOX4$^+$ Arabidopsis plants were previously shown to have increased levels of MIOX4 mRNA (Lorence *et al*., 2004). As such, these plants present an opportunity to examine the impact of MIOX overexpression on the regulation of Ins metabolism and signaling during physiologically and developmentally distinct stages in the plant life cycle.

According to Genevestigator data, MIOX4 is a developmentally regulated gene. Native MIOX4 expression is highest in pollen, flowers siliques, and the shoot apex, while MIOX2 is expressed more constitutively, and MIOX1 and MIOX5 generally have low expression levels (Figure 20A) (Zimmermann *et al*., 2004). To confirm that the MIOX4 gene is overexpressed in different tissues from MIOX4$^+$ plants, we performed quantitative PCR (qPCR) on seedlings, leaves, flowers, and siliques. Figure 20B shows that there is approximately 8-fold more expression of MIOX4 in seedling and leaf tissue from MIOX4$^+$ plants as compared to WT plants. In contrast, although we detect high levels of native MIOX4 expression in both flowers and siliques, MIOX4 is not expressed at a higher level in these tissues from MIOX4$^+$ plants as compared to WT plants (Figure 20B).

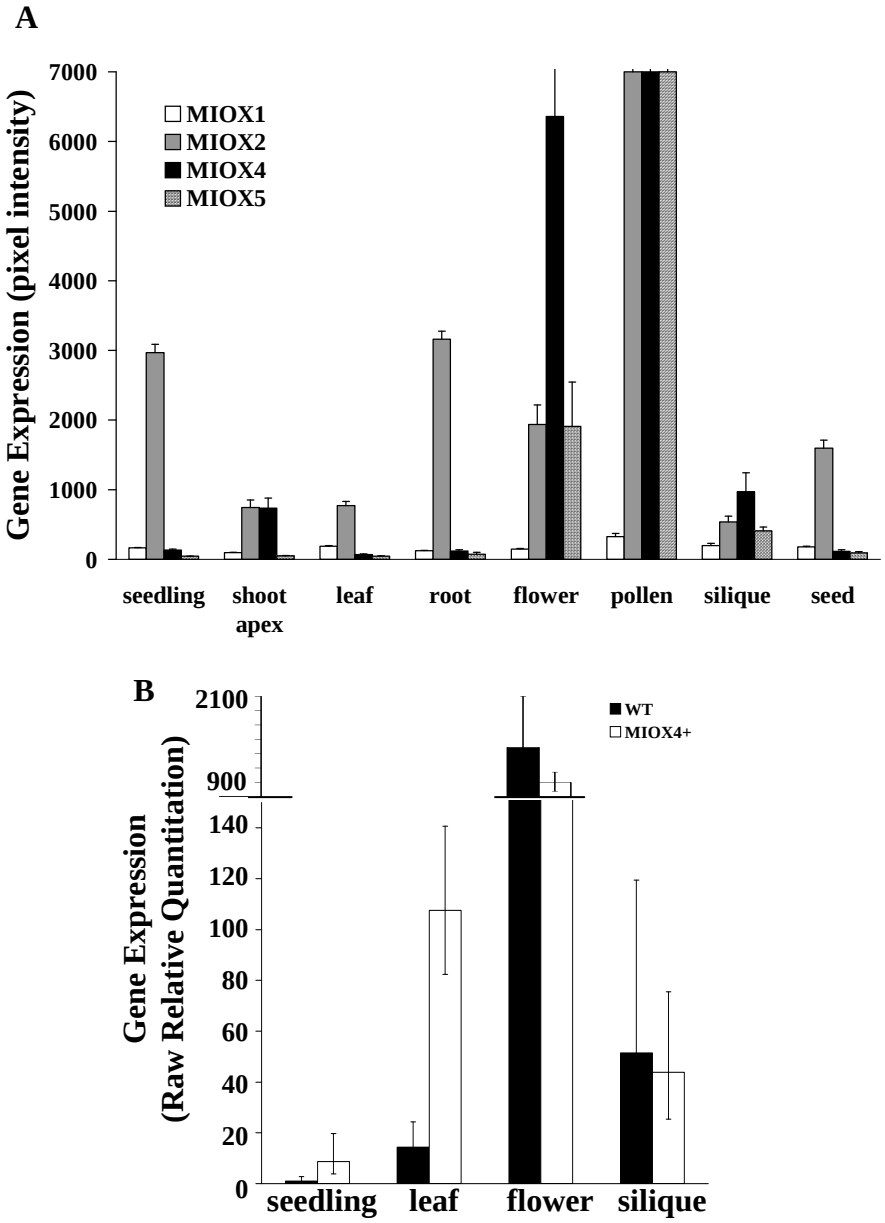

Figure 20. Gene expression of MIOX. **A)**. Genevestigator microarray data was queried to determine MIOX1, 2, 4, and 5 expression in various tissues. Values represent the mean ± SD of three replicates. **B).** RNA was extracted from flash-frozen tissue and cDNA was synthesized from the RNA. Quantitative PCR was performed using SYBR green reagents. Values represent the mean ± SE (n= 3 to 5 biological replicates) compared to WT seedling, which has expression normalized to 1.

MIOX4 Overexpression Alters Levels of Ins and Other Metabolites

To address whether oxidation of Ins in MIOX4$^+$ plants is altered, we measured Ins pathway metabolites with a gas chromatography (GC) assay that allowed us to quantify metabolites (Fiehn *et al.*, 2000) in selected developmental stages/tissues of MIOX4$^+$ and WT plants. Metabolites of interest included Ins, DGlcA, and other known or hypothesized compounds in the AsA synthesis pathways (Wheeler *et al.*, 1998; Smirnoff *et al.*, 2001) (Michell, 2007, 2008), including L-gulonic acid γ-lactone, AsA, L-galactonic acid γ-lactone, D/L-galactose, and D-glucose (see Figure 1). Sample chromatograms from separation of metabolites in WT and MIOX4$^+$ siliques are presented in Figure 21A and standards used are shown in Figure 21B.

We found that Ins levels were only reduced in MIOX4$^+$ imbibed seeds and 5-day-old seedlings (Figure 22). In contrast, at later stages of development, Ins levels are not decreased in MIOX4$^+$ plants as compared to WT plants. In 6-week-old rosette leaf tissue from MIOX4$^+$ plants, Ins levels are reproducibly increased by 11% despite the 8-fold overexpression of MIOX4 (Figure 20B). Ins levels are also increased in flower (22%) and silique (20%), where overexpression was not detected (Figure 22). Examination of Ins levels in MIOX4$^+$ dry seeds reveals that this stage tissue also has increased Ins, indicating that a switch in Ins levels in MIOX4$^+$ plants occurs during germination.

Examination of DGlcA levels from these same tissues shows that as expected, there are corresponding changes in DGlcA levels indicative of increased Ins oxidation in some, but not all, MIOX4$^+$ tissues. For example, imbibed seeds and seedlings that contain reduced Ins also contain increased DGlcA (Figure 22). In contrast, in MIOX4$^+$ tissues with increased Ins, there is no change or a decrease in DGlcA, suggesting that decreased oxidation of Ins is taking place. We conclude that overexpression of MIOX4 in transgenic plants results in an Ins depletion in imbibed seeds and seedlings and an unexpected increase in Ins at later stages of development.

Lorence *et al.* (2004) showed that increasing MIOX expression in transgenic plants resulted in a 2- to 3-fold increase of AsA levels in leaves, and Endres and Tenhaken (2008) recently found no evidence for altered AsA in MIOX4$^+$ leaves. We measured AsA levels (Figure 22) and found that AsA remains relatively unchanged in rosette leaves and flowers; however, MIOX4$^+$ green siliques, a tissue with high endogenous MIOX4 expression, contains a 2-fold increase in AsA (Figure 22).

Since alterations in Ins levels have the ability to impact metabolites in the AsA pathway, we examined L-gulonic acid γ-lactone, L-galactonic acid γ-lactone, and D/L-galactose levels. The major route to AsA synthesis in plants is from GDP-mannose through L-galactose and L-galactonic acid γ-lactone (see Figure 1, gray highlight) (Smirnoff *et al*., 2001). In contrast, L-gulonic acid γ-lactone is a proposed intermediate on an alternate pathway from Ins to AsA (Valpuesta and Botella, 2004). Thus a comparison of these metabolites in MIOX4$^+$ plants as compared to WT plants can be informative regarding AsA synthesis pathways at different developmental stages. As was apparent with Ins, levels of L-gulonic acid γ-lactone were decreased (53%) in MIOX4$^+$ seedlings as compared to WT seedlings (Table 1). Similarly, levels of AsA, L-galactonic acid γ-lactone, and D/L-galactose are reduced in MIOX4$^+$ seedlings. We conclude that metabolites from both, the Smirnoff-Wheeler pathway and via the *myo*-inositol oxidation pathway (MIOP) (see Figure 1), are reduced in MIOX4$^+$ seedlings; therefore, the change in metabolite levels is not specific to AsA synthesis via Ins.

In rosette leaves, we found no changes in L-gulonic acid γ-lactone and L-galactonic acid γ-lactone, however D/L-galactose levels are increased. It is interesting to note that neither the increase in Ins or D/L-galactose appear to be affecting an increase in AsA in this tissue in the MIOX4$^+$ plants. Similarly, in flowers, with high endogenous MIOX4 expression, the mass increase in Ins (22%) and D/L-galactose (39%) is not translated into an AsA increase. In fact, there is a decrease (37%) in the AsA precursor, L-galactonic acid γ-lactone, which is synthesized from L-galactose catalyzed by L-galactose-1-dehydrogenase (Wheeler *et al*., 1998). We conclude that MIOX4$^+$ leaf and flower tissue contains alterations in a few metabolites, but these do not result in increased AsA levels.

In MIOX4$^+$ green siliques, a tissue with high endogenous MIOX4 levels (Figure 20A-B) and AsA levels, L-gulonic acid γ-lactone and L-galactonic acid γ-lactone are not significantly altered. In contrast, D/L-galactose levels are less than in WT siliques (62% of WT). We conclude that MIOX4$^+$ siliques contain no significant increase in metabolites downstream of Ins involved in AsA synthesis. Thus the increase in AsA seen in siliques suggests that either key metabolites in AsA synthesis are metabolized quickly, or that transport of AsA from other tissues, such as leaves, results in the elevated AsA level in siliques from MIOX4$^+$ transgenic plants.

When creating overlays of GC data as shown in Figure 21, we noted that two unidentified peaks increased in flowers and siliques from MIOX4^{+} plants as compared to WT plants. We compared retention times of known standards and used mass spectrometry to identify both peaks as conformers of D-glucose, which have been previously observed (Sawardeker and Sloneker, 1965). Levels of D-glucose thus mirror those of Ins in flowers and siliques, with MIOX4^{+} tissues containing an increase in D-glucose. We conclude that levels of D-glucose also change when the MIOX4 transgene is present in Arabidopsis.

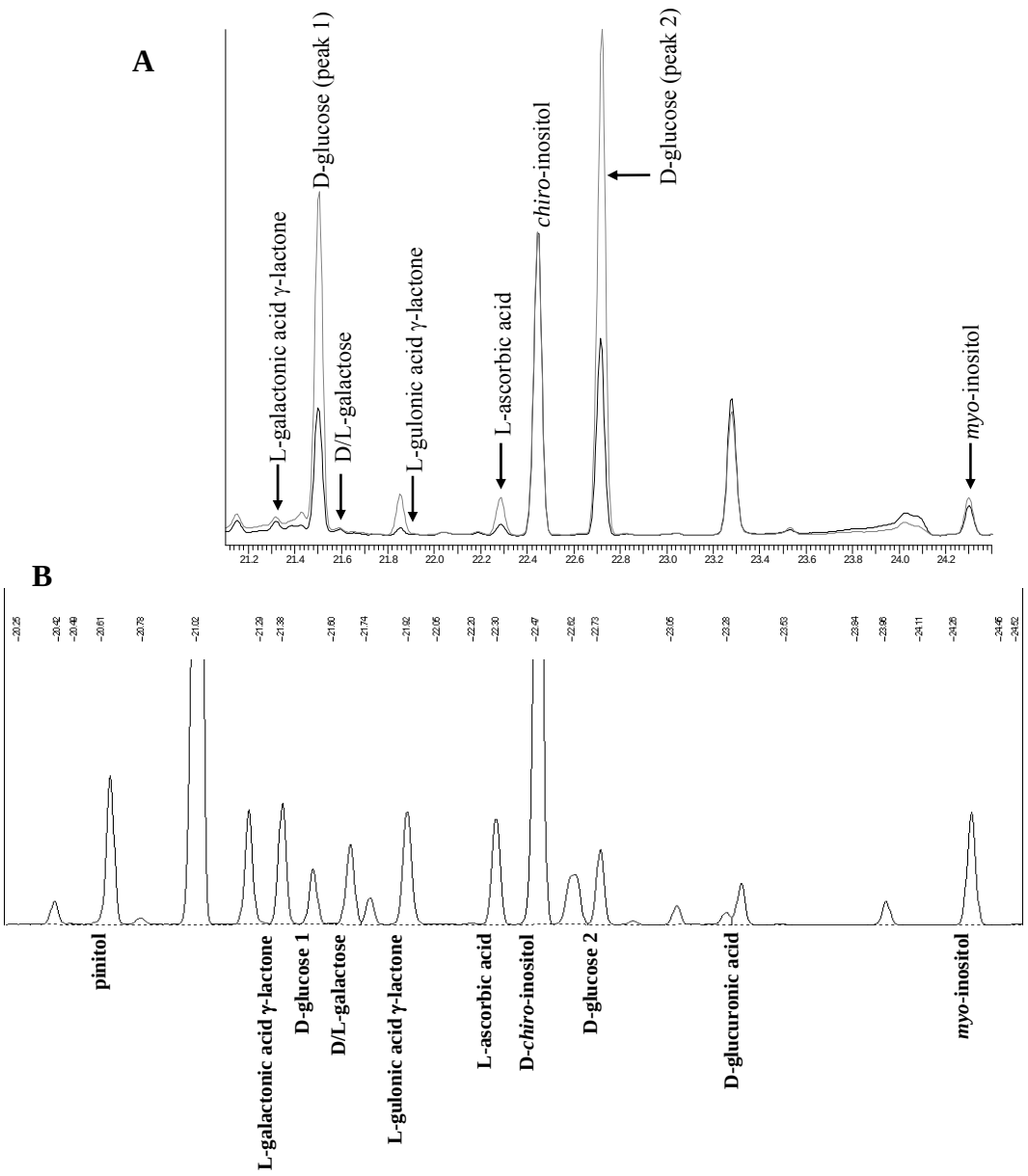

Figure 21. Gas Chromatograms of Samples and Standards. A). Chromatograms from analysis of WT (solid) and MIOX4^{+} (dashed) silique tissue are overlaid. These chromatograms are representative of samples with similar amounts of starting material (95.4 mg and 96.1 mg) for a visible comparison of metabolites. **B)**. A chromatogram of metabolite standards at 50 μg/mL is shown. The retention times are as follows: pinitol 20.61 min, L-galactonic acid γ-lactone 21.38 min, Peak 1 D-glucose 21.5 min, D/L-galactose 21.60 min, L-gulonic acid γ-lactone 21.92 min, AsA 22.30 min, D-*chiro*-inositol 22.47 min, Peak 2 D-glucose 22.73 min, DGlcA 23.3 min, and *myo*-inositol 24.3 min. Other peaks are visible in each individual standard solution and are therefore attributed to compounds found in the reducing or derivatizing reagents.

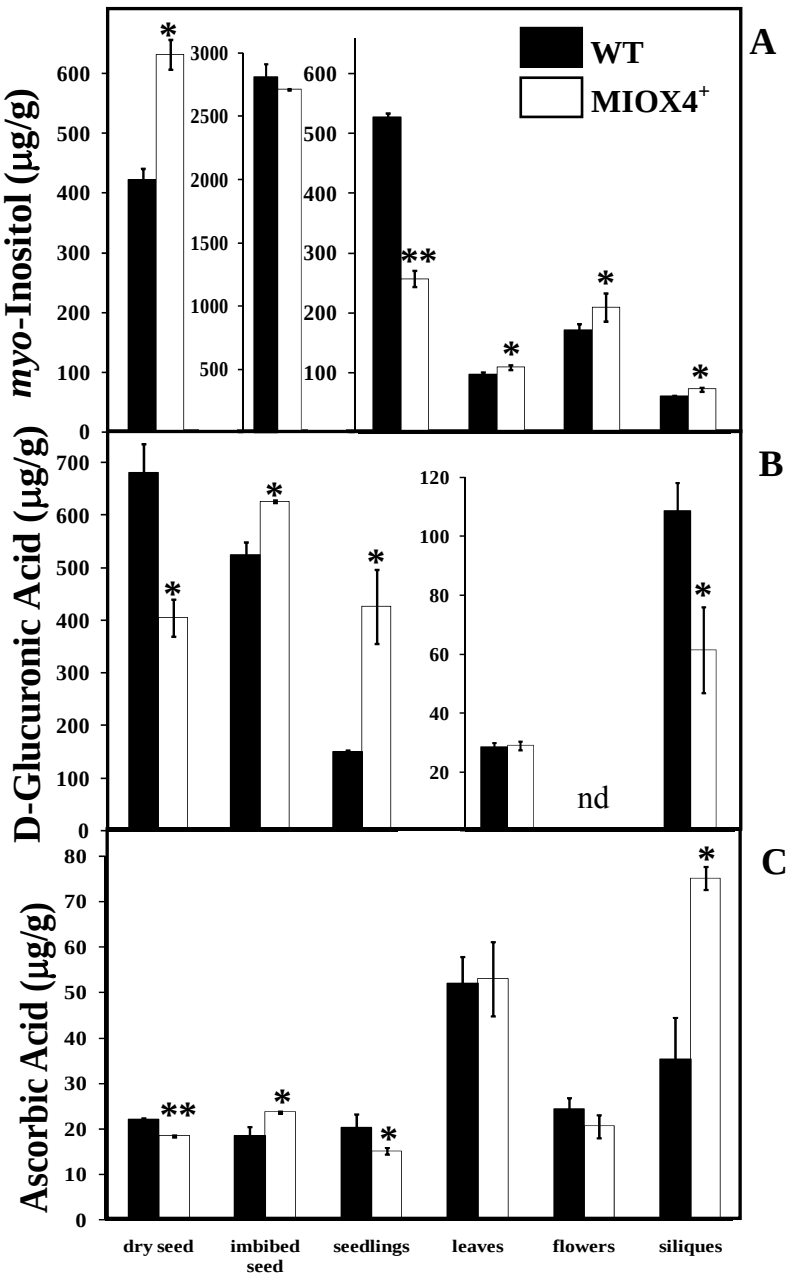
A
B
C
WT
MIOX4+
myo-Inositol (µg/g)
D-Glucuronic Acid (µg/g)
Ascorbic Acid (µg/g)
nd
dry seed
imbibed seed
seedlings
leaves
flowers
siliques

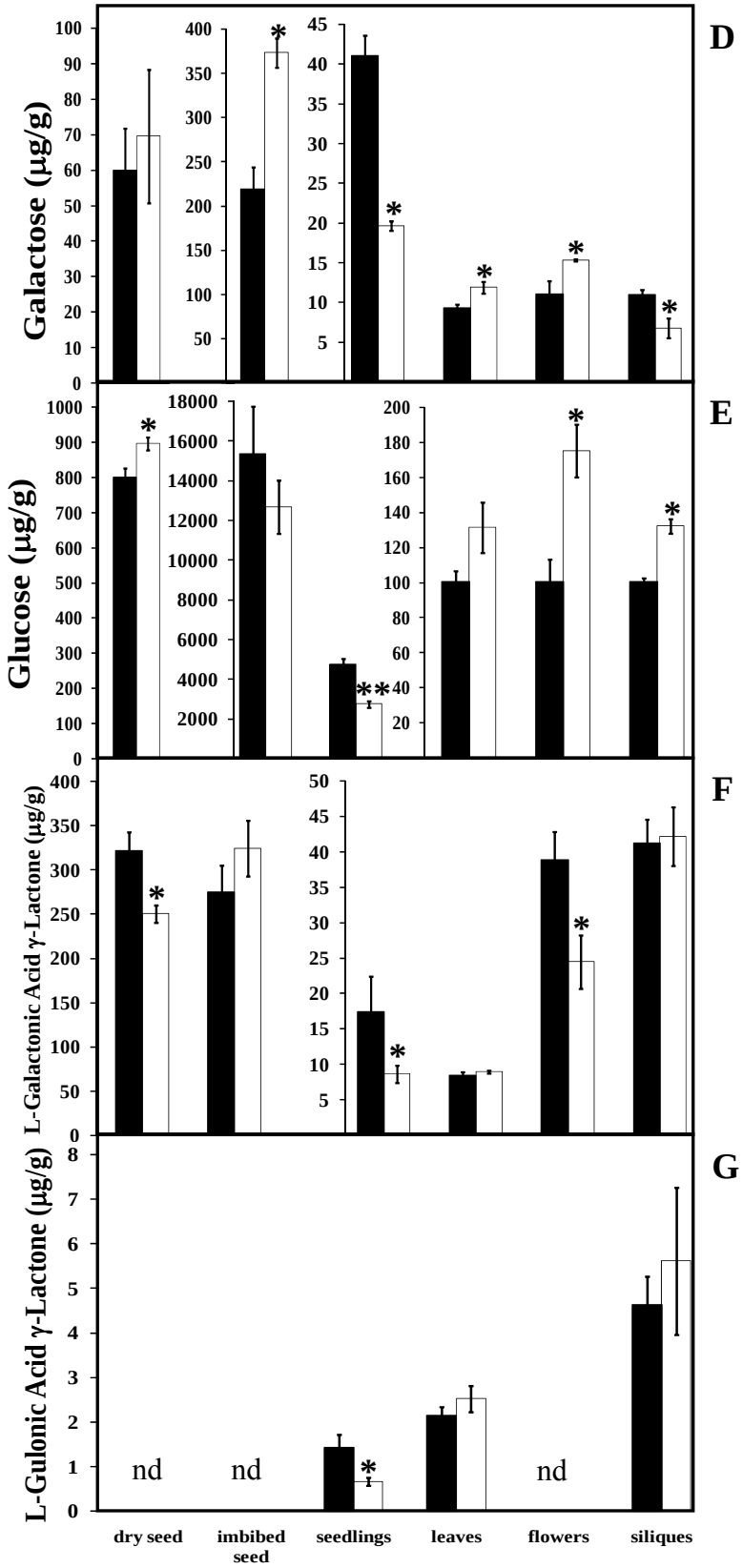
D
Galactose (µg/g)
E
Glucose (µg/g)
F
L-Galactonic Acid γ-Lactone (µg/g)
G
L-Gulonic Acid γ-Lactone (µg/g)
nd
nd
nd
dry seed
imbibed seed
seedlings
leaves
flowers
siliques

Figure 22. Metabolite Levels of WT and MIOX4$^+$ Tissues. Tissues were harvested, ground in liquid nitrogen, extracted, reduced, derivatized, and analyzed by GC. Amounts are given in μg/g fresh tissue. **A)** Ins, **B)** DGlcA, **C)** AsA, **D)** galactose, **E)** glucose, **F)** L-galactonic acid γ-lactone, **G)** L-gulonic acid γ-lactone were measured by GC for WT and MIOX4$^+$ plants. Bars represent the mean ±SE where n=3-5 independent, biological replicates, with each seedling replicate containing hundreds of 5-day-old seedlings, each leaf replicate contained 3-5 6-wk-old leaves, each flower replicate contained 50-100 open flowers, and each silique replicate contained 30-50 green, elongated siliques. ** indicates p-value ≤0.005, and * indicates p-value ≤0.05 as compared to WT. "nd" represents values below detectable limits.

MIOX4 Overexpression Alters Ins(1,4,5)P_3 Levels

Because our metabolite analysis revealed that MIOX overexpression results in an Ins depletion in seedlings, but not at later stages of development, we decided to focus on characterizing alterations within MIOX4$^+$ seedlings. To determine if the mass Ins depletion present in MIOX4$^+$ seedlings impacts production of the second messenger Ins(1,4,5)P_3, we measured mass Ins(1,4,5)P_3 levels in five day-old light-grown MIOX4$^+$ and WT seedlings using a commercially available Ins(1,4,5)P_3 mass assay kit (Amersham-Pharmacia Biotech, UK). In this assay, [^{3}H]Ins(1,4,5)P_3 is incubated with plant extracts, and a partially purified Ins(1,4,5)P_3 receptor is used in a competitive binding assay. Values from the competition assay are then compared to a standard curve, and mass Ins(1,4,5)P_3 is calculated. The results in Figure 23 indicate that MIOX4$^+$ transgenic seedlings contain a 50% decrease in Ins(1,4,5)P_3 as compared to WT seedlings. We conclude that overexpression of MIOX4 results in decreased Ins(1,4,5)P_3 second messenger in light-grown seedlings, which correlates well with the decrease of Ins in these seedlings.

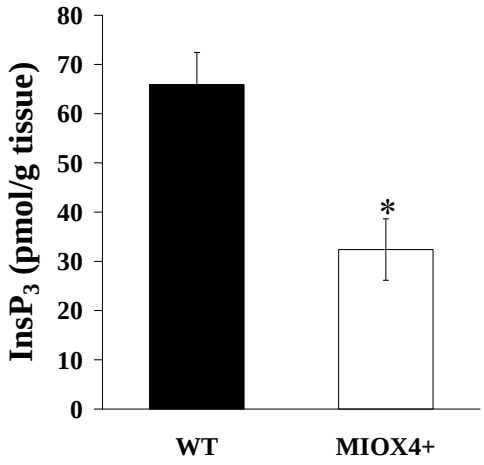

Figure 23. Mass Inositol-(1,4,5)-Trisphosphate Levels in WT and MIOX4$^+$ Seedlings. Five-day-old light-grown seedlings were frozen in liquid nitrogen, ground, and analyzed for mass Ins(1,4,5)P_3 levels as described in the Methods. Bars represent the mean ± SE (n= 6 biological replicates, where each replicate contained hundreds of small seedlings) from two independent experiments. * indicates a 2-tailed p value ≤ 0.05.

MIOX4 Overexpression Alters Phosphatidic Acid Levels

Changes in Ins(1,4,5)P_3 in MIOX4$^+$ seedlings could occur as a result of decreased Ins incorporation into phosphatidylinositol (PI), so we analyzed the lipid profile of seedlings to observe if changes occurred in phospholipids. We extracted lipids from 5-day-old light-grown seedlings and analyzed the lipid extracts using mass spectrometry protocols from the Kansas State Lipidomics facility. The results in Figure 24 indicate no difference in PI or phosphatidylcholine (PC) species. There are significant increases in phosphatidic acid (PA) in the MIOX4$^+$ seedlings (Figure 24). PA is a signaling molecule that can be synthesized from PLC products such as DAG or from PLD action on PC (see Figure 1) (Munnik *et al*., 2000). We conclude that the decrease in Ins(1,4,5)P_3 noted in MIOX4$^+$ seedlings correlates with increased PA levels. Since PC and PI levels are not affected in MIOX4$^+$ seedlings, the PA increase is most likely a result of compensatory DAG phosphorylation in response to altered Ins metabolism.

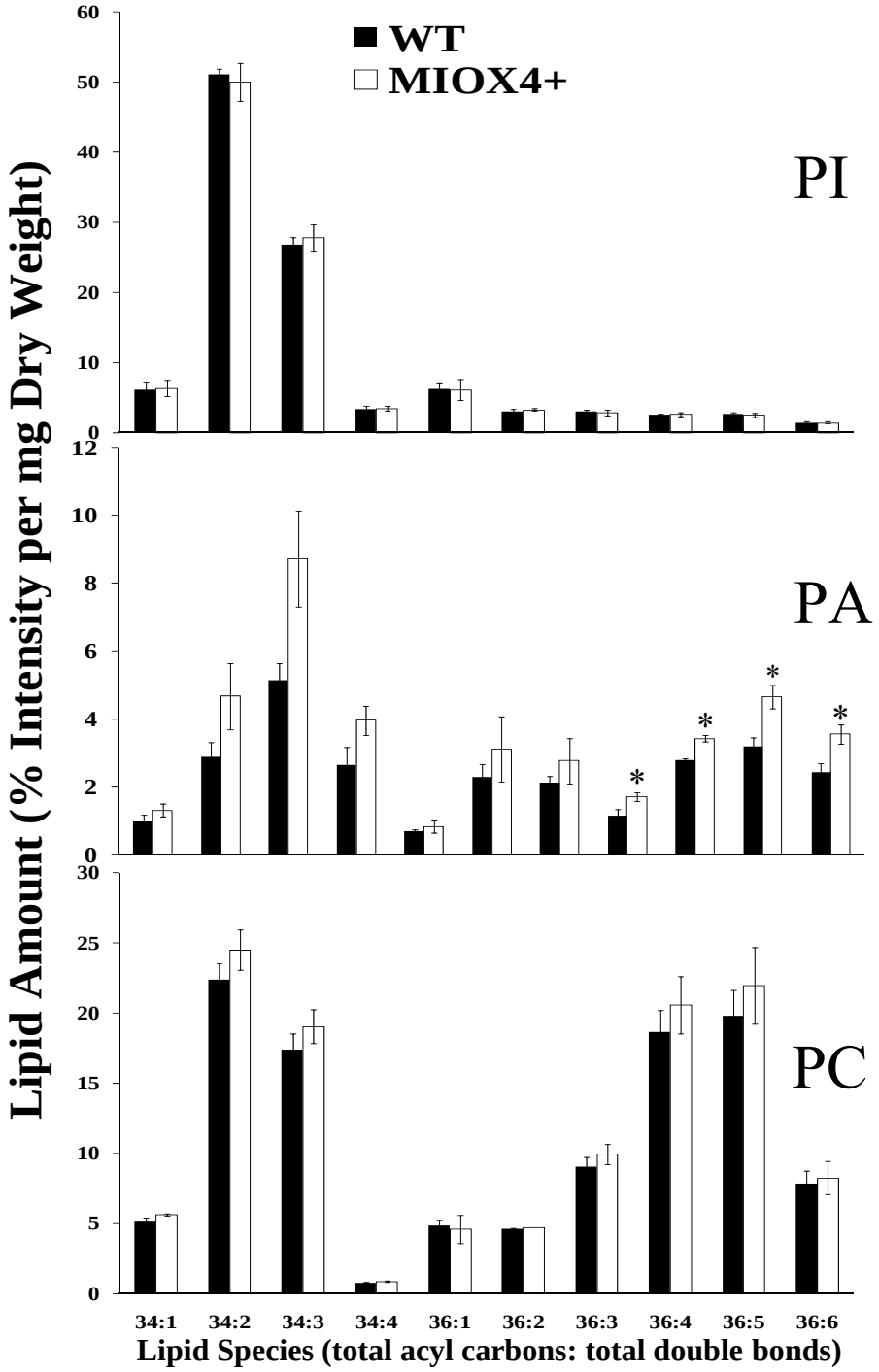

Figure 24. Lipid Analysis of WT and MIOX4^{+} Seedlings. Five-day-old light-grown seedlings were analyzed for lipid content as described in Methods. PI= phosphatidylinositol, PA= phosphatidic acid, and PC= phosphatidylcholine. Bars represent the mean ± SE (n=2-3 biological replicates, where each replicate contained hundreds of small seedlings). * indicates a p-value <0.05.

MIOX4 Overexpression Alters Seed Dormancy

Since imbibed seed and seedlings overexpressing MIOX4 contain decreased Ins, and seedlings have decreased Ins(1,4,5)P_3, they present an opportunity to determine the physiological impact of these alterations. We and others have previously examined seedlings altered in Ins(1,4,5)P_3 levels; however, the alterations examined thus far have resulted from altering Ins(1,4,5)P_3 hydrolysis by InsP-degrading enzymes including the *myo*-inositol polyphosphate 5-phosphatases (5PTases) (Berdy *et al*., 2001; Sanchez and Chua, 2001; Burnette *et al*., 2003; Williams *et al*., 2005; Gunesekera *et al*., 2007). Arabidopsis *5ptase* mutants contain elevated Ins(1,4,5)P_3 (Gunesekera *et al*., 2007), while ectopic expression of human or plant 5PTase genes in Arabidopsis and tobacco reduces Ins(1,4,5)P_3 levels (Sanchez and Chua, 2001; Perera *et al*., 2002; Burnette *et al*., 2003). These alterations thus impact InsP accumulation and Ins signaling, but do not alter other Ins metabolic events in the plant cell. The elevation of Ins(1,4,5)P_3 in *5ptase* mutants is associated with faster seed germination, increased sensitivity to ABA, and increased hypocotyl elongation in the dark, indicating a role for Ins(1,4,5)P_3 in these seedling events (Gunesekera *et al*., 2007).

To examine if MIOX4$^+$ seed dormancy and germination are altered, we produced age-matched seed populations that were harvested from WT and MIOX4$^+$ plants grown at the same time under identical conditions. Germination of seeds on 0.5x MS was determined by radicle protrusion from the seed coat. Harvested seeds were either after-ripened at room temperature (Figure 25A) or were germinated directly after surface sterilization (Figure 25B). When seed were after-ripened for 12 days, there was no difference in germination of MIOX4$^+$ and WT seeds (Figure 25A). However, when MIOX4$^+$ seed are germinated directly after harvest, they exhibit a small increase in dormancy as seen by an approximately 6-hour lag in germination as compared to WT seed (Figure 25B). Non-dormant seed were analyzed as a control by stratifying ripened seed for 3 days at 4^{o}C before germination. After this cold stratification, MIOX4$^+$ and WT seed reached 100% germination by 24 hrs, indicating no difference in germination after stratification (data not shown). We conclude that the overexpression of MIOX4 is correlated with a small increase in seed dormancy. In contrast, MIOX4 overexpression does not alter seed germination of non-dormant seeds that have been after-ripened or stratified.

We next examined whether the decrease in Ins and Ins(1,4,5)P_3 levels in MIOX4$^+$ seedlings was associated with alterations in seedling hypocotyl growth, as was noted for *5ptase*

mutants (Gunesekera *et al*., 2007). We found no evidence for a change in hypocotyl growth when MIOX4^{+} and WT seedlings were germinated on 0.5x MS and grown in the dark in a vertical orientation (Figure 26), nor was there a change in root length (data not shown). We conclude that the decrease in Ins and Ins(1,4,5)P_3 in MIOX4^{+} seedlings is not associated with growth changes in the hypocotyl and/or root.

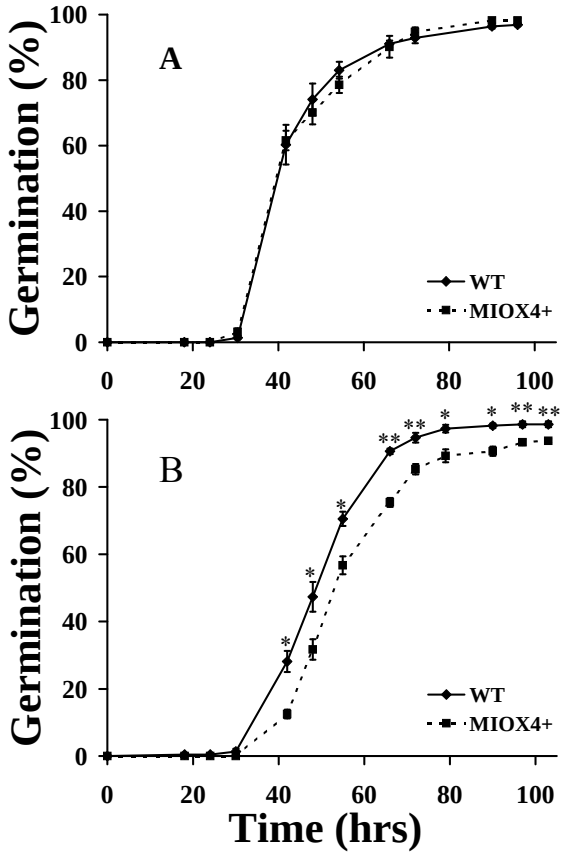

Figure 25. Dormancy of WT and MIOX4$^+$ Seeds. Seed from WT (solid line) and MIOX4$^+$ (dashed line) were harvested from plants, surface-sterilized, and germinated on 0.5x MS agar medium. Seeds were placed at 23°C under continuous light. Germination was scored over 100 hours. **A).** Seeds were allowed to ripen at room temperature for 12 days before the assay. **B).** Seeds were not allowed to ripen and were germinated 1 day after harvesting. Values represent the mean ± SE (n= 4 biological replicates, where each replicate contained 56 seeds) from one of two independent experiments with similar results. * indicates a 2-tailed p-value <0.05, and ** indicates a 2-tailed p-value < 0.005.

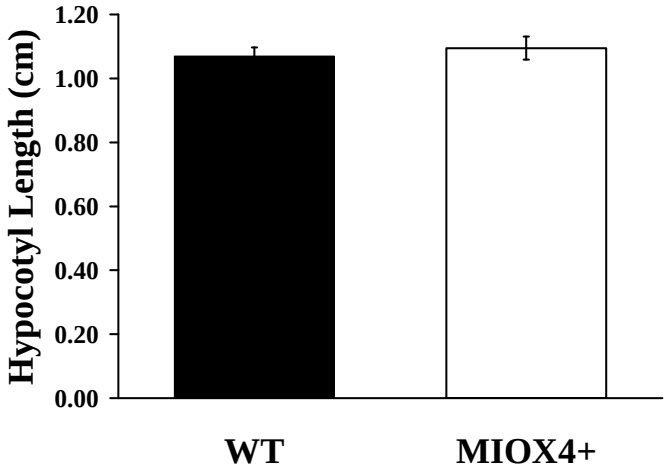

Figure 26. Hypocotyl Growth of WT and MIOX4^{+} Seedlings. Seeds were germinated and grown in the dark for 3 days on 0.5x MS agar medium. Hypocotyls from WT and MIOX4^{+} seedlings were measured. Bars represent the mean ± SE (n= 40 biological replicates) from one of two independent experiments with similar results.

MIOX4 Overexpression Alters Abscisic Acid Sensitivity of Seeds

Many studies have linked Ins(1,4,5)P_3 accumulation in plants with ABA sensitivity. ABA application to seedlings induces a transient increase in Ins(1,4,5)P_3, indicated in Figure 1 by ABA stimulation of phospholipase C, and changes in Ins(1,4,5)P_3 have been correlated with altered ABA sensitivity in seed germination and stomatal closure assays (Gilroy *et al*., 1990; Burnette *et al*., 2003). For example, *5ptase* mutants containing elevated Ins(1,4,5)P_3 are ABA hypersensitive (Gunesekera *et al.*, 2007), while seed overexpressing the At5PTase2 gene contain reduced Ins(1,4,5)P_3 and are ABA-insensitive in seed germination assays (Sanchez and Chua, 2001). To determine whether the increased oxidation of Ins and decrease in Ins(1,4,5)P_3 in MIOX4$^+$ plants alters ABA sensitivity, we performed seed germination assays in the presence of ABA. We produced age-matched seed populations were plated on 0.5x MS medium containing 0, 0.5, 1 and 2 μM ABA. After stratification for 6 days at 4^o C in the dark, plates were moved to continuous light and examined for radicle protrusion from the seed coat (germination) after 6 days. MIOX4$^+$ seeds were insensitive to 0.5 and 1 μM ABA as compared to WT seeds (Figure 27A). We also compared the time course for germination of MIOX4$^+$ seed in the presence of 1 μM ABA and found that this ABA insensitivity continued over the course of 10 days (Figure 27B). We conclude that overexpression of MIOX4 results in ABA-insensitivity during seed germination. This ABA-insensitivity is similar to that noted for plants overexpressing the At5PTase2 gene and for other ABA-insensitive mutants (Sanchez and Chua, 2001). Further, these data are consistent with a decrease in Ins upon imbibition of the seeds, and the known role of Ins(1,4,5)P_3 as a second messenger in the inhibitory effects of ABA on seed germination.

We also tested whether leaves of MIOX4$^+$ plants, which do not have an Ins depletion (Figure 28), contained alterations in ABA sensitivity. Endogenous ABA in leaves is known to cause stomatal closure during drought conditions. To test if MIOX4$^+$ leaves contain an alteration in response to endogenous levels of ABA, we measured water loss in detached leaves. Leaves from age-matched WT and MIOX4$^+$ plants were detached, and leaves were weighed at time points from 0 to 450 minutes. Water loss was calculated by converting dry weight to a percentage of the total fresh weight. Water loss did not differ between MIOX4$^+$ and WT leaves (Figure 28). We conclude that overexpression of MIOX4 does not impact the endogenous response to ABA in leaves.

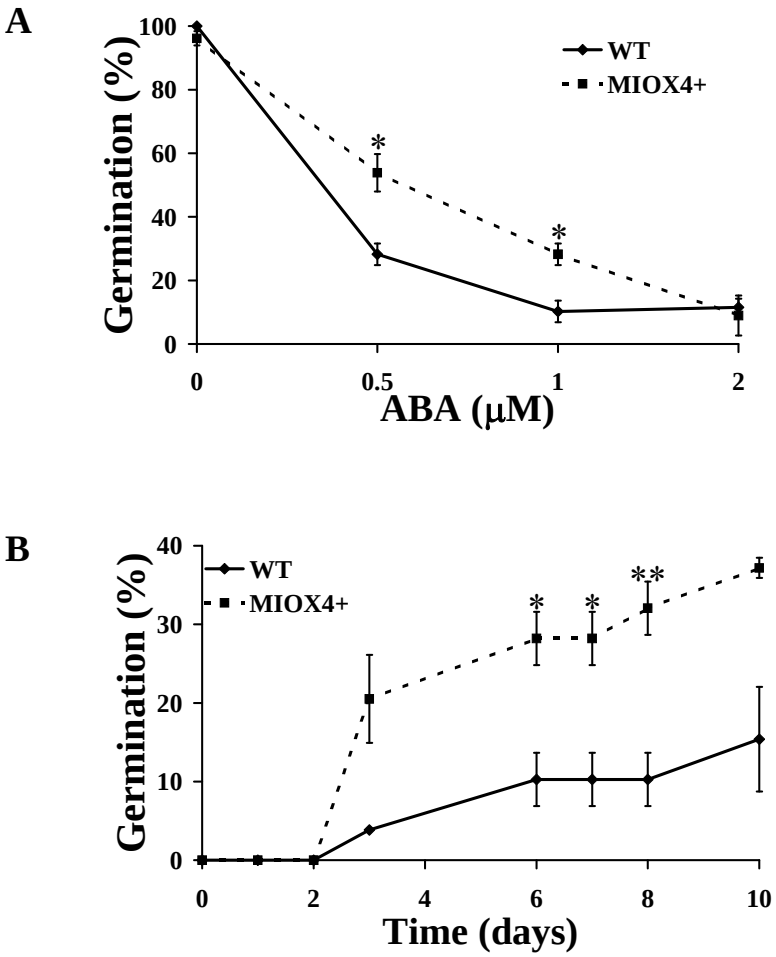

Figure 27. WT and MIOX4^{+} Seed Germination on ABA. WT (solid line) and MIOX4^{+} (dashed line) seeds were surface sterilized and plated on 0.5x MS agar medium with ABA. Seeds were stratified at 4°C for 6 days then placed at 23°C under continuous light. Germination was scored daily for 10 days. **A).** Germination was measured on increasing doses of ABA. Germination at day 6 is shown. **B).** Germination at 1 μM ABA is shown. Values represent the mean ± SE (n= 3 biological replicates, where each replicate contained 26 seeds) from one of six independent experiments with similar results. * indicates a 2-tailed p-value < 0.05, and ** indicates a 2-tailed p-value = 0.01.

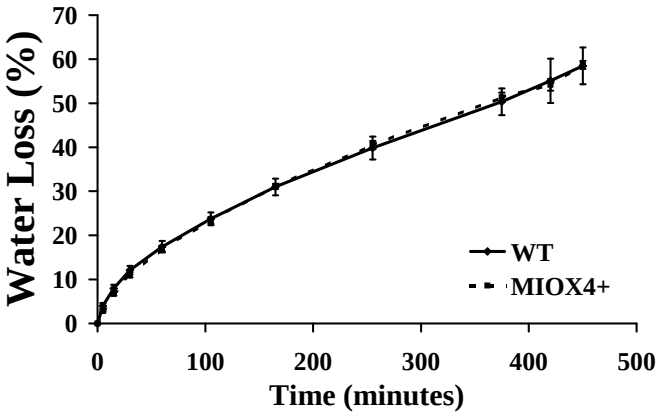

Figure 28. Water Loss of WT and MIOX4^{+} Expanded Leaves. WT (solid line) and MIOX4^{+} (dashed line) leaves were detached from 5-week-old plants and placed under continuous light. The weights of the leaves were measured over a time course. Water loss was calculated as percent of fresh weight. Bars represent the mean ± SE of three independent experiments (n= 5 biological replicates for each experiment).

MIOX4 Overexpression Alters NaCl-Sensitivity of Seeds

Increased Ins synthesis has been previously associated with osmolyte (pinitol) production and salt tolerance in certain halophytic plants such as ice plant (*Mesembryanthemum crystallinum*) (Nelson *et al*., 1998; Nelson *et al*., 1999). In contrast, data exists supporting a role for Ins(1,4,5)P_3 as a second messenger produced after salt stimulation of seedlings (DeWald *et al*., 2001; Takahashi *et al*., 2001). Thus, it was of interest to test whether MIOX4$^+$ seeds, which contain an increase in Ins when dry and a decrease in Ins upon imbibition, have altered responses to salt treatment. To determine whether the switch from increased Ins to Ins depletion in MIOX4$^+$ seed upon imbibition impacts responses to salt, we performed germination assays in the presence of different amounts of NaCl. MIOX4$^+$ and WT age-matched seeds were plated on 0.5x MS medium containing 0, 75, 100 and 125 mM NaCl and were stratified for 3 days at 4^o C in the dark. Plates were moved to continuous light and scored for germination. The MIOX4$^+$ seeds were slightly sensitive to 75 and 100 mM NaCl as compared to WT seed (Figure 29A). We also compared the time course for seed germination of MIOX4$^+$ seed in the presence of 100 mM NaCl and found that NaCl-sensitivity continued over the course of 96 hrs (Figure 29B). We conclude that overexpression of MIOX4 results in NaCl-sensitivity during seed germination.

The increase in NaCl-sensitivity in MIOX4$^+$ seeds suggests that the Ins depletion present at this stage may have resulted in a decrease in Ins-containing osmolytes such as pinitol, which is formed in halophytic plants by methylation of Ins. We measured Ins and pinitol in 5 day-old control and NaCl-treated MIOX4$^+$ and WT seedlings. Under control conditions, Ins levels were reduced in MIOX4$^+$ seedlings (as noted previously), and pinitol levels were unchanged in MIOX4$^+$ seedlings as compared to WT (Figure 29C). When seedlings were grown in the presence of salt, we found no significant difference of pinitol in MIOX4$^+$ seedlings compared to WT seedlings (Figure 29C). This indicates that the NaCl-sensitivity of MIOX4$^+$ seed compared to WT does not correlate with a decrease in pinitol. We also note that pinitol levels did not increase in either genotype upon salt stress compared to control conditions. This lack of pinitol increase upon salt treatment is in agreement with published data on Arabidopsis, indicating that osmolytes such as pinitol do not accumulate during salt stress (Ishitani *et al*., 1996). Together, these results suggest that NaCl-sensitivity of MIOX4$^+$ seed and Ins depletion in MIOX4$^+$ seedlings do not correlate with a decreased pinitol accumulation.

One unexpected finding we made during this experiment is that a 5-day NaCl treatment increased Ins levels 40% in MIOX4^{+} seedlings as compared to WT seedlings (Figure 29C). This finding indicates that overexpression of the MIOX4 gene allows seedlings to increase mass Ins levels after a NaCl treatment, possibly by eliciting down-regulation of the MIOX4 transgene. This ability to increase Ins levels is reminiscent of halophytic plants.

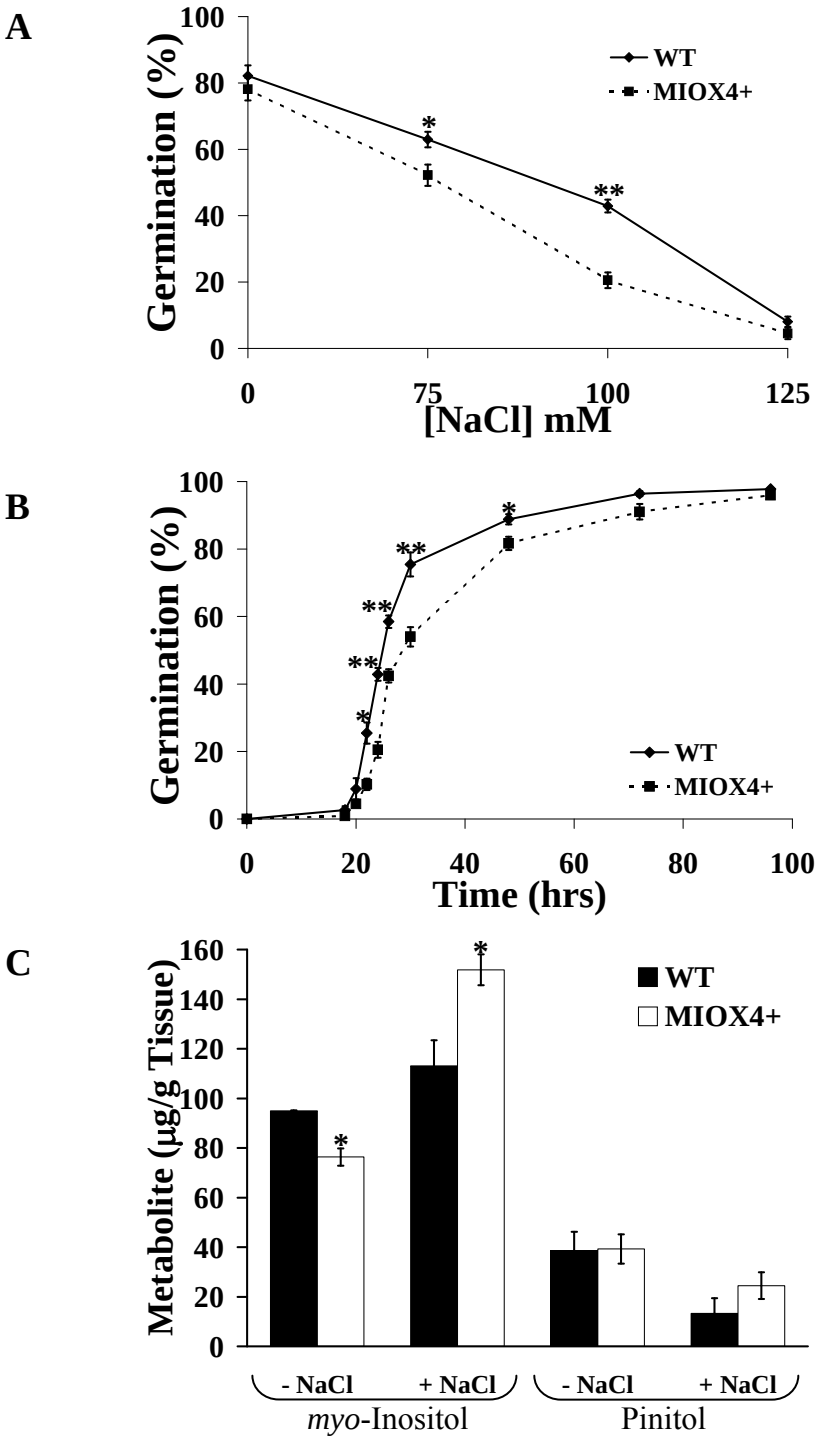

Figure 29. Germination and Metabolite Data of Seedlings Grown on NaCl. A and **B**). WT (solid line) and MIOX4^{+} (dashed line) seeds were plated on 0.5x MS agar medium with NaCl. Seeds were stratified at 4°C for 3 days then placed at 23°C under continuous light. Values represent the mean ± SE (n= 3 biological replicates, where each replicate contained 56 seeds) from one of two independent experiments with similar results. **A)**. Germination was measured on increasing doses of NaCl. Germination at 24 hrs is shown. **B)**. Germination was scored

periodically for 96 hours. Germination at 100 mM is shown. **C)**. NaCl-treated and control seedlings were frozen in liquid nitrogen, ground, extracted, reduced, derivatized, and analyzed by GC. Levels of Ins and pinitol are shown for WT (black bars) and MIOX4^{+} (white bars) seedlings grown on 0 and 100 mM NaCl. Bars represent the mean ± SE (n= 3 to 5 biological replicates, where each replicate contained hundreds of small seedlings) from one of two independent experiments with similar results. * indicates a p value ≤ 0.05. ** indicates a p value ≤ 0.005.

MIOX4 Overexpression Does Not Result in MIOX Protein Accumulation

Because we observed limited alterations of Ins in some tissues of MIOX4$^+$ plants, we decided to examine MIOX protein accumulation in these plants. A MIOX4 antibody was obtained from the laboratory of Dr. Craig Nessler, Virginia Tech. To produce this antibody, a MIOX4 recombinant protein was injected into rabbits (Cocalico Biologicals Inc.), producing a polyclonal antisera which recognizes both the MIOX4 recombinant protein and a MIOX2 fusion protein from transgenic plant extracts (Figure 30). We confirmed the identity of the MIOX2 fusion protein with an anti-GFP antibody, which shows that our MIOX2 fusion protein accumulates and is detectable by both antibodies (Figure 30A). We conclude that the anti-MIOX4 antibody is immuno-reactive with both MIOX2 and MIOX4 proteins. When this antibody is used on a membrane with crude plant extract, there are two immunoreactive bands present in seedlings. The upper abundant band is ~50 kD in size; and the lower band is ~45 kD in size. We think the upper 50 kD band is not MIOX because it is not reduced in a previously identified *miox2* mutant (Kanter *et al*., 2005), and it is not present in flowers, a tissue with high levels expression of both MIOX2 and MIOX4 (see Figure 20). This 50kD band is also not likely MIOX1 or MIOX5 because they have the similar predicted isoform identity and molecular masses (36.57 kD and 36.54 kD, respectively) as MIOX2 and MIOX4. The lower 45 kD immunoreactive band is closer to the predicted molecular masses of MIOX isoforms (MIOX2 37.05 kD and MIOX4 36.90 kD), and it is absent in seedling extract from the abovementioned *miox2* mutant (Kanter *et al*., 2005). Because of the similarity in MIOX isoform identity and size, this 45 kD band likely represents a combination of the MIOX isoforms present in the plant.

We sought to determine whether the MIOX4 protein accumulates in MIOX4$^+$ seedlings, leaves, and flowers. Figure 30B indicates that there is no difference in accumulation of the 45kD band between WT and MIOX4+ seedling and flowers. In leaves, the 45kD band is not present, which corresponds well with published data on MIOX2 and MIOX4 expression in leaves (Kanter *et al*., 2005) (also see Figure 20 and Ch II Figure 6). We conclude that, even though MIOX4$^+$ transgenic plants accumulate 8-fold MIOX4 RNA in seedlings and leaves, there is not a corresponding large increase in MIOX4 protein accumulation in either tissue, which is indicative of post-transcriptional control over MIOX4. However, given the limitations of our western blotting procedure, we cannot rule out that there are small increases in MIOX4 protein in the MIOX4$^+$ plants.

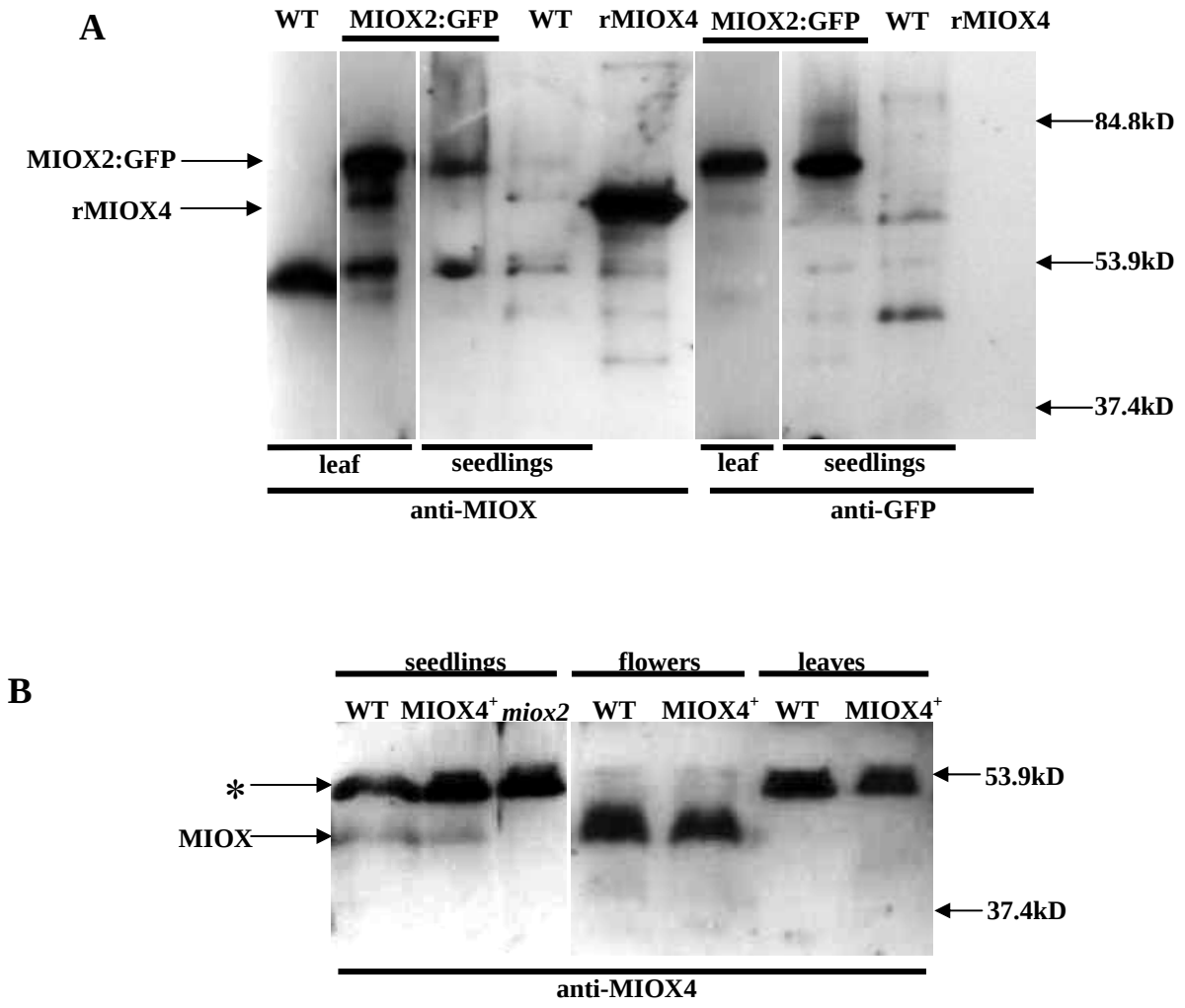

Figure 30. Western Blot of MIOX Transgenic Plants. Crude protein extracts were separated by SDS-PAGE, transferred to a membrane, and blotted. **A)** recombinant MIOX4 protein (rMIOX4), WT and MIOX2:GFP leaf and seedling extracts were blotted with the anti-MIOX4 antibody and with the anti-GFP antibody. **B)** WT, MIOX4^{+}, and *miox2* seedling and WT and MIOX4^{+} flower and leaf extracts were blotted with the anti-MIOX4 antibody. * denotes the 50kD non-specific band.

MIOX2 Overexpression Alters Levels of Ins and Other Metabolites

Our data suggests that the MIOX4 transgene is active in imbibed seed and seedlings of MIOX4^{+} plants and functions to lower Ins levels, increase DGlcA levels, and alter seed germination sensitivity to ABA and NaCl. However, our data also indicates that the expression of the MIOX4 transgene does not result in dramatically increased protein levels in mature tissue (Figure 30B) nor does it decrease Ins levels. Since the native MIOX2 gene is expressed at high levels in all these tissues (see Figure 20), we examined whether MIOX2 expression in transgenic plants has a greater overall impact on the Ins metabolic pathway. The 35S CaMV promoter was used to direct expression of the MIOX2 gene fused to the green fluorescent protein (GFP) gene, resulting in 14 transformants. Of those 14 transformants, two homozygous lines were identified and examined. The resulting MIOX2 transgenic plants (MIOX2^{+} plants) accumulate high levels of MIOX2:GFP fusion protein in leaves as seen in western blots (Figure 30A).

Metabolite data for MIOX2^{+} plants, shows that there are decreased Ins levels in all tissues examined, increased DGlcA in all tissues except seedlings, and increased downstream product, AsA, in all tissues except seedlings (Figure 31). These data indicate that expression of the MIOX2 fusion protein drives oxidation of Ins, and strongly suggests that the fusion protein is catalytically active in all tissues examined. Furthermore, these data support the idea that Ins can be channeled into AsA production when MIOX is overexpressed.

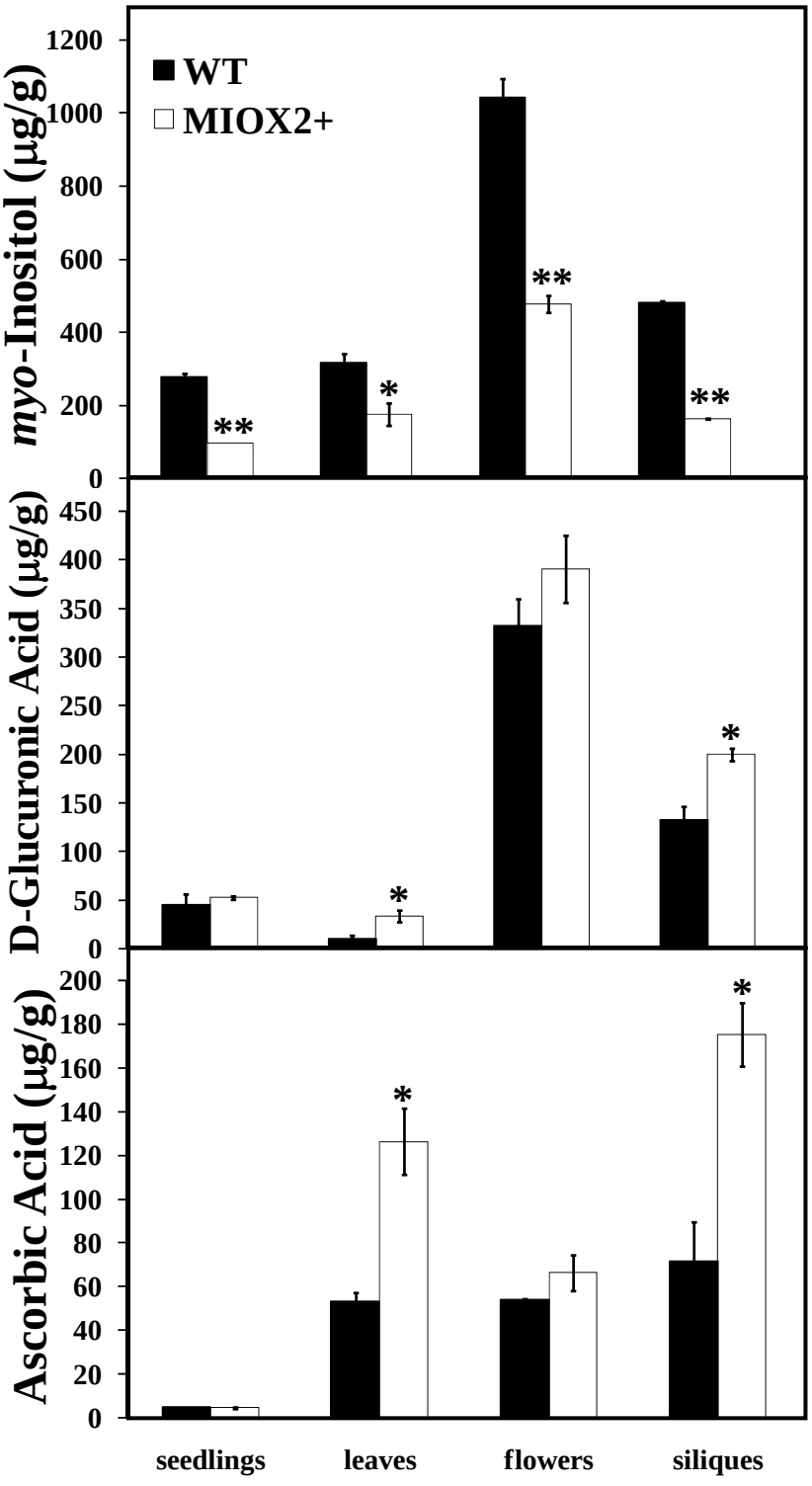

Figure 31. Metabolite Levels of WT and MIOX2$^+$ Tissues. MIOX2 was overexpressed in Arabidopsis and examined for metabolic changes. Tissues were harvested, ground in liquid nitrogen, extracted, reduced, derivatized, and analyzed by GC. Amounts are given in µg/g fresh tissue. **A)** Ins, **B)** DGlcA, and **C)** AsA were measured by GC for WT and MIOX2$^+$ plants. Bars

represent the mean ±SE where n= 3-5 independent, biological replicates, with each seedling replicate containing hundreds of seedlings, each leaf replicate contained 3-5 leaves, each flower replicate contained 50-100 flowers, and each silique replicate contained 30-50 siliques. * indicates p-value <0.05, ** indicates p-value <0.0005.

DISCUSSION

In plants, Ins is an important precursor to InsP signaling molecules, cell wall components, and more recently it's role as an AsA precursor has been debated (Lorence *et al*., 2004; Endres and Tenhaken, 2008) . Plant cells maintain a pool of free Ins to distribute for various needs, and oxidation of Ins, by MIOX, results in a commitment to cell wall and/or AsA synthesis as opposed to use in signal transduction pathways (Loewus and Murthy, 2000). MIOX is therefore positioned at a potentially important point for regulating the use of Ins in signaling versus metabolism. Plants overexpressing MIOX were previously shown to have increased levels of AsA (Lorence *et al*., 2004), demonstrating the possibility of directing Ins into AsA synthesis. Given that such a strategy has important implications for genetic engineering of AsA synthesis, we wanted to determine if the allocation of Ins in MIOX4$^+$ plants impacted Ins signaling and associated physiological events. We report here that MIOX4 overexpression leads to an Ins depletion and a reduction of the Ins second messenger, Ins(1,4,5)P_3, in seedlings, but not in tissues from later developmental stages. Furthermore, we show that the Ins and Ins(1,4,5)P_3 reductions in seedlings correlate with an impact on seed physiology.

Ins and Ins(1,4,5)P_3 Reductions in MIOX4$^+$ Seeds and Seedlings Correlates with Physiological Changes

We have shown that overexpression of MIOX4 impacts Ins levels differently at several stages of plant development. Of primary importance is our finding that MIOX4$^+$ seedlings contain reduced Ins and Ins(1,4,5)P_3 levels. This Ins depletion in MIOX4$^+$ seedlings is similar in nature to the Li^+-induced Ins depletion hypothesized in humans (Berridge, 1989) and proven experimentally in developing frog embryos (Maslanski *et al.*, 1992). It is important to note that the MIOX4$^+$ plants are the first transgenic plants characterized with alterations in Ins(1,4,5)P_3 resulting from manipulation of Ins catabolism, as opposed to manipulating Ins signaling. Additionally, these plants were observed to have increased levels of PA and unchanged levels of PC and PI. The mechanism for increased PA in the MIOX4$^+$ seedlings is unclear; however, we propose that the elevated PA results from compensatory phosphorylation of DAG stimulated indirectly by the reduction in Ins levels.

By analyzing MIOX4$^+$ seed and seedlings, we were able to correlate the Ins and Ins(1,4,5)P_3 reductions with ABA-insensitivity, increased seed dormancy, and NaCl-sensitivity

(Figures 22, 23, 25, 27, & 29). This ABA-insensitivity is not surprising given that MIOX4$^+$ seedlings have decreased Ins(1,4,5)P_3, which can serve as a second messenger in ABA signaling pathways. For example, reducing levels of Ins(1,4,5)P_3 by ectopic expression of the At5PTase2 gene in Arabidopsis results in ABA-insensitivity in seed germination assays, while ectopic expression of the At5PTase1 gene reduces ABA-sensitivity of guard cells (Sanchez and Chua, 2001; Burnette *et al*., 2003). In contrast, genetic loss-of-function mutants in 5PTases and other genes such as *sac9*, often contain elevated Ins(1,4,5)P_3 levels and ABA-hypersensitivity, indicating a role for Ins(1,4,5)P_3 in mediating the effects of ABA (Williams *et al*., 2005). It is important to note that we did not find evidence for ABA-insensitivity in MIOX4$^+$ leaves in water loss assays (Figure 28), which is not surprising, given that this tissue does not contain reduced Ins levels and is not expected to have altered Ins(1,4,5)P_3 levels as a result.

In contrast to the ABA-insensitivity noted in seed germination assays, we found that MIOX4$^+$ seed have increased seed dormancy (Figure 25B), and no changes in seed germination after dormancy is broken (Figure 25A). Since we observed increased levels of Ins in the MIOX4$^+$ dry seed, we speculate that the increase in Ins in MIOX4$^+$ dry seed is the primary determinant of the small increase in seed dormancy. Furthermore, we observed a dramatic increase of Ins levels, in general, in imbibed seed as compared to dry seed. This increase in absolute Ins levels, is likely due to the increased hydrolysis of an Ins-containing molecule called phytate ($InsP_6$) which is deposited during seed development, and its hydrolysis may be important for breaking seed dormancy (Scott and Loewus, 1986; Quick *et al*., 1997). $InsP_6$ levels decrease during the breaking of dormancy, while activity of the $InsP_6$–degrading enzyme, phytase increases (Andriotis *et al*., 2005). With more Ins available for $InsP_6$ synthesis in the MIOX4$^+$ silique and dry seed, we could expect increased hydrolysis required for the breaking of seed dormancy.

We also tested MIOX4$^+$ seed for salt-sensitivity in seed germination assays (Figure 29A-B). Ins and Ins(1,4,5)P_3 are expected to impact salt-sensitivity in unique ways. Similar to ABA, NaCl can stimulate an increase in Ins(1,4,5)P_3 levels, and genetic mutants such as *fry1* (an Ins polyphosphate bisphosphatase) contain elevated Ins(1,4,5)P_3 and are salt-, cold- and ABA-hypersensitive (Xiong *et al*., 2001). However, the NaCl sensitivity seems to be opposite the ABA-insensitivity. Therefore, the NaCl sensitivity might occur specifically because of the reduction in Ins, beginning with imbibed seeds and becoming exaggerated in 5-day-old

seedlings. Since Ins is a known osmolyte (Nelson *et al*., 1998), a decrease in Ins could result in salt-sensitivity, irrespective of Ins(1,4,5)P_3 levels. Alternatively, the decrease in AsA in MIOX4$^+$ dry seed could also result in salt sensitivity as judged by the fact that mutants with reduced AsA are often stress-sensitive (Conklin *et al*., 1996; Conklin *et al*., 2000).

Developmental Regulation of Ins Levels

Our data supports a tissue-specific control of the MIOX4 transgene and effects on Ins levels. We found that MIOX4$^+$ overexpression in seedlings negatively impacts Ins levels, but does not reduce Ins levels in leaves (Figure 22). In addition, our qPCR data indicate that the MIOX4 transgene does not increase MIOX4 expression in tissues with high endogenous MIOX4 expression such as flowers and siliques (Figure 20), and western blots indicate that the MIOX4 protein does not accumulate much higher in MIOX4$^+$ tissues compared to WT tissues (Figure 30). However, MIOX4$^+$ leaves, flowers, and siliques contained elevated Ins levels. This elevated Ins may indicate that increased MIOX4 expression in these tissues stimulates additional Ins synthesis. Alternatively, because Ins and DGlcA could be rapidly metabolized, we cannot rule out the possibility that elevated Ins in a tissue such as leaves is transported to sink tissues such as flowers and siliques (Figure 22). A third possible explanation for elevated Ins in MIOX4$^+$ leaves, flowers and siliques is MIOX gene silencing. In this scenario, elevated MIOX4 transgene expression could trigger an endogenous miRNA pathway and silence MIOX4 or other MIOX gene expression.

Another indication of altered Ins synthesis in MIOX4$^+$ plants was found when we measured an increase in Ins levels in NaCl-treated seedlings (Figure 29C). In halophytic plants, salt treatment can induce Ins synthesis as seen by an increase in *myo*-inositol phosphate synthase RNA and increased Ins levels (Wang *et al*., 2002; Kore-eda *et al*., 2004). In contrast, glycophytic plants such as Arabidopsis have been shown to lack RNA induction of *myo*-inositol phosphate synthase and the subsequent increase in Ins after salt stress (Ishitani *et al*., 1996; Gong *et al*., 2005). Thus, the overexpression of MIOX4$^+$ in seedlings could result in increased Ins accumulation during NaCl stress. Conversely, the MIOX4 overexpression might be depressed upon salt treatment resulting in MIOX4 silencing and increased Ins.

Ins as a Precursor for Ascorbic Acid Synthesis

There is a debate about whether Ins is used as a precursor for AsA synthesis in plants. We have shown that overexpression of MIOX2 results in decreased Ins in all tissues examined, increased DGlcA in all tissues except seedlings, and increased AsA in all tissues except seedlings (Figure 31). This data strongly supports a role of Ins as a precursor for AsA; however, only metabolic flux analyses would resolve this role. We have shown that overexpression of MIOX4 results in greatly reduced Ins only in seedlings, and although there is a corresponding increase of DGlcA, there is not an increase in AsA (Figure 22). There is not a decrease of Ins in other tissues examined. Furthermore, in MIOX4^{+} plants, we have shown that the overexpression of MIOX4 does not yield a robust accumulation of MIOX4 protein in mature tissues, including leaves, (Figure 30B), making this tissue an inappropriate source for examination of MIOX direction of carbon into AsA synthesis. We suspect that overexpression of MIOX2 yields more protein accumulation and Ins oxidation than overexpression of MIOX4 (Figure 30A) because native MIOX2 gene expression occurs almost constitutively throughout development, while MIOX4 is most highly expressed in reproductive tissues (see Figure 20). This could result in less down-regulation of MIOX2 when overexpressed in the plant.

Given the connections to salt tolerance and AsA synthesis (Benavides *et al*., 2000; He *et al*., 2004; Anitha *et al*., 2005; Eltayeb *et al*., 2007), the Ins metabolism and signaling pathway is an attractive pathway to manipulate for desired traits. We conclude that MIOX4 overexpression can negatively impact Ins signaling capacity of seedlings because of the signaling alterations in ABA and salt sensitivities. Additionally, MIOX4 is subject to post-transcriptional regulation; however, MIOX2 overexpression is more constitutive, indicating that MIOX2 is a better candidate for manipulation by overexpression. Our work presented here illustrates that successful manipulation of this pathway will require a thorough understanding of the role of Ins in both signaling and metabolism and the integration between these areas.

CHAPTER IV

SUMMARY AND FUTURE DIRECTIONS

Ins has many functions and destinations within the plant cell (Loewus and Loewus, 1983). Ins is the precursor to InsP signaling molecules (Munnik and Testerink, 2008), cell wall components (Kanter *et al*., 2005), hormone conjugates (Bandurski, 1979), phosphorous storage (Grabau, 2002), and it has been shown as a precursor in AsA synthesis (Lorence *et al*., 2004), a debated topic. Understanding the enzymes that interact with Ins is key to defining, and even manipulating, Ins use in plants. Plant cells maintain a pool of free Ins to distribute for various needs, and oxidation of Ins, by MIOX, results in a commitment to cell wall and/or AsA synthesis as opposed to use in signal transduction pathways (Loewus and Murthy, 2000). MIOX is therefore positioned at a potentially important point for regulating the use of Ins in signaling versus metabolism.

To gain more understanding of how MIOX is involved in Ins signaling and metabolism, I have performed the following work: examined transcription of MIOX2 and MIOX4 spatially within the plant and in response to varying conditions; identified and further analyzed phenotypic alterations in loss-of-function mutants for MIOX2 and MIOX 4 genes with a focus on nutrient and signaling responses; measured inositol-related metabolites under conditions where altered phenotypes are present; created GFP fusions to determine subcellular localization in whole plants; and characterized a gain-of-function transgenic in the MIOX4 gene.

I have shown that MIOX2 and MIOX4 play a role in metabolism of Ins and the inositol-signaling pathway. Overexpression of MIOX4 impacts the Ins(1,4,5)P_3 signaling pathway by removing Ins from the pool, thus altering the Ins(1,4,5)P_3 levels and signaling mechanisms; however this does not occur via alterations of phosphatidylinositol levels. This finding connecting metabolism and signaling demonstrates the need to fully understand how physiology is altered for the purpose of genetically engineering a metabolic pathway. MIOX4 has been implicated in increased AsA synthesis in plants; however I and others (Endres and Tenhaken, 2008) have shown evidence that this overexpression is tempered by the plant's innate post-transcriptional control of MIOX4. I would recommend manipulating MIOX2 for the purpose of

increased AsA in plants, as I have shown that its activity is not diminished as a plant matures. MIOX2 orthologs in crop species could be identified and manipulated.

Other members of the Gillaspy lab and I are beginning to explore how Ins and its associated proteins are involved in nutrient-sensing and regulation in the plant. I have presented evidence that two of the four MIOX proteins in Arabidopsis play a role in plant growth and development dependent upon nutrient conditions in which the plant is grown, and there expression patterns are correspondingly altered. We know that an Ins polyphosphate 5-phosphatase (At5PTase13) directly binds with the nutrient sensor, SnRK1.1, and regulates its stability in various nutrient conditions (Ananieva *et al*., 2008). It is reasonable to hypothesize that MIOX is another protein-binding partner in the SnRK complex, and regulates levels of Ins available for use as an alternate carbon source. In fact, the GFP localization pattern of MIOX4:GFP closely mimics that of At5PTase13 (Ananieva *et al*., 2008), suggesting that an At5PTase13: MIOX4 complex could be forming in the nucleus. It is also known that InsPs are involved in chromatin remodeling in yeast (Steger *et al*., 2003). Therefore, a nutrient-sensing complex that binds InsPs could potentially regulate gene function at the level of transcription.

MIOX function is understood to play a role in diabetes in animals, specifically catalyzing the oxidation of two Ins isomers, *myo* and D-*chiro*-inositol (Arner *et al.*, 2001). Both *myo*- and D-*chiro* Ins are known components of endogenous Ins phosphoglycans, which have been reported to act as insulin mediators (Frick *et al*., 1998; Nascimento *et al*., 2006). There is evidence that administration of inositols lowers blood glucose in diabetes and enhances insulin action (Brautigan *et al*., 2005; Nascimento *et al*., 2006). Therefore, it seems clear that the animal MIOX also plays a role in the nutrient status of animal cells. Perhaps increased understanding of MIOX function in plant systems can enhance the body of knowledge available for diabetes research.

Although I have characterized MIOX2 and MIOX4 in Arabidopsis, the question remains as to the role of MIOX1 and MIOX5 in Ins catabolism. Even though examination of these genes is outside the scope of this work, it would be beneficial to understand how these genes function and why Arabidopsis utilizes four different MIOX genes. Indeed, their existence could be the result of gene duplication. However, they may control more specialized roles involving Ins signaling or metabolism, or both, that have yet to be discovered.

As the efforts are ongoing to feed and fuel a hungry world, I think understanding the basics of plant metabolism is key to developing plants that are more nutritious and can thrive in a wider range of growth conditions.

REFERENCES

Alonso JM, Stepanova AN, Leisse TJ, Kim CJ, Chen H, Shinn P, Stevenson DK, Zimmerman J, Barajas P, Cheuk R, Gadrinab C, Heller C, Jeske A, Koesema E, Meyers CC, Parker H, Prednis L, Ansari Y, Choy N, Deen H, Geralt M, Hazari N, Hom E, Karnes M, Mulholland C, Ndubaku R, Schmidt I, Guzman P, Aguilar-Henonin L, Schmid M, Weigel D, Carter DE, Marchand T, Risseeuw E, Brogden D, Zeko A, Crosby WL, Berry CC, Ecker JR (2003) Genome-wide insertional mutagenesis of *Arabidopsis thaliana*. Science **301:** 653-657

Ananieva E, Gillaspy G, Ely A, Burnette R, Erickson FL (2008) *Myo*-Inositol Polyphosphate 5-Phosphatase 13 Functions in Glucose and ABA Responses. Plant Physiology **148:** 1868-1882

Andersson MX, Kourtchenko O, Dangl JL, Mackey D, Ellerstrom M (2006) Phospholipase-dependent signalling during the AvrRpm1- and AvrRpt2-induced disease resistance responses in *Arabidopsis thaliana*. Plant J **47:** 947-959

Andriotis VME, Smith SB, Ross JD (2005) Phytic acid mobilization is an early response to chilling of the embryonic axes from dormant oilseed of hazel (*Corylus avellana*). Journal of Experimental Botany **56:** 537-545

Anitha T, Suriyavathana M, Thiyagarajan K (2005) Effect of salt stress on ascorbic acid and DNA content in the seedlings of rice (*Oryza sativa*). Journal of Ecotoxicology & Environmental Monitoring **15:** 37-40

Arner R, Prabhu K, Krishnan V, Johnson M, Reddy C (2006) *myo*-Inositol oxygenase: molecular cloning and expression of a unique enzyme that oxidizes *myo*-inositol and D-*chiro*-inositol. Biochem Biophys Res Commun **339:** 816–820

Arner RJ, Prabhu KS, Thompson JT, Hildenbrandt GR, Liken AD, Reddy CC (2001) *myo*-Inositol oxygenase: molecular cloning and expression of a unique enzyme that oxidizes *myo*-inositol and D-*chiro*-inositol. Biochem J **360:** 313-320.

Baena-Gonzalez E, Rolland F, Thevelein JM, Sheen J (2007) A central integrator of transcription networks in plant stress and energy signalling. Nature (London, United Kingdom) **448:** 938-942

Bandurski RS (1979) Chemistry and physiology of *myo*-inositol esters of indole 3-acetic acid. *In* WW Wells, F Eisenberg, Jr., eds, Cyclitols and Phosphoinositides. Academic Press, London, New York, pp 35-54

Banhegyi G, Braun L, Csala M, Puskas F, Mandl J (1997) Ascorbate metabolism and its regulation in animals. Free Radic Biol Med **23:** 793-803

Bechtold N, Ellis J, Pelletier G (1993) *In planta* Agrobacterium mediated gene transfer by infiltration of adult *Arabidopsis thaliana* plants. Comptes Rendus De L'academic Des Sciences Serie Iii Sciences De La Vie **316:** 1194-1199

Benavides MP, Marconi PL, Gallego SM, Comba ME, Tomaro ML (2000) Relationship between antioxidant defence systems and salt tolerance in *Solanum tuberosum*. Australian Journal of Plant Physiology **27:** 273-278

Berdy S, Kudla J, Gruissem W, Gillaspy G (2001) Molecular characterization of *At*5PTase1, an inositol phosphatase capable of terminating IP_3 signaling. Plant Physiol **126:** 801-810

Berridge MJ (1989) Inositol trisphosphate, calcium, lithium, and cell signaling. Jama **262:** 1834-1841

Berridge MJ (1993) Inositol trisphosphate and calcium signaling. Nature **361:** 315-325
Berridge MJ (2005) Unlocking the secrets of cell signaling. Annu Rev Physiol **67:** 1-21
Bohnert HJ, Nelson DE, Jensen RG (1995) Adaptations to environmental stresses. Plant Cell **7:** 1099-1111
Brautigan DL, Brown M, Grindrod S, Chinigo G, Kruszewski A, Lukasik SM, Bushweller JH, Horal M, Keller S, Tamura S (2005) Allosteric activation of protein phosphatase 2C by D-*chiro*-inositol-galactosamine, a putative mediator mimetic of insulin action. Biochemistry **44:** 11067–11073
Brown PM, Caradoc-Davies TT, Dickson JM, Cooper GJS, Loomes KM, Baker EN (2006) Purification, crystallization and preliminary crystallographic analysis of mouse *myo*-inositol oxygenase. Acta Crystallographica, Section F: Structural Biology and Crystallization Communications **F62:** 811-813
Burnette RN, Gunesekera BM, Gillaspy GE (2003) An Arabidopsis inositol 5-phosphatase gain-of-function alters abscisic acid signaling. Plant Physiol **132:** 1011-1019
Chen IW, Charalampous CF (1966) Biochemical studies on D-Inositol 1-phosphate as an intermediate in the biosynthesis of inositol from glucose-6-phosphate, and characteristics of two reactions in this biosynthesis. J. Biol. Chem. **241:** 2194-2199
Chen X, Lin WH, Wang Y, Luan S, Xue HW (2008) An Inositol Polyphosphate 5-Phosphatase Functions in PHOTOTROPIN1 Signaling in Arabidopis by Altering Cytosolic $Ca2^{+}$. Plant Cell
Cho M, Shears S, Boss W (1993) Changes in phosphatidylinositol metabolism in response to hyperosmotic stress in *Daucus carota* L. cells grown in suspension culture. Plant Physiol. **103:** 637-647
Conklin PL, Saracco SA, Norris SR, Last RL (2000) Identification of ascorbic acid-deficient *Arabidopsis thaliana* mutants. Genetics **154:** 847-856
Conklin PL, Williams EH, Last RL (1996) Environmental stress sensitivity of an ascorbic acid-deficient Arabidopsis mutant. Proc. Natl. Acad. Sci. **93:** 9970-9974
Devaiah SP, Roth MR, Baughman E, Li M, Tamura P, Jeannotte R, Welti R, Wang X (2006) Quantitative profiling of polar glycerolipid species from organs of wild-type Arabidopsis and a PHOSPHOLIPASE Da1 knockout mutant. Phytochemistry (Elsevier) **67:** 1907-1924
DeWald DB, Torabinejad J, Jones CA, Shope JC, Cangelosi AR, Thompson JE, Prestwich GD, Hama H (2001) Rapid accumulation of phosphatidylinositol 4,5-bisphosphate and inositol 1,4,5-trisphosphate correlates with calcium mobilization in salt-stressed arabidopsis. Plant Physiol. **126:** 759-769.
Eisenberg F, Bolden AH, Loewus FA (1964) Inositol formation by cyclization of glucose chain in rat testis. Biochemical and Biophysical Research Communications **14:** 419-424
Eltayeb AE, Kawano N, Badawi GH, Kaminaka H, Sanekata T, Shibahara T, Inanaga S, Tanaka K (2007) Overexpression of monodehydroascorbate reductase in transgenic tobacco confers enhanced tolerance to ozone, salt and polyethylene glycol stresses. Planta **225:** 1255-1264
Endres S, Tenhaken R (2008) *myo*-Inositol oxygenase controls the level of *myo*-inositol in Arabidopsis but does not increase ascorbic acid. Plant Physiol. **10.1104:** pp.108.130948
Ercetin M, Ananieva EA, Safaee NM, Torabinejad J, Robinson J, Gillaspy GE (2008) A Phosphotidylinositol Phosphate-Specific *myo*-Inositol Polyphosphate 5-Phosphatase Required for Seedling Growth. Plant Molecular Biology **67**:375-388

Fiehn O, Kopka J, Dormann P, Altmann T, Trethewey RN, Willmitzer L (2000) Metabolite profiling for plant functional genomics. Nat. Biotechnol. **18:** 1157-1161

Frick WW, Bauer A, Bauer J, Wied S, Muller G (1998) Insulin-mimetic signalling of synthetic phosphoinositolglycans in isolated rat adipocytes. The Biochemical Journal **336:** 163-181

Gibon Y, Usadel B, Blaesing Oliver E, Kamlage B, Hoehne M, Trethewey R, Stitt M (2006) Integration of metabolite with transcript and enzyme activity profiling during diurnal cycles in Arabidopsis rosettes. Genome Biol. **7:** R76

Gillaspy GE, Ercetin ME, Burnette RN (2004) Inositol metabolism in plant cells: a genomics perspective. *In* A Hemantaranjan, ed, Advances in Plant Physiology, Vol 7, India, pp 145-158

Gilroy S, Read ND, Trewavas AJ (1990) Elevation of cytoplasmic calcium by caged calcium or caged inositol triphosphate initiates stomatal closure. Nature **346:** 769-771

Gong Q, Li P, Ma S, Indu Rupassara S, Bohnert HJ (2005) Salinity stress adaptation competence in the extremophile *Thellungiella halophila* in comparison with its relative *Arabidopsis thaliana*. The Plant Journal **44:** 826-839

Grabau EA (2002) Phytase expression in transgenic plants. *In* NR Reddy, SK Sathe, eds, Food Phytates. CRC Press, Boca Raton, FL, pp 85-105

Gunesekera B, Torabinejad J, Robinson J, Gillaspy GE (2007) Inositol polyphosphate 5-phosphatases 1 and 2 are required for regulating seedling growth. Plant Physiol. **143:** 1408-1417

He W, Huang C, Yang Y, Zhang F, Zhang L (2004) Protective function of ascorbic acid in plant against salt stress. Xibei Zhiwu Xuebao **24:** 2196-2201

Hong Y, Pan X, RuthWelti, XueminWang (2008) Phospholipase Da3 Is Involved in the Hyperosmotic Response in Arabidopsis. The Plant Cell **20:** 803–816

Horton P, Park K-J, Obayashi T, Nakai K (2006) Protein subcellular localization prediction with WoLF PSORT. Series on Advances in Bioinformatics and Computational Biology **3:** 39-48

Ishitani M, Majumder AL, Bornhouser A, Michalowski CB, Jensen R, Bohnert H (1996) Coordinate transcription induction of *myo*-inositol metabolism during environmental stress. Plant Journal **9:** 537-548

Jefferson RA (1987) Assaying chimeric genes in plants: The GUS fusion system. Plant Mol. Biol. Rep. **5:** 387-405

Jung P, Tanner W, Wolter K (1972) The fate of *myo*-insoitol infraxinus tissue culture. Phytochemistry **11:** 1655-1659

Kanter U, Usadel B, Guerineau F, Li Y, Pauly M, Tenhaken R (2005) The inositol oxygenase gene family of Arabidopsis is involved in the biosynthesis of nucleotide sugar precursors for cell-wall matrix polysaccharides. Planta **221:** 243-254

Koller F, Hoffmann-Ostenhof O (1979) *myo*-Inositol oxygenase from rat kidneys. I: Purification by affinity chromatography; physical and catalytic properties. Hoppe Seylers Z Physiol. Chem. **360:** 507-513

Kore-eda S, Cushman MA, Akselrod I, Bufford D, Fredrickson M, Clark E, Cushman JC (2004) Transcript profiling of salinity stress responses by large-scale expressed sequence tag analysis in *Mesembryanthemum crystallinum*. Gene **341:** 83-92

Krinke O, Novotna Z, Valentova O, Martinec J (2007) Inositol trisphosphate receptor in higher plants: is it real? Journal of Experimental Botany **58:** 361–376

Loewus F (1965) Inositol metabolism and cell wall formation in plants. Fed. Proc. **24:** 855-862.
Loewus FA, Loewus MW (1983) *Myo*-inositol: its biosynthesis and metabolism. Annu. Rev. Plant Physiol. **34:** 137-161
Loewus FA, Murthy PPN (2000) *Myo*-Inositol Metabolism in Plants. Plant Sci. **150:** 1-19
Loewus MW (1977) Hydrogen isotope effects in the cyclization of D-glucose 6-phosphate by *myo*-inositol-1-phosphate synthase. J. Biol. Chem. **252:** 7221-7223.
Loewus MW, Loewus FA (1980) The C-5 hydrogen isotope-effect in *myo*-inositol 1-phosphate synthase as evidence for the *myo*-inositol oxidation-pathway. Carbohydr. Res. **82:** 333-342.
Loewus MW, Loewus FA, Brillinger GU, Otsuka H, Floss HG (1980) Stereochemistry of the *myo*-inositol-1-phosphate synthase reaction. J. Biol. Chem. **255:** 11710-11712.
Lorence A, Chevone BI, Mendes P, Nessler CL (2004) *myo*-inositol oxygenase offers a possible entry point into plant ascorbate biosynthesis. Plant Physiol. **134:** 1200-1205
Majumder AL, Johnson MD, Henry SA (1997) 1-L-*myo*-inositol-1-phosphate synthase. Biochim. Biophys. Acta **1348:** 245-256.
Maslanski JA, Leshko L, Busa WB (1992) Lithium-Sensitive Production of Inositol Phosphates During Amphibian Embryonic Mesoderm Induction. Science **256:** 243-245
Michell RH (2007) Evolution of the diverse biological roles of inositols. Biochem. Soc. Symp.**:** 223-246
Michell RH (2008) Inositol derivatives: evolution and functions. Nat. Rev. Mol. Cell Biol. **9:** 151-161
Moskala R, Reddy CC, Minard RD, Hamilton GA (1981) An oxygen-18 tracer investigation of the mechanism of *myo*-inositol oxygenase. Biochemical and Biophysical Research Communications **99:** 107-113
Munnik T, Meijer HJ, Ter Riet B, Hirt H, Frank W, Bartels D, Musgrave A (2000) Hyperosmotic stress stimulates phospholipase D activity and elevates the levels of phosphatidic acid and diacylglycerol pyrophosphate. Plant J. **22:** 147-154
Munnik T, Testerink C (2008) Plant phospholipid signaling - 'in a nutshell'. J. Lipid Res.**:** jlr.R800098-JLR800200
Nascimento NRF, Lessa LMA, Kerntopf MR, Sousa CM, Alves RS, Queiroz MGR, Price J, Heimark DB, Larner J, Du X, Brownlee M, Gow A, Davis C, Fonteles MC (2006) Inositols prevent and reverse endothelial dysfunction in diabetic rat and rabbit vasculature metabolically and by scavenging superoxide. Proc. Natl. Acad. Sci. **103:** 218-223
Nayak B, Xie P, Akagi S, Yang Q, Sun L, Wada J, Thakur A, Danesh F, Chugh S, Kanwar Y (2005) Modulation of renal-specific oxidoreductase/*myo*-inositol oxygenase by high-glucose ambience. Proc. Natl. Acad. Sci. USA **102:** 17952–17957
Nelson DE, Koukoumanos M, Bohnert HJ (1999) *Myo*-inositol-dependent sodium uptake in ice plant. Plant Physiol. **119:** 165-172
Nelson DE, Rammesmayer G, Bohnert H (1998) Regulation of cell specific inositol metabolism and transport in plant salinity tolerance. Plant Cell **10:** 753-764
Nelson DE, Rammesmayer G, Bohnert HJ (1998) Regulation of cell-specific inositol metabolism and transport in plant salinity tolerance. Plant Cell **10:** 753-764
Nishikimi M, Fukuyama R, Minoshima S, Shimizu N, Yagi K (1994) Cloning and chromosomal mapping of the human nonfunctional gene for L- gulono-gamma-lactone

oxidase, the enzyme for L-ascorbic acid biosynthesis missing in man. J. Biol. Chem. **269:** 13685-13688.

Ohto M-a, Onai K, Furukawa Y, Aoki E, Araki T, Nakamura K (2001) Effects of Sugar on Vegetative Development and Floral Transition in Arabidopsis. Plant Physiol. **127:** 252-261

Ortega X, Perez LM (2001) Participation of the phosphoinositide metabolism in the hypersensitive response of Citrus limon against *Alternaria alternata*. Biol. Res. **34:** 43-50

Parthasarathy L, Vadnal RE, Parthasarathy R, Shyamala, Devi CS (1994) Biochemical and molecular properties of lithium-sensitive *myo*-inositol monophosphatase. Life Sci. **54:** 1127-1142

Perera IY, Heilmann I, Boss WF (1999) Transient and sustained increases in inositol 1,4,5-trisphosphate precede the differential growth response in gravistimulated maize pulvini. Proc. Natl. Acad. Sci. **96:** 5838-5843

Perera IY, Heilmann I, Chang SC, Boss WF, Kaufman PB (2001) A role for inositol 1,4,5-trisphosphate in gravitropic signaling and the retention of cold-perceived gravistimulation of oat shoot pulvini. Plant Physiol. **125:** 1499-1507.

Perera IY, Hung CY, Brady S, Muday GK, Boss WF (2006) A universal role for inositol 1,4,5-trisphosphate-mediated signaling in plant gravitropism. Plant Physiol. **140:** 746-760

Perera IY, Love J, Heilmann I, Thompson WF, Boss WF (2002) Up-regulation of phosphoinositide metabolism in tobacco cells constitutively expressing the human type I inositol polyphosphate 5-phosphatase. Plant Physiol. **129:** 1795-1806

Quick WA, Hsiao AI, Hanes JA (1997) Dormancy implications of phosphorus levels in developing caryopses of wild oats (Avena fatua L.). Journal of Plant Growth Regulation **16:** 27-34

Raboy V (2001) Seeds for a better future: 'low phytate' grains help to overcome malnutrition and reduce pollution. Trends Plant Sci. **6:** 458-462.

Raboy V (2003) myo-Inositol-1,2,3,4,5,6-hexakisphosphate. Phytochemistry **64:** 1033-1043

Reddy CC, Swan JS, Hamilton GA (1981) *myo*-Inositol oxygenase from hog kidney. I. Purification and characterization of the oxygenase and of an enzyme complex containing the oxygenase and D-glucuronate reductase. J. Biol. Chem. **256:** 8510-8518

Roberts RM, Shah R, Loewus F (1967) Conversion of *myo*-inositol-2-14C to labeled 4-O-methyl-glucuronic acid in the cell wall of maize root tips. Arch. Biochem. Biophys. **119:** 590-593.

Sanchez JP, Chua NH (2001) Arabidopsis plc1 is required for secondary responses to abscisic acid signals. Plant Cell **13:** 1143-1154.

Sawardeker JS, Sloneker JH (1965) Determination of monosaccharides by gas chromatography. Anal. Chem. **37:** 945-947

Scott JJ, Loewus FA (1986) Phytate metabolism in plants. Phytic Acid, [Symp. \"Appl. Phytic Acid,\"]**:** 23-42

Seitz B, Klos C, Wurm M, Tenhaken R (2000) Matrix polysaccharide precursors in Arabidopsis cell walls are synthesized by alternate pathways with organ-specific expression patterns. Plant J **21:** 537-546.

Sherman WR, Stewart MA, Zinbo M (1969) Mass spectrometric study on the mechanism of D-glucose 6-phosphate-L- *myo*-inositol 1-phosphate cyclase. J. Biol. Chem. **244:** 5703-5708.

Smirnoff N, Conklin PL, Loewus FA (2001) Biosynthesis of ascorbic acid in plants: A renaissance. Annual Review of Plant Physiology and Plant Molecular Biology **52:** 437-467, 431 plate

Steger DJ, Haswell ES, Miller AL, Wente SR, O'Shea EK (2003) Regulation of chromatin remodeling by inositol polyphosphates. Science **299:** 114-116

Stevenson JM, Perera IY, Heilmann II, Persson S, Boss WF (2000) Inositol signaling and plant growth. Trends Plant Sci. **5:** 357

Takada S, Goto K (2003) TERMINAL FLOWER2, an Arabidopsis Homolog of HETEROCHROMATIN PROTEIN1, Counteracts the Activation of FLOWERING LOCUS T by CONSTANS in the Vascular Tissues of Leaves to Regulate Flowering Time. Plant Cell **15:** 2856-2865

Takahashi S, Katagiri T, Hirayama T, Yamaguchi-Shinozaki K, Shinozaki K (2001) Hyperosmotic stress induces a rapid and transient increase in inositol 1,4,5-trisphosphate independent of abscisic acid in Arabidopsis cell culture. Plant Cell Physiol. **42:** 214-222.

Testerink C, Munnik T (2005) Phosphatidic acid: A multifunctional stress signaling lipid in plants. Trends in Plant Science **10:** 368-375

Torabinejad J, Gillaspy GE (2005) Functional Genomics of Inositol Metabolism, Volume 39: Biology of Inositols and Phosphoinositide

Valpuesta V, Botella M (2004) Biosynthesis of L-ascorbic acid in plants: new pathways for an old antioxidant. Trends in Plant Science **9:** 573-577

Vera-Estrella R, Barkla BJ, Bohnert HJ, Pantoja O (1999) Salt stress in *Mesembryanthemum crystallinum L.* cell suspensions activates adaptive mechanisms similar to those observed in the whole plant. Planta **207:** 426-435

Wang P, Ma C, Cao Z, Zhao Y, Zhang H (2002) Molecular cloning and differential expression of a *myo*-inositol-1-phosphate synthase gene in *Suaeda salsa* under salinity stress. Zhiwu Shengli Yu Fenzi Shengwuxue Xuebao **28:** 175-180

Wang X (2005) Regulatory functions of phospholipase D and phosphatidic acid in plant growth, development, and stress responses. Plant Physiol. **139:** 566-573

Wheeler GL, Jones MA, Smirnoff N (1998) The biosynthetic pathway of vitamin C in higher plants. *In* Nature, Vol 393, pp 365-369.

Williams ME, Torabinejad J, Cohick E, Parker K, Drake EJ, Thompson JE, Hortter M, Dewald DB (2005) Mutations in the Arabidopsis phosphoinositide phosphatase gene SAC9 lead to overaccumulation of PtdIns(4,5)P2 and constitutive expression of the stress-response pathway. Plant Physiol. **138:** 686-700

Xiong L, Lee B, Ishitani M, Lee H, Zhang C, Zhu JK (2001) FIERY1 encoding an inositol polyphosphate 1-phosphatase is a negative regulator of abscisic acid and stress signaling in Arabidopsis. Genes Dev. **15:** 1971-1984.

Zhang L, Wang Z, Xia Y, Kai G, Chen W, Tang K (2007) Metabolic engineering of plant L-ascorbic acid biosynthesis: recent trends and applications. Crit. Rev. Biotechnol. **27:** 173-182

Zimmermann P, Hirsch-Hoffmann M, Hennig L, Gruissem W (2004) GENEVESTIGATOR. Arabidopsis microarray database and analysis toolbox. Plant Physiol. **136:** 2621-2632